HUMAN RNA POLYMERASE III TRANSCRIPTOMES AND PHOSPHATASE REGULATION OF YEAST MAF1

by

Andrew Joseph Oler

A dissertation submitted to the faculty of
The University of Utah
in partial fulfillment of the requirements for the degree of

Doctor of Philosophy

Department of Oncological Sciences

The University of Utah

May 2011

The University of Utah Graduate School

STATEMENT OF DISSERTATION APPROVAL

The dissertation of **Andrew Joseph Oler**

has been approved by the following supervisory committee members:

Bradley R. Cairns	, Chair	**February 9, 2011** Date Approved
Stephen L. Lessnick	, Member	**February 9, 2011** Date Approved
Jared Rutter	, Member	**February 9, 2011** Date Approved
Matthew Topham	, Member	**February 9, 2011** Date Approved
Katharine Ullman	, Member	**February 9, 2011** Date Approved

and by **Donald E. Ayer**, Chair of the Department of **Oncological Sciences**

and by Charles A. Wight, Dean of The Graduate School.

ABSTRACT

RNA Polymerase (Pol) III transcribes small noncoding RNAs (e.g., tRNAs) important for translational capacity. Maf1 is a repressor of Pol III conserved from yeast to human, required for repression of Pol III in response to multiple environmental stresses, such as nutrient deprivation. Interestingly, Maf1 is a phosphoprotein, being phosphorylated in good growth conditions and dephosphorylated in poor growing conditions. The phosphatase acting on Maf1 has not been determined. I investigated the identity of the phosphatase in yeast *Saccharomyces cerevisiae* using a genetic Maf1-Pol III fusion construct in combination with molecular and biochemical assays. I queried members of Protein Phosphatase 2A and 4 complexes (PP2A and PP4, respectively) for their role in dephosphorylation of Maf1 and determined that PP4—containing Pph3 and Psy2, together with accessory factors Rrd1 and Tip41—is the major Maf1 phosphatase, acting in response to multiple stresses. Maf1 interacts with Pph3 *in vivo*, and biochemical purification of TAP-tagged Pph3-bound complex shows activity on purified, endogenously phosphorylated Maf1 *in vitro*, suggesting that PP4 is a direct phosphatase of Maf1.

In human cells, regulation of Pol III also involves chromatin regulation, not apparent in studies of Pol III in yeast. The full repertoire of Pol III-transcribed genes in human cells has not been defined. I determined the full Pol III

transcriptome in human (HeLa) cells by chromatin immunoprecipitation (ChIP), coupled with microarray (ChIP-array) or high throughput sequencing (ChIP-seq), for Pol III subunit Rpc32, and Pol III transcription factors Brf1, Brf2 and TFIIIC63. I also determined the Pol III transcriptome in other cell types to address the possibility of cell type-specific activation of Pol III genes. Although many active Pol III genes were shared between all cell types assayed, a large number of genes were differentially enriched with Pol III. I compared enrichment of Pol III with chromatin modifications, transcription factors, and Pol II ChIP-seq profiles and found a significant correlation for active Pol III genes with active chromatin modifications and occupancy of transcription factors and Pol II. These results suggest that active chromatin gates Pol III accessibility to the human genome.

To Shannon, my greatest source of encouragement.

TABLE OF CONTENTS

LIST OF TABLES

LIST OF FIGURES

ACKNOWLEDGMENTS

I would like to thank those who have helped me along the path of graduate school. I thank members of the Molecular Biology Program, especially Barb Saffel, Tammy Brunson, and Steve Lessnick, for their dedication to helping students transition into the Ph.D. program and to have a successful graduate school experience. I thank the teachers and mentors I had during my first year while I was without a home lab, including my first year advisor Dennis Winge.

I thank the faculty and others in the department of Oncological Sciences for the encouragement and mentorship I have received during my development as a scientist. I am also grateful for the help that I received with administrative aspects of graduate school, in particular from Jessica Askin and Dee DalPonte, as they helped ensure that I would complete the things necessary to graduate one day. I thank my committee members for their helpful suggestions and encouragement during my development as a scientist. I thank David Nix and Brett Milash for training in genomics and for helpful discussions.

I thank the Cairns lab for providing me with an environment that has been enormously stimulating and valuable. I thank Brad Cairns for his enthusiasm for science and for the many, many helpful ideas. Brad has been a superb mentor and has been very supportive during my time in his lab. Other people of special mention who have entertained my countless questions are Alisha Schlichter,

Maggie Kasten, Kaede Hinata, Tim Parnell, and Cedric Clapier. I thank Ravi Alla for his direct contributions to this work. I thank everyone in the lab for their friendship.

I thank my family for their love and encouragement throughout my Ph.D. candidacy. I thank my wife Shannon for her constant support in all aspects of my life, and for offering many needed diversions. I thank my daughter Lucy and my son Benjamin for their smiles, their hugs and their love, which have helped me to feel like a whole person. To all who have tried to understand what I do, and to all who have offered love and interest, thank you.

CHAPTER 1

INTRODUCTION

RNA Polymerase III Target Gene Products and Functions

Biology of Known Pol III Products

RNA synthesis in eukaryotes is conducted by three RNA Polymerases, termed Pols I, II, and III, with an additional two polymerases (IV and V) present in plants. Pol III transcriptional activity is required for many basic cellular functions, as well as regulatory processes in the cell. All transcripts produced by Pol III are short (<400bp) and of a noncoding nature. This short length is partially determined by the frequency of Pol III terminators in the genome[1] (i.e., a stretch of ≥4 thymine residues). These noncoding RNAs (ncRNAs) play structural or catalytic roles in ribonucleoprotein particles (RNPs). As a group, these RNPs have a myriad of functions in cellular biology. Pol III transcribes small ncRNAs important for translational capacity[2], such as the 5S rRNA, RNase P, RNase MRP, and all tRNAs (and snoRNAs in *C. elegans*[3]). In addition, Pol III also transcribes a growing list of ncRNAs with alternative functions[4], providing interesting connections to the biology of splicing (U6), viral RNAs (VA-I/II), microRNAs, DNA repeat-derived RNAs (SINEs, including MIR and Alu elements), neuronal disease and protein translation (BC200), Pol II

transcriptional regulation (7SK, BC2), spermatogenesis (BC1), and multidrug resistance (Vault).

Potential to Identify Novel Pol III Targets

In the past decade, there has come an increasing awareness of the fact that a large fraction of the human genome is transcribed to some degree[5]. In 2007, based on methods largely reliant on various forms of microarray techniques and querying the Encyclopedia of DNA Elements (ENCODE) regions of the human genome (comprising ~30Mb total, or about 1% of the human genome), it was extrapolated that 74% of the genome was transcribed if two independent technologies were considered, or 93% if only one technology is considered[6]. Most of the novel transcripts identified in large-scale studies have no potential to be translated into protein[7], and are defined as “noncoding” RNAs.

Pol III is well-known for its production of many different types of ncRNAs[4]. In addition to the known functional ncRNAs, there have also been reported several microRNAs (miRNAs) transcribed by Pol III whose function is as yet unknown[8]. Generally, miRNAs are involved in post-transcriptional regulation of protein expression, so the potential for Pol III transcripts in regulating specific Pol II genes is intriguing. These miRNAs are reportedly driven by Alus, short interspersed element (SINE) class repeats. An Alu repeat contains an A and a B box that allow for TFIIIC binding and Pol III recruitment. It is predicted that approximately 10% of the known miRNAs may be transcribed by Pol III based on their proximity to Alu repeats[8]. In 2007, one report showed the discovery of a functional type 3 promoter Pol III gene starting from a bioinformatics search for

Pol III promoter elements in the human genome[9]. Also in 2007, another Pol III-transcribed gene was discovered—CBL3—which may be a novel vault RNA, or it could be a miRNA[10]. Finally, in 2007, an entirely new family of Pol III genes was discovered, called small NF90-associated RNAs (snaRs)[11]. Thus, the repertoire of Pol III genes continues to expand.

The human transcriptome study by Affymetrix identified many unannotated transcribed RNA fragments (transfrags) in human cells[12]. Their study catalogued RNA expression genomewide, covering the nonrepeat human genome (approximately 45% coverage of the human genome sequence), tiled at an average of 5 bp resolution for seven human cell lines. Included in their study was a comparison of long (>200 nt) versus short (<200 nt) RNAs, cytoplasmic vs. nuclear RNAs and sense vs. antisense short RNAs. Their findings showed that roughly half of the transfrags corresponded to annotated genes and expressed sequence tags (ESTs), while the other half represented unannotated transfrags. Given that new human Pol III genes have been discovered as recently as 2007, and that unbiased whole genome discovery technology has not yet probed into repeat regions of the genome, it is highly likely that other Pol III target genes exist among unannotated regions of the genome, which could be part of new RNPs, miRNAs, or another class of ncRNA.

Pol III Basal Transcription Machinery and Promoter Types

Extensive work on Pol III target genes in yeasts, invertebrates, and vertebrates has revealed the factors required for directing Pol III to target genes[1,13,14]. The three 'Types' of Pol III genes in humans (Fig. 1.1) have been

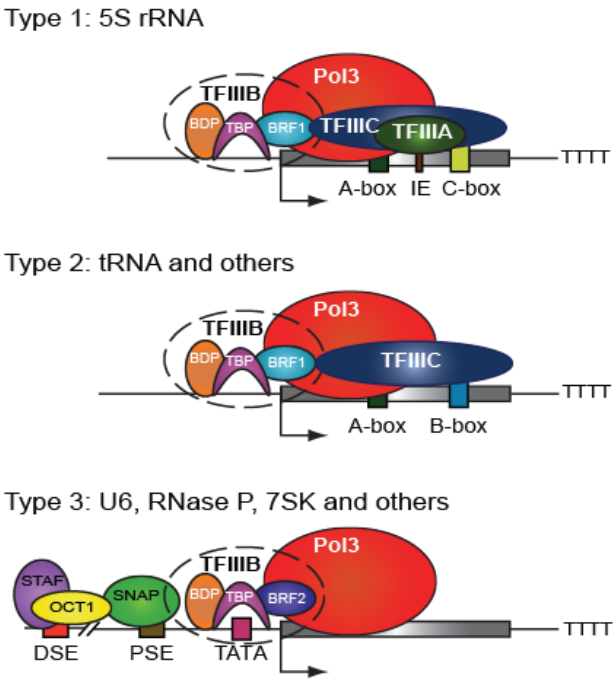

Figure 1.1 Pol III promoter types. Pol III–transcribed genes are classified into three types on the basis of sequence elements and transcription factors. IE, intermediate element; DSE, distal sequence element; PSE, proximal sequence element. Adapted from ref. 19

defined based on the presence and positions of *cis* regulatory elements, and the requirement for particular basal or accessory transcription factors. Briefly, *5S* rRNA is the sole Type 1 gene, uniquely requiring TFIIIA. Type 1 and Type 2 genes both require TFIIIC, a basal factor and targeting complex that recognizes gene-internal *A-box* and *B-box* elements at Type 2, but not Type 1 genes. The TFIIIB complex includes the TATA-binding protein (TBP), needed for TATA/promoter recognition and Pol III initiation. Type 2 and 3 genes utilize alternative assemblies of TFIIIB: BRF1 for Type 2 and BRF2 for Type 3 genes. Type 3 genes lack an internal *A*- or *B-box*, and lack reliance on TFIIIC, relying instead on upstream proximal and distal sequence elements (PSE and DSE) and specific factors (Oct1, SNAP, others) for targeting. Notably, Type 3 Pol III

promoters resemble Pol II genes in their architecture, which utilizes upstream regulatory elements rather than gene-internal elements.

Pol III Is Implicated in Cancer Progression

Pol III is overactive in many types of cancer. For over one hundred years, it has been understood clinically that cancer tissue often exhibits enlargement of the nucleoli[15]. It is in the nucleolus of a nucleus that ribosomal DNA (rDNA) is transcribed into ribosomal RNA (rRNA) and where ribosomes are assembled from their protein and RNA parts. It is also the location of tRNA transcription by Pol III and tRNA processing[16,17]. This enlargement of nucleoli is suggestive of overactive Pol I and III, since nucleoli size has been correlated with the rate of rDNA transcription[18]. Once molecular characterization of cancer became possible, it was also determined that many Pol III factors and target gene products are overexpressed in cancer. Multiple members of TFIIIC are overexpressed in ovarian cancer[20]. TFIIIB members Bdp1 and Brf1 have been found overexpressed in cervical cancer[21]. Overexpression of Pol III targets including tRNAs, 7SL, rRNA, Alu, and BC200 have been reported in multiple types of cancer[21,22]. Whether overexpression of any these products plays a role in cancer outside of generally accelerating cell growth is not known, although one study reports that specific types of tRNAs isotypes are consistently overexpressed in breast cancer, and that these isotypes show a statistically significant enrichment in codons required for cancer-related gene translation but not housekeeping genes[23]. To support the idea that overexpression of these transcripts can support more rapid growth, induced overexpression of $tRNA_i^{Met}$,

the methionine that initiates translation of messenger RNA (mRNA) in mouse fibroblasts leads to higher overall rate of protein synthesis, proliferation, and oncogenic transformation[22]. In contrast, one small family of Pol III gene products has shown a direct clinical relationship with cancer: the Vault RNAs (or HVG RNAs). The expression and overexpression of Vault RNAs and their associated proteins has been associated with multidrug resistance (MDR) in cancer treatment, against chemotherapeutic drugs such as mitoxantrone and doxorubicin[24-27] and is associated with poor outcome in multiple types of cancers[28,29]. Importantly, Pol III is also a target of many tumor suppressors, including direct repressive interaction of TFIIIB by Retinoblastoma protein (Rb) and p53[30-33], as well as indirect repression by phosphatase and tensin homolog (PTEN) via the phosphoinositide 3-kinase (PI3K) signaling pathway[34]. Pol III is also a target of oncogenes, including direct activating interaction by the oncogenic Myc protein[35]. Together, these data suggest that deregulation of Pol III might be one step in the process that could lead to cancer and that Pol III might be a effective target for therapeutic intervention. In addition, a better understanding of the breadth of Pol III targets, as well as the RNP complexes of which they are a part could help us to understand what other potential mechanisms there could be for deregulated Pol III to lead to cancer progression. Since several novel Pol III target genes have recently emerged (e.g., snaR family of ncRNAs), it will be interesting to determine their function and to determine whether they too might be involved in cancer progression.

Chromatin Regulation of Pol III Transcription

Coordinate Regulation of RNA Polymerases

Transcription of the protein synthetic machinery (PSM) by all three RNA Polymerases coordinately responds to nutrient availability and growth conditions (Fig. 1.2). The RNA Polymerases work together to produce the PSM, accounting for ~80% of nuclear transcription in proliferating cells[36]. The transcripts produced by these polymerases are all required for protein synthesis, including ribosomal RNAs (mostly transcribed by Pol I except for 5S rRNA, which is transcribed by Pol III), ribosomal protein genes (Pol II), and tRNAs (Pol III). In response to multiple stresses, such as nutrient availability and DNA damage, repression of all components of PSM is observed. Because of the high energy requirement of PSM production, it makes sense that all three polymerases would be coordinately repressed in poor growth conditions in order to conserve energy until conditions are more favorable for growth. In this study I will focus on RNA Polymerase III regulation: what is already known, and how I have investigated this further.

Pol III Activity Default States in Yeast and Human

To better understand Pol III regulation, it is important to understand the default state for Pol III transcription and to know what differences there are for yeast and human Pol III. Unlike Pol II transcription, which requires regulated, gene-specific activation of its targets, Pol III transcription in yeast has a “default on” state. In a genome-wide Pol III ChIP-on-chip study in *S. cerevisiae*, the Pol

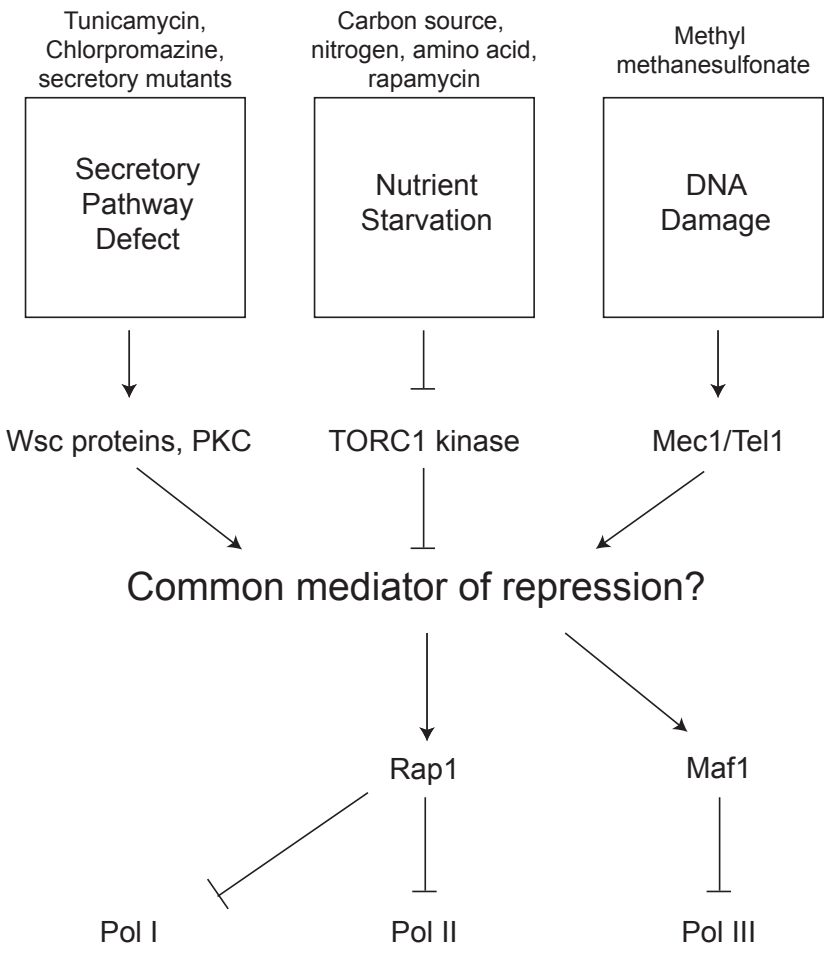

Figure 1.2 All RNA Polymerases are coordinately repressed in cellular stress. Adapted from ref. 37.

III machinery was found to be enriched at *all* predicted Pol III genes (275 tRNA genes, in addition to *5S rDNA, SNR6, SCR1*, and *RPR1*), although there was some variability in the level of enrichment at different genes[38]. When growth conditions are poor and the demand for protein synthesis is decreased, attenuation of the Pol III system requires the master repressor Maf1. Although Maf1 plays a conserved role in metazoans, it appears there are other levels of regulation in metazoan cells that are not present in yeast. For example, there

are 513 predicted tRNA genes in the contiguous human (hg18) genome, not including tRNA pseudogenes (109 total), but there is evidence that there is fractional usage in different cell types. This has been shown for tRNA genes as well as other Pol III targets. It was shown that particular tRNAs are overexpressed in brain tissue[39], and the snaR family of ncRNAs are specific to testes[11]. This is also true in other metazoans. In both human and mouse, BC200 shows neuron-specific expression[40]. In *Xenopus*, an oocyte-specific 5S rRNA is overexpressed during oogenesis and early embryogenesis[41]. In *Bombyx mori*, $tRNA^{Ala}$ is overexpressed specifically in the silk gland[42], likely to aid in producing silk fibroin protein, which is a 391 kDa protein that is 30% alanine by composition. One potential cause for a differential use Pol III targets in metazoans compared to yeast is the dynamic regulation of the chromatin environment of genes throughout the development of a multicellular organism, and advanced mechanisms of producing repressive chromatin not present in yeast.

Chromatin Effects on Gene Expression

"Chromatin" refers to the DNA in the nucleus of a cell plus the proteins that are bound to the DNA. The proteins associated with DNA make up part of the packaging of the DNA, and they provide information content about the genes that are located there as well. Inside the nucleus of a cell, DNA is packaged into a higher order structure to allow organized retrieval of information (Fig. 1.3). The information that is needed by the cell consists of genes, which need to be

Figure 1.3 Histone code. DNA in the nucleus of a cell is packaged with histone proteins as chromatin. Histone tails can receive modifications, which represent active and repressed chromatin. Ac, Acetyl; Me, Methyl; P, Phosphate; Ub, Ubiquitin. Reprinted by permission from Macmillan Publishers Ltd: *Nature Reviews Cancer*, ref. 50, copyright 2006.

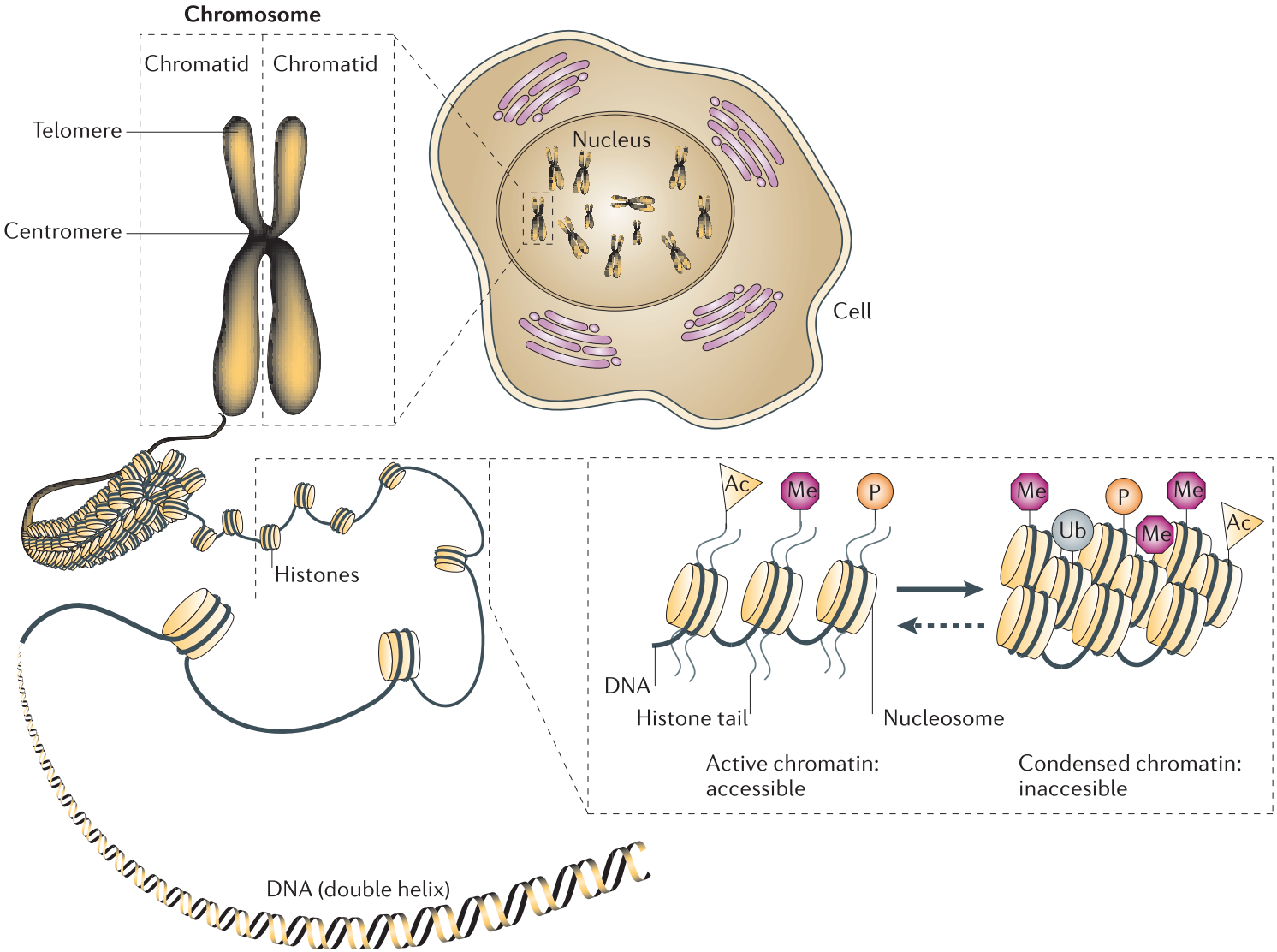
Chromosome
Chromatid
Chromatid
Telomere
Centromere
Nucleus
Cell
Histones
DNA (double helix)
Ac
Me
P
Me
P
Me
Ub
Me
Ac
DNA
Histone tail
Nucleosome
Active chromatin:
accessible
Condensed chromatin:
inaccesible

available for expression at the appropriate time and place. At the basic level, a nucleosome consists of DNA wrapped around a histone protein core. This "beads on a string" structure of repeating nucleosomes is organized into larger fibers and ultimately into a fractal-like higher order structure that allows opening of individual sections without interfering with the rest of the structure[43,44]. Some of the information that is contained in chromatin is information about which genes need to become activated or repressed, and within each gene region, chromatin provides information about where transcription should start, where splicing should occur, etc. Much of this information content is stored in the form of histone modifications[45]. The amino acids that make up amino-terminal histone tails can be modified on their functional groups in certain ways to act as a flag to other factors in the cell, such as chromatin remodelers and modifiers. For example, histone H3 is often modified by trimethylation at lysine 4 (H3K4me3) to signal to Pol II where to begin transcription at active genes[46]. Transcriptionally active chromatin, or "euchromatin," is characterized by positive histone modifications, including H3K4me3, as well as histone acetylation, which can be recognized by bromodomain-containing proteins such as the RSC chromatin remodeler[47]. Transcriptionally inactive chromatin, or "heterochromatin," displays modifications that are repressive, such as DNA methylation, H3K27me3, H3K36me3, and H3K9me3, which can recruit repressor complexes such as Polycomb (recruited by H3K27me3[48]), histone deacetylases (HDACs; e.g., binding of heterochromatin protein 1 (HP1) to H3K9me3 allows recruitment of HDAC4 and HDAC5[49]), or other co-repressors.

Yeast Chromatin Lacks Many Repressive Mechanisms

While all of these types of modifications are present in human cells, many of these are greatly simplified or absent in yeast. Absent from yeast are DNA methylation, H3K27me3, Polycomb, and H3K9me3. This reduces the ability of yeast to form large domains of repressive chromatin. Instead, repression occurs on a gene-by-gene basis where DNA-binding transcription factors (TFs) recruit histone deacetylases to inactive a particular gene. For example, during sporulation, many genes are repressed by binding of either Sum1 or Ume6 TFs in the promoter, which recruit Hst1 or Rpd3 HDACs, respectively[51,52]. It is quite reasonable that yeast would not have the ability to create large repressive chromatin domains, since the gene density is quite high, with a very short average distance between genes compared to metazoans. In addition, the yeast genome has a much smaller amount of "junk" DNA compared to the human genome. The "junk" DNA in the human genome is made up largely of ancient retrotransposons[53] but includes some that could potentially be retrotranspositionally active if they were allowed to be expressed, so mechanisms have been developed to repress their transcription. In the absence of most repressive mechanisms, the yeast genome is considered much more permissive to transcription than that of higher eukaryotes. One other evidence of highly permissive transcription is the characteristically unstable nucleosome particle present in yeast compared to higher eukaryotes[54-57]. With less stable nucleosomes, disassembly of a nucleosome to allow gene activation is much easier to accomplish. In light of all of these differences between

human/metazoan and yeast, it is very likely that chromatin regulation is a layer of Pol III regulation that could be seen in human cells although absent in yeast.

In summary, it appears that human Pol III is regulated on two levels: 1) access to Pol III genes via chromatin regulatory mechanisms and 2) strength of transcription, via Maf1; yeast Pol III appears to be regulated primarily by the latter mechanism.

Maf1-Dependent Regulation of Pol III

Regulators of Pol III Present in Human but not in Yeast

In addition to the added complexity of tissue-specific expression of Pol III targets and chromatin regulatory mechanisms, there are also other activators and repressors of Pol III in metazoans not present in yeast. As mentioned previously, many of these repressors are tumor suppressors, which could be why some Pol III targets are overexpressed in cancers that have certain compromised tumor suppressor genes. The relationship of these metazoan regulators of Pol III to Maf1 is not known, although it is clear that repression of Pol III in response to environmental stress is dependent on Maf1 in both yeast and humans.

Identification of Maf1 Involvement in Pol III Regulation

Maf1 was first identified in yeast *Saccharomyces cerevisiae* and conserved homologs have been found in eukaryotes from yeast to human. The *maf1* strain was identified as a mutant that caused an antisuppression phenotype in an *ade2-1 SUP11* background, caused by an overproduction of tRNAs, suggesting that Maf1 may be involved in Pol III transcription[58].

There are several lines of evidence that prove that Maf1 is the master repressor of Pol III. Yeast *maf1* mutant cells produce a higher basal level of tRNAs than WT cells and it was reported that mutations in the large subunit of Pol III—Rpc160—that lower tRNA levels rescue the phenotype of *maf1* mutant cells, demonstrating that Maf1 plays a role in regulating Pol III[59]. Mutations in the large subunit of Pol III—Rpc160—that lowered tRNA levels could rescue the phenotype of *maf1* mutant cells, suggesting that Maf1 might play a role in regulating Pol III[59]. Maf1 interacts *in vivo* with several subunits of the Pol III machinery, including Pol III components Rpc160, Rpc34, and Rpc82, as well as TFIIIB component Brf1[59-61]. There is also reported a direct interaction of Maf1 with the N-terminus of Rpc160 *in vitro*, suggesting that this is a subunit to which Maf1 binds within the complex[62], further verified by the crystal structure of Maf1 bound to Pol III[63]. Importantly, all repression signals for Pol III appear to converge on Maf1, including response to nutrient deprivation, DNA damage, oxidative stress, and cell wall stress[64,65]. Maf1 is not required for repression of ribosomal protein genes or Pol I-encoded ribosomal RNAs, suggesting that Maf1 is specifically dedicated to repression of Pol III[64]. In summary, the data indicate that Maf1 specifically represses Pol III transcription in response to multiple stresses by direct interaction with the Pol III machinery.

Mechanism of Maf1-dependent Repression of Pol III

Previous work has elucidated many of the factors involved in regulating Maf1. Maf1 is a serine-rich protein that is phosphorylated and mostly cytoplasmic in favorable growth conditions[61]. Phosphorylation by Sch9 and PKA,

and nuclear export by Msn5 are important for maintaining its cytoplasmic localization[66-68]. Upon stress, Maf1 is dephosphorylated, it accumulates in the nucleus, and it becomes highly enriched at Pol III target genes as shown by whole genome ChIP-on-chip studies[61,62]. *In vitro* systems have demonstrated that Maf1 can block recruitment of TFIIIB to preformed TFIIIC-DNA complexes[60]. However, *in vivo*, Maf1 is also able to repress Pol III at a time when all three subcomplexes remain on DNA (TFIIIB, TFIIIC, and Pol III). The resolution of these data can be explained by two phases of repression: acute phase (< 30 min.), in which Maf1 associates with Pol III on DNA and represses transcription, and the prolonged phase, in which TFIIIB and Pol III are displaced from DNA and recruitment of new active Pol III complexes is inhibited.

Both molecular and genetic data support the idea that phosphorylation is a key regulatory modification for Maf1. A previous study in our lab established that Maf1 migration in SDS-PAGE is faster in stressed cells versus unstressed cells, due to loss of phosphate[61]. Dephosphorylation of Maf1 is correlated with its nuclear localization and only the hypophosphorylated form of Maf1 interacts with Pol III, suggesting that dephosphorylation is important for repression. To test whether dephosphorylation was required for repression, conserved residues of Maf1 were mutated in order to create mutants that were not dephosphorylatable. These constitutively phosphorylated mutants were also defective for nuclear localization, association with Pol III, and repression of Pol III transcription. These results suggest that dephosphorylation of Maf1 is a key step in repression of Pol III. Since Pol III specifically interacts with the hypophosphorylated form of Maf1,

it is likely that the major role of Maf1 dephosphorylation is in the acute phase of repression[61].

Identifying the Phosphatase of Maf1

Since Maf1 dephosphorylation is a common mechanism in all reports of Maf1-dependent repression of Pol III to date, the identity of the phosphatase(s) is an intriguing question. Since Pol III repression occurs in a Maf1-dependent manner in response to multiple cellular insults, representing multiple signaling pathways, it could be that there are multiple phosphatases acting on Maf1 in response to the different stress treatments. Or, alternatively, there could be one phosphatase that accounts for the majority of Maf1 dephosphorylation in response to all Pol III-repressive stresses. Many phosphatases in yeast have been tested for their requirement in dephosphorylation of Maf1, including Sit4, Yhv1, Ppz1, His2, Msg5, and Cdc14, showing no effect[61], but there is one report strongly pointing to the PP2A family of serine/threonine phosphatases as playing a role[62], discussed in detail below. Although human Maf1 is also regulated by phosphorylation[69-73], no study has sought to the identity of the phosphatase of human Maf1. Perhaps studies in yeast will again be fruitful here in directing future studies of Pol III regulation, as has been the case in the history of Maf1 and Pol III.

PP2A Family Phosphatases

The PP2A family of phosphatases are interesting as a group, since they are regulated by the target of rapamycin complex (TOR), and specific inhibition of

TOR nutrient signaling with the macrolide antibiotic rapamycin induces rapid inhibition of Pol III transcription[74]. The regulation of PP2A phosphatases by TOR suggests a possible mechanism of integrating nutrient availability and other stresses to dephosphorylation of Maf1. Regulation of PP2A family phosphatases by TOR occurs via the protein Tap42. Tap42 interacts with the PP2A family catalytic subunits Pph21, Pph22, Pph3, and Sit4[75-77] (Fig. 1.4A) and this interaction is reinforced by TOR phosphorylation of Tap42[78]. Upon inhibition of TOR by the drug rapamycin or by poor nutrient source, the phosphatases become active, probably by dissociating from Tap42 and associating in their respective holoenzymes[79] (Fig. 1.4B, C). While Sit4 is not involved in Pol III repression[37,61], a potential role for Pph21/22 or Pph3 has been reported[62]. The triple catalytic mutant of phosphatases *pph21*Δ, *pph22-ts*, and *pph3*Δ was shown to be defective for Maf1 dephosphorylation and Pol III repression. These three have frequently been reported as alternative catalytic subunits of the PP2A phosphatase complex (see below), therefore, the conclusion of a former study was that PP2A is the phosphatase of Maf1. However, the PP2A scaffold and catalytic mutants *tpd3*Δ and *pph21*Δ *pph22*Δ, respectively, are not defective for Maf1 dephosphorylation, initially raising the possibility that Pph3 may be the phosphatase of Maf1 rather than PP2A[61].

Confusion Between PP2A and PP4

I digress briefly to discuss potential reasons for the perpetuation of the idea that yeast PP2A contains three alternative catalytic subunits. The basis for calling the three mentioned phosphatases (Pph21, Pph22, Pph3) alternative

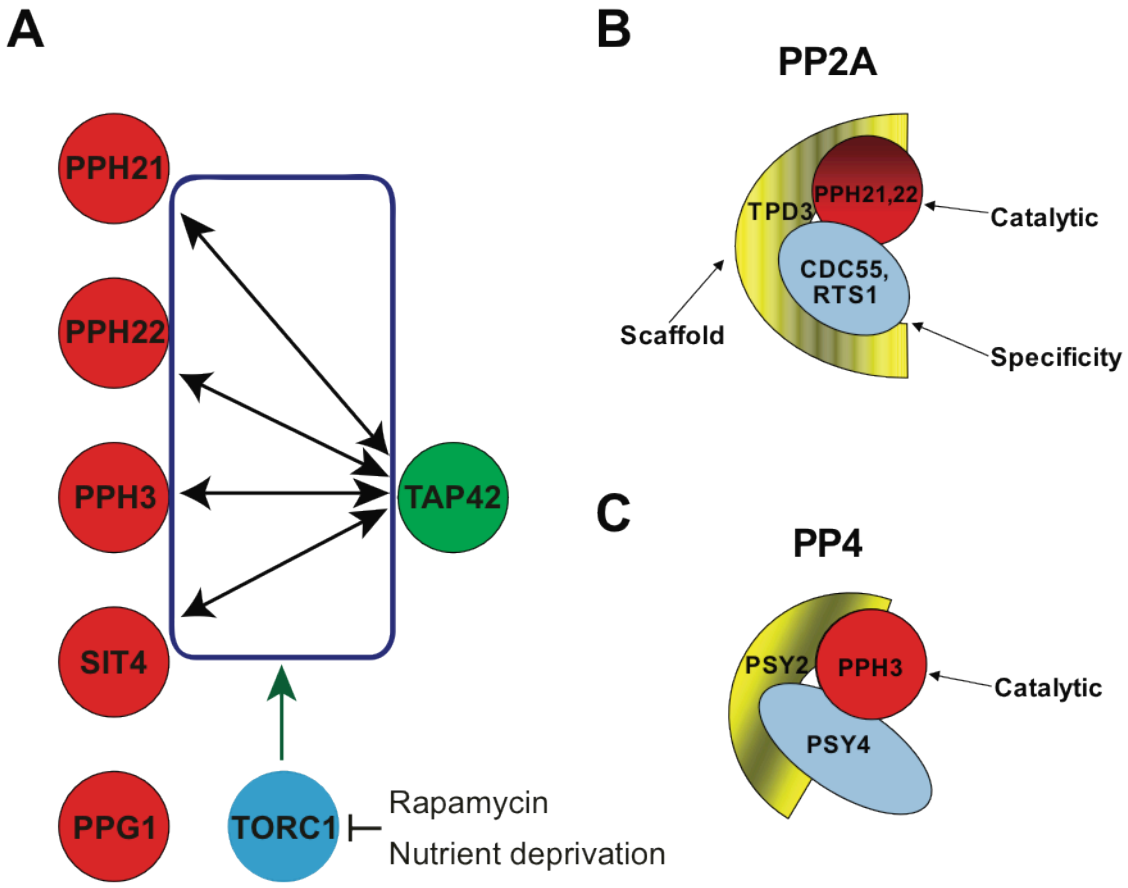

Figure 1.4 PP2A family phosphatases in yeast. (A) Canonical view of nutrient-responsive TORC1 regulation of PP2A family phosphatases. Phosphatases Pph21, Pph22, Pph3, and Sit4 (but not Ppg1) interact with a repressor, Tap42. This interaction is enhanced by TORC1. When interacting with Tap42, the phosphatase subunits are likely excluded from their respective holoenzymes. TORC1 complex can be inhibited by rapamycin or nutrient deprivation (B) PP2A holoenzyme with alternative subunits specified. (C) PP4 holoenzyme.

catalytic subunits of PP2A stems from early work by Ronne et al. in defining the phenotype of these mutants[80]. The single mutant of Pph21 or Pph22 produces no detectable growth phenotype, consistent with the functional redundancy between the two genes. A double *pph21*Δ*pph22*Δ mutant has a severe slow growth phenotype and the combined disruption of Pph21, Pph22, and Pph3 is lethal. Some have interpreted this result, in combination with the sequence similarity between the proteins, to mean that Pph3 is an alternative catalytic subunit of PP2A (e.g., ref. 81). This is not an acceptable conclusion, according to the authors of the paper in which the disruption was created. The authors are clear that the Pph3 is not homologous with PP2A: "these two genes [*PPH21 and PPH22*] encode true homologs of PP2A in budding yeast….The PPH3 protein is not closely related to PPH1/SIT4, PPH21 or PPH22"[80]. And with reference to the death in the triple mutant, they state the following:

> This finding is surprising for two reasons. First, it differs from the results of Sneddon et al., who found that spores disrupted for both *PPH21* and *PPH22* either fail to germinate or arrest as microcolonies with less than 32 cells. Second, the sequence of PPH3 does not suggest that it is a PP2A homolog. Instead, it belongs to the group of PP2A-like proteins that includes PPH1, PPV, and PPX. We think that these results should be interpreted as a partial suppression of the PP2A deficiency by PPH3, even though the latter enzyme probably has a function distinct from that of PP2A[80].

There are nearly a dozen papers that have referred to Pph21, Pph22 and Pph3 as orthologs of mammalian PP2A and which state (or strongly imply) that all three are alternative catalytic subunits of PP2A, most of which have cited one of two papers as evidence: i.e., papers citing Ronne et al. (1991)[62,65,81-85]; papers citing Evans and Stark (1997)[62,81,86-88]. Evans and Stark are also clear in their

understanding that though they were working with strains that have mutations in *PPH21*, *PPH22*, and *PPH3*, that Pph3 is not a part of PP2A, evidenced by phrases such as “we investigated the influence of *SSD1-v1* on growth in the absence of both the PP2A C subunits and Pph3p”[89]. With the thoughts of the authors of these seminal papers in mind, it is surprising to realize that many who have investigated Pph3 since the time these papers were published have interpreted their findings to mean the opposite, or have misinterpreted these papers. This is part of the reason why the phosphatase complex important for dephosphorylation of Maf1 was unknown until our study.

Protein Phosphatase 4

Instead of Pph3 being a part of PP2A, there is an expanding body of evidence that shows that Pph3 is part of an evolutionarily conserved phosphatase complex, Protein Phosphatase 4 (PP4). Pph3 homologs have been studied in amoeba, budding yeast, human, worms, and fruit flies and found to have a conserved role in the regulation of the DNA damage response[90-92]. In addition, interaction of Pph3 (or its homologues) with PP4-specific subunits has been shown in human, *S. cerevisiae*, *D. discoideum,* and *C. elegans*[90-92].

It is becoming clear that PP4 is a complex that is involved in the cellular response to environmental stress in yeast. The Target of Rapamycin complex 1 (TORC1) is a kinase complex that regulates PP2A family phosphatases, including PP2A, PP4, and PP6 in response to environmental nutrient status. Inhibition of TORC1 in yeast leads to G_0 stationary phase, since the cells “think” they are deprived of nutrients[74]. Stresses that inhibit TORC1, such as starvation

of good sources of amino acids, nitrogen, or carbon[93], as well as the antibiotic rapamycin, which specifically inhibits TORC1 activity, are also known to repress Pol III transcription, implicating the Tor pathway in regulation of Pol III[37]. Since Tap42 inhibition of PP2A family phosphatase subunits is sensitive to TORC1 activity, all PP2A family phosphatases are prime candidates for Maf1-dependent repression of Pol III in response to nutritional status. In addition, *pph3Δ* cells are resistant to rapamycin-induced growth arrest, suggesting that PP4 activity plays a role in the starvation-mediated growth arrest that is not redundant with other PP2A family phosphatases[94]. It is possible that one function of PP4 in rapamycin/starvation-induced growth arrest is repression of Pol III transcription.

As already mentioned, PP4 plays a role in DNA damage, which is another cellular perturbation that causes Pol III repression. PP4 dephosphorylates Rad53 and γH2AX in order to recover from the intra-S cell cycle checkpoint induced by DNA damage[95,96]. Recent data show that in the nuclear exportin *msn5Δ* mutant strain, Maf1 is constitutively localized in the nucleus but still requires dephosphorylation to repress Pol III[67]. This suggests that the phosphatase of Maf1 must be capable of localizing to the nucleus during stress. Both of the known substrates of yeast PP4 are nuclear proteins[97], and PP4 is activated towards these substrates in DNA damaging conditions, putting PP4 in the proper time and place for filling the role of a Maf1 phosphatase in yeast.

Dissertation Overview

In this study, I have characterized the Pol III transcriptome in human cells and have investigated mechanisms of Maf1 regulation of Pol III in yeast.

I characterized the Pol III transcriptome in an unbiased, genome-wide fashion by chromatin immunoprecipitation (ChIP) of multiple subunits of the Pol III machinery, coupled with microarray or high-throughput sequencing technology. This work is presented in Chapter 2 as previously published in *Nature Structural and Molecular Biology*[19]. ChIP is a technique used to identify binding sites of proteins in the genomic DNA of an organism. Briefly, cells are cross-linked with formaldehyde to covalently link DNA to its associated proteins; the proteins are immunoprecipitated from extracts (along with DNA) using antibodies specific to the protein; DNA is isolated, amplified, and subjected to competitive hybridization microarray or high-throughput sequencing to determine bound regions. Pol III ChIP on a scale as large as this had never been previously performed. I used whole genome microarrays (tiled at ~150 bp resolution, consisting of ten 1 million feature arrays) representing the nonrepeat genome for Pol III (RPC32) ChIP-on-chip. In addition, ChIP DNA bound by Pol III (RPC32), Brf1, Brf2, or TFIIIC63 was subjected to sequencing. Using two platforms, I was able to comprehensively determine the binding locations of the Pol III machinery and catalogue active genes in multiple cells lines. I also determined Pol III occupancy relationships with chromatin status in two cell types to determine correlations between active Pol III genes and positive chromatin modifications, transcription factor occupancy, and Pol II occupancy.

In my mechanistic study in yeast, I have investigated the basis of Maf1 dephosphorylation in repression of Pol III. This work is presented in Chapter 3 as a manuscript in preparation for publication. I verified the hypothesis that Pph3

is the catalytic subunit of PP4 and not PP2A in yeast, and (more importantly) that PP4 is the major phosphatase of Maf1 in response to multiple stress pathways in yeast. I used strains genetically disrupted for components of PP4 and PP2A to test for ability for Maf1 dephosphorylation and Pol III repression. I purified PP4 from yeast and tested for its ability to dephosphorylate Maf1 *in vitro*. I also developed a novel Maf1-Pol III fusion protein that has proven useful in identifying PP4 components and associated factors and may be a valuable tool in elucidating other components of the pathway of Pol III repression.

References

1. Schramm, L. & Hernandez, N. Recruitment of RNA polymerase III to its target promoters. *Genes Dev* **16**, 2593-620 (2002).

2. White, R.J. *RNA Polymerase III Transcription*, (Springer-Verlag, New York, NY, 1998).

3. Li, T. et al. In vivo analysis of Caenorhabditis elegans noncoding RNA promoter motifs. *BMC Mol Biol* **9**, 71 (2008).

4. Dieci, G., Fiorino, G., Castelnuovo, M., Teichmann, M. & Pagano, A. The expanding RNA polymerase III transcriptome. *Trends Genet* **23**, 614-22 (2007).

5. Griffiths-Jones, S. Annotating noncoding RNA genes. *Annu Rev Genomics Hum Genet* **8**, 279-98 (2007).

6. Birney, E. et al. Identification and analysis of functional elements in 1% of the human genome by the ENCODE pilot project. *Nature* **447**, 799-816 (2007).

7. Guttman, M. et al. Chromatin signature reveals over a thousand highly conserved large non-coding RNAs in mammals. *Nature* **458**, 223-7 (2009).

8. Borchert, G.M., Lanier, W. & Davidson, B.L. RNA polymerase III transcribes human microRNAs. *Nat Struct Mol Biol* **13**, 1097-101 (2006).

9. Pagano, A. et al. New small nuclear RNA gene-like transcriptional units as sources of regulatory transcripts. *PLoS Genet* **3**, e1 (2007).

10. Mrazek, J., Kreutmayer, S.B., Grasser, F.A., Polacek, N. & Huttenhofer, A. Subtractive hybridization identifies novel differentially expressed ncRNA species in EBV-infected human B cells. *Nucleic Acids Res* **35**, e73 (2007).

11. Parrott, A.M. & Mathews, M.B. Novel rapidly evolving hominid RNAs bind nuclear factor 90 and display tissue-restricted distribution. *Nucleic Acids Res* **35**, 6249-58 (2007).

12. Kapranov, P. et al. RNA maps reveal new RNA classes and a possible function for pervasive transcription. *Science* **316**, 1484-8 (2007).

13. Willis, I.M. RNA polymerase III. Genes, factors and transcriptional specificity. *Eur J Biochem* **212**, 1-11 (1993).

14. Geiduschek, E.P. & Kassavetis, G.A. The RNA polymerase III transcription apparatus. *J Mol Biol* **310**, 1-26 (2001).

15. Pianese, G. Beitrag zur Histologie und Aetiologie der Carcinoma Histologische und experimentelle Untersuchungen. *Beitr Pathol Anat* **142(suppl 1)**, 1-193 (1896).

16. Thompson, M., Haeusler, R.A., Good, P.D. & Engelke, D.R. Nucleolar clustering of dispersed tRNA genes. *Science* **302**, 1399-401 (2003).

17. Bertrand, E., Houser-Scott, F., Kendall, A., Singer, R.H. & Engelke, D.R. Nucleolar localization of early tRNA processing. *Genes Dev* **12**, 2463-8 (1998).

18. Altmann, G.G. & Leblond, C.P. Changes in the size and structure of the nucleolus of columnar cells during their migration from crypt base to villus top in rat jejunum. *J Cell Sci* **56**, 83-99 (1982).

19. Oler, A.J. et al. Human RNA polymerase III transcriptomes and relationships to Pol II promoter chromatin and enhancer-binding factors. *Nat Struct Mol Biol* **17**, 620-8 (2010).

20. Winter, A.G. et al. RNA polymerase III transcription factor TFIIIC2 is overexpressed in ovarian tumors. *Proc Natl Acad Sci U S A* **97**, 12619-24 (2000).

21. White, R.J. RNA polymerase III transcription and cancer. *Oncogene* **23**, 3208-16 (2004).

22. Marshall, L. & White, R.J. Non-coding RNA production by RNA polymerase III is implicated in cancer. *Nat Rev Cancer* **8**, 911-4 (2008).

23. Pavon-Eternod, M. et al. tRNA over-expression in breast cancer and functional consequences. *Nucleic Acids Res* **37**, 7268-80 (2009).

24. Kitazono, M. et al. Multidrug resistance and the lung resistance-related protein in human colon carcinoma SW-620 cells. *J Natl Cancer Inst* **91**, 1647-53 (1999).

25. Kitazono, M. et al. Reversal of LRP-associated drug resistance in colon carcinoma SW-620 cells. *Int J Cancer* **91**, 126-31 (2001).

26. Gopinath, S.C., Matsugami, A., Katahira, M. & Kumar, P.K. Human vault-associated non-coding RNAs bind to mitoxantrone, a chemotherapeutic compound. *Nucleic Acids Res* **33**, 4874-81 (2005).

27. Gopinath, S.C., Wadhwa, R. & Kumar, P.K. Expression of noncoding vault RNA in human malignant cells and its importance in mitoxantrone resistance. *Mol Cancer Res* **8**, 1536-46.

28. List, A.F. et al. Overexpression of the major vault transporter protein lung-resistance protein predicts treatment outcome in acute myeloid leukemia. *Blood* **87**, 2464-9 (1996).

29. Izquierdo, M.A. et al. Drug resistance-associated marker Lrp for prediction of response to chemotherapy and prognoses in advanced ovarian carcinoma. *J Natl Cancer Inst* **87**, 1230-7 (1995).

30. Chesnokov, I., Chu, W.M., Botchan, M.R. & Schmid, C.W. p53 inhibits RNA polymerase III-directed transcription in a promoter-dependent manner. *Mol Cell Biol* **16**, 7084-8 (1996).

31. White, R.J., Trouche, D., Martin, K., Jackson, S.P. & Kouzarides, T. Repression of RNA polymerase III transcription by the retinoblastoma protein. *Nature* **382**, 88-90 (1996).

32. Cairns, C.A. & White, R.J. p53 is a general repressor of RNA polymerase III transcription. *EMBO J* **17**, 3112-23 (1998).

33. Felton-Edkins, Z.A. et al. Direct regulation of RNA polymerase III transcription by RB, p53 and c-Myc. *Cell Cycle* **2**, 181-4 (2003).

34. Woiwode, A. et al. PTEN represses RNA polymerase III-dependent transcription by targeting the TFIIIB complex. *Mol Cell Biol* **28**, 4204-14 (2008).

35. Gomez-Roman, N., Grandori, C., Eisenman, R.N. & White, R.J. Direct activation of RNA polymerase III transcription by c-Myc. *Nature* **421**, 290-4 (2003).

36. Moss, T. & Stefanovsky, V.Y. At the center of eukaryotic life. *Cell* **109**, 545-8 (2002).

37. Willis, I.M., Desai, N. & Upadhya, R. Signaling repression of transcription by RNA polymerase III in yeast. *Prog Nucleic Acid Res Mol Biol* **77**, 323-53 (2004).

38. Roberts, D.N., Stewart, A.J., Huff, J.T. & Cairns, B.R. The RNA polymerase III transcriptome revealed by genome-wide localization and activity-occupancy relationships. *Proc Natl Acad Sci U S A* **100**, 14695-700 (2003).

39. Dittmar, K.A., Goodenbour, J.M. & Pan, T. Tissue-specific differences in human transfer RNA expression. *PLoS Genet* **2**, e221 (2006).

40. Martignetti, J.A. & Brosius, J. BC1 RNA: transcriptional analysis of a neural cell-specific RNA polymerase III transcript. *Mol Cell Biol* **15**, 1642-50 (1995).

41. Wakefield, L. & Gurdon, J.B. Cytoplasmic regulation of 5S RNA genes in nuclear-transplant embryos. *EMBO J* **2**, 1613-9 (1983).

42. Meza, L., Araya, A., Leon, G. & Krauskopf, M. Specific alanine-tRNA species associated with fibroin biosynthesis in the posterior silk-gland of Bombyx mori. *FEBS Lett* **77**, 255-60 (1977).

43. Lieberman-Aiden, E. et al. Comprehensive mapping of long-range interactions reveals folding principles of the human genome. *Science* **326**, 289-93 (2009).

44. van Berkum, N.L. et al. Hi-C: a method to study the three-dimensional architecture of genomes. *J Vis Exp*.

45. Strahl, B.D. & Allis, C.D. The language of covalent histone modifications. *Nature* **403**, 41-5 (2000).

46. Santos-Rosa, H. et al. Active genes are tri-methylated at K4 of histone H3. *Nature* **419**, 407-11 (2002).

47. Kasten, M. et al. Tandem bromodomains in the chromatin remodeler RSC recognize acetylated histone H3 Lys14. *EMBO J* **23**, 1348-59 (2004).

48. Fischle, W. et al. Molecular basis for the discrimination of repressive methyl-lysine marks in histone H3 by Polycomb and HP1 chromodomains. *Genes Dev* **17**, 1870-81 (2003).

49. Zhang, C.L., McKinsey, T.A. & Olson, E.N. Association of class II histone deacetylases with heterochromatin protein 1: potential role for histone methylation in control of muscle differentiation. *Mol Cell Biol* **22**, 7302-12 (2002).

50. Sparmann, A. & van Lohuizen, M. Polycomb silencers control cell fate, development and cancer. *Nat Rev Cancer* **6**, 846-56 (2006).

51. Robert, F. et al. Global position and recruitment of HATs and HDACs in the yeast genome. *Mol Cell* **16**, 199-209 (2004).

52. Kadosh, D. & Struhl, K. Repression by Ume6 involves recruitment of a complex containing Sin3 corepressor and Rpd3 histone deacetylase to target promoters. *Cell* **89**, 365-71 (1997).

53. Lander, E.S. et al. Initial sequencing and analysis of the human genome. *Nature* **409**, 860-921 (2001).

54. Lee, K.P., Baxter, H.J., Guillemette, J.G., Lawford, H.G. & Lewis, P.N. Structural studies on yeast nucleosomes. *Can J Biochem* **60**, 379-88 (1982).

55. Pineiro, M., Puerta, C. & Palacian, E. Yeast nucleosomal particles: structural and transcriptional properties. *Biochemistry* **30**, 5805-10 (1991).

56. White, C.L., Suto, R.K. & Luger, K. Structure of the yeast nucleosome core particle reveals fundamental changes in internucleosome interactions. *Embo J* **20**, 5207-18 (2001).

57. Jin, C. & Felsenfeld, G. Nucleosome stability mediated by histone variants H3.3 and H2A.Z. *Genes Dev* **21**, 1519-29 (2007).

58. Murawski, M. et al. maf1 mutation alters the subcellular localization of the Mod5 protein in yeast. *Acta Biochim Pol* **41**, 441-8 (1994).

59. Pluta, K. et al. Maf1p, a negative effector of RNA polymerase III in Saccharomyces cerevisiae. *Mol Cell Biol* **21**, 5031-40 (2001).

60. Desai, N. et al. Two steps in Maf1-dependent repression of transcription by RNA polymerase III. *J Biol Chem* **280**, 6455-6462 (2005).

61. Roberts, D.N., Wilson, B., Huff, J.T., Stewart, A.J. & Cairns, B.R. Dephosphorylation and genome-wide association of Maf1 with Pol III-transcribed genes during repression. *Mol Cell* **22**, 633-44 (2006).

62. Oficjalska-Pham, D. et al. General repression of RNA polymerase III transcription is triggered by protein phosphatase type 2A-mediated dephosphorylation of Maf1. *Mol Cell* **22**, 623-32 (2006).

63. Vannini, A. et al. Molecular basis of RNA polymerase III transcription repression by Maf1. *Cell* **143**, 59-70.

64. Upadhya, R., Lee, J. & Willis, I.M. Maf1 is an essential mediator of diverse signals that repress RNA polymerase III transcription. *Mol Cell* **10**, 1489-94 (2002).

65. Boisnard, S. et al. H2O2 activates the nuclear localization of Msn2 and Maf1 through thioredoxins in Saccharomyces cerevisiae. *Eukaryot Cell* **8**, 1429-38 (2009).

66. Moir, R.D. et al. Protein kinase A regulates RNA polymerase III transcription through the nuclear localization of Maf1. *Proc Natl Acad Sci U S A* **103**, 15044-9 (2006).

67. Towpik, J., Graczyk, D., Gajda, A., Lefebvre, O. & Boguta, M. Derepression of RNA polymerase III transcription by phosphorylation and nuclear export of its negative regulator, Maf1. *J Biol Chem* **283**, 17168-74 (2008).

68. Lee, J., Moir, R.D. & Willis, I.M. Regulation of RNA polymerase III transcription involves SCH9-dependent and SCH9-independent branches of the target of rapamycin (TOR) pathway. *J Biol Chem* **284**, 12604-8 (2009).

69. Reina, J.H., Azzouz, T.N. & Hernandez, N. Maf1, a new player in the regulation of human RNA polymerase III transcription. *PLoS ONE* **1**, e134 (2006).

70. Rollins, J., Veras, I., Cabarcas, S., Willis, I. & Schramm, L. Human Maf1 negatively regulates RNA polymerase III transcription via the TFIIB family members Brf1 and Brf2. *Int J Biol Sci* **3**, 292-302 (2007).

71. Shor, B. et al. Requirement of the mTOR kinase for the regulation of Maf1 phosphorylation and control of RNA polymerase III-dependent transcription in cancer cells. *J Biol Chem* **285**, 15380-92.

72. Michels, A.A. et al. mTORC1 directly phosphorylates and regulates human MAF1. *Mol Cell Biol* **30**, 3749-57.

73. Kantidakis, T., Ramsbottom, B.A., Birch, J.L., Dowding, S.N. & White, R.J. mTOR associates with TFIIIC, is found at tRNA and 5S rRNA genes, and targets their repressor Maf1. *Proc Natl Acad Sci U S A* **107**, 11823-8.

74. Zaragoza, D., Ghavidel, A., Heitman, J. & Schultz, M.C. Rapamycin induces the G0 program of transcriptional repression in yeast by interfering with the TOR signaling pathway. *Mol Cell Biol* **18**, 4463-70 (1998).

75. Di Como, C.J. & Arndt, K.T. Nutrients, via the Tor proteins, stimulate the association of Tap42 with type 2A phosphatases. *Genes Dev* **10**, 1904-16 (1996).

76. Jacinto, E., Guo, B., Arndt, K.T., Schmelzle, T. & Hall, M.N. TIP41 interacts with TAP42 and negatively regulates the TOR signaling pathway. *Mol Cell* **8**, 1017-26 (2001).

77. Wang, H., Wang, X. & Jiang, Y. Interaction with Tap42 is required for the essential function of Sit4 and type 2A phosphatases. *Mol Biol Cell* **14**, 4342-51 (2003).

78. Jiang, Y. & Broach, J.R. Tor proteins and protein phosphatase 2A reciprocally regulate Tap42 in controlling cell growth in yeast. *EMBO J* **18**, 2782-92 (1999).

79. Inoki, K., Ouyang, H., Li, Y. & Guan, K.L. Signaling by target of rapamycin proteins in cell growth control. *Microbiol Mol Biol Rev* **69**, 79-100 (2005).

80. Ronne, H., Carlberg, M., Hu, G.Z. & Nehlin, J.O. Protein phosphatase 2A in Saccharomyces cerevisiae: effects on cell growth and bud morphogenesis. *Mol Cell Biol* **11**, 4876-84 (1991).

81. Wang, Y. & Ng, T.Y. Phosphatase 2A negatively regulates mitotic exit in Saccharomyces cerevisiae. *Mol Biol Cell* **17**, 80-9 (2006).

82. Snaith, H.A., Armstrong, C.G., Guo, Y., Kaiser, K. & Cohen, P.T. Deficiency of protein phosphatase 2A uncouples the nuclear and centrosome cycles and prevents attachment of microtubules to the kinetochore in Drosophila microtubule star (mts) embryos. *J Cell Sci* **109 (Pt 13)**, 3001-12 (1996).

83. Zhao, Y., Boguslawski, G., Zitomer, R.S. & DePaoli-Roach, A.A. Saccharomyces cerevisiae homologs of mammalian B and B' subunits of protein phosphatase 2A direct the enzyme to distinct cellular functions. *J Biol Chem* **272**, 8256-62 (1997).

84. Richard, M., Quijano, R.R., Bezzate, S., Bordon-Pallier, F. & Gaillardin, C. Tagging morphogenetic genes by insertional mutagenesis in the yeast Yarrowia lipolytica. *J Bacteriol* **183**, 3098-107 (2001).

85. Eckert-Boulet, N. et al. Deletion of RTS1, encoding a regulatory subunit of protein phosphatase 2A, results in constitutive amino acid signaling via increased Stp1p processing. *Eukaryot Cell* **5**, 174-9 (2006).

86. Duvel, K., Santhanam, A., Garrett, S., Schneper, L. & Broach, J.R. Multiple roles of Tap42 in mediating rapamycin-induced transcriptional changes in yeast. *Mol Cell* **11**, 1467-78 (2003).

87. Tang, X. & Wang, Y. Pds1/Esp1-dependent and -independent sister chromatid separation in mutants defective for protein phosphatase 2A. *Proc Natl Acad Sci U S A* **103**, 16290-5 (2006).

88. Pal, G., Paraz, M.T. & Kellogg, D.R. Regulation of Mih1/Cdc25 by protein phosphatase 2A and casein kinase 1. *J Cell Biol* **180**, 931-45 (2008).

89. Evans, D.R. & Stark, M.J. Mutations in the Saccharomyces cerevisiae type 2A protein phosphatase catalytic subunit reveal roles in cell wall integrity, actin cytoskeleton organization and mitosis. *Genetics* **145**, 227-41 (1997).

90. Gingras, A.C. et al. A novel, evolutionarily conserved protein phosphatase complex involved in cisplatin sensitivity. *Mol Cell Proteomics* **4**, 1725-40 (2005).

91. Kim, S.H., Holway, A.H., Wolff, S., Dillin, A. & Michael, W.M. SMK-1/PPH-4.1-mediated silencing of the CHK-1 response to DNA damage in early C. elegans embryos. *J Cell Biol* **179**, 41-52 (2007).

92. Mendoza, M.C., Booth, E.O., Shaulsky, G. & Firtel, R.A. MEK1 and protein phosphatase 4 coordinate Dictyostelium development and chemotaxis. *Mol Cell Biol* **27**, 3817-27 (2007).

93. Crespo, J.L. & Hall, M.N. Elucidating TOR signaling and rapamycin action: lessons from Saccharomyces cerevisiae. *Microbiol Mol Biol Rev* **66**, 579-91, table of contents (2002).

94. Douville, J., David, J., Lemieux, K.M., Gaudreau, L. & Ramotar, D. The Saccharomyces cerevisiae phosphatase activator RRD1 is required to modulate gene expression in response to rapamycin exposure. *Genetics* **172**, 1369-72 (2006).

95. Keogh, M.C. et al. A phosphatase complex that dephosphorylates gammaH2AX regulates DNA damage checkpoint recovery. *Nature* **439**, 497-501 (2006).

96. O'Neill, B.M. et al. Pph3-Psy2 is a phosphatase complex required for Rad53 dephosphorylation and replication fork restart during recovery from DNA damage. *Proc Natl Acad Sci U S A* **104**, 9290-5 (2007).

97. Huh, W.K. et al. Global analysis of protein localization in budding yeast. *Nature* **425**, 686-91 (2003).

CHAPTER 2

HUMAN RNA POLYMERASE III TRANSCRIPTOMES AND RELATIONSHIPS TO POL II PROMOTER CHROMATIN AND ENHANCER-BINDING FACTORS

This material was originally published in *Nat Struct Mol Biol* 2010 May;17(5):620-8. Epub 2010 Apr 25; doi:10.1038/nsmb.1801.

RESOURCE

nature structural & molecular biology

Human RNA polymerase III transcriptomes and relationships to Pol II promoter chromatin and enhancer-binding factors

Andrew J Oler[1,2], Ravi K Alla[1,2], Douglas N Roberts[3], Alexander Wong[3], Peter C Hollenhorst[1], Katherine J Chandler[1], Patrick A Cassiday[4], Cassie A Nelson[4], Curt H Hagedorn[4], Barbara J Graves[1] & Bradley R Cairns[1,2]

RNA polymerase (Pol) III transcribes many noncoding RNAs (for example, transfer RNAs) important for translational capacity and other functions. We localized Pol III, alternative TFIIIB complexes (BRF1 or BRF2) and TFIIIC in HeLa cells to determine the Pol III transcriptome, define gene classes and reveal 'TFIIIC-only' sites. Pol III localization in other transformed and primary cell lines reveals previously uncharacterized and cell type–specific Pol III loci as well as one microRNA. Notably, only a fraction of the *in silico*–predicted Pol III loci are occupied. Many occupied Pol III genes reside within an annotated Pol II promoter. Outside of Pol II promoters, occupied Pol III genes overlap with enhancer-like chromatin and enhancer-binding proteins such as ETS1 and STAT1. Moreover, Pol III occupancy scales with the levels of nearby Pol II, active chromatin and CpG content. These results suggest that active chromatin gates Pol III accessibility to the genome.

RNA synthesis in mammals is conducted by three RNA polymerases, termed Pol I, Pol II and Pol III, with an additional two polymerases (IV and V) present in plants. Pol III transcribes small noncoding RNAs important for translational capacity[1], such as the 5S ribosomal RNA, RNase P, RNase MRP and all tRNAs. In addition, there is a growing list of noncoding RNAs with alternative functions that Pol III is known to transcribe[2], which connects this polymerase to the biology of splicing (U6), viral RNAs (VA-I and VA-II), microRNAs (miRNAs), DNA repeat–derived RNAs (short interspersed nuclear elements, including mammalian-wide interspersed repeat (MIR) and Alu elements), neuronal disease and messenger RNA translation (BC200), Pol II transcriptional regulation (7SK, BC2), spermatogenesis (BC1) and multidrug resistance (Vault). However, the full repertoire of Pol III genes in the human genome is not known and must be determined in multiple cell types to understand the full scope of Pol III biology. Also of high interest is Pol III regulation—whether the Pol III transcriptome is constitutive or instead highly regulated, and if it is regulated, by what mechanism. For example, there are 513 predicted tDNAs (genes encoding tRNAs) in the contiguous genome (hg18 human genome assembly), not including tRNA pseudogenes (172 total), but their fractional usage in different cell types is entirely unknown. Also, high levels of Pol III transcription and tRNA pools are correlated with the growth of cancer cells[3,4]. A better understanding of Pol III dynamics and regulation is needed for understanding normal Pol III biology and its misregulation in cancer and disease.

Extensive work on Pol III genes in yeasts, invertebrates and vertebrates has revealed the factors required for directing Pol III to target genes[5–7] and has defined the three types of Pol III genes in humans (**Fig. 1a**), on the basis of (i) the presence and positions of *cis* regulatory elements and (ii) the requirement for particular basal or accessory transcription factors. Briefly, 5S rRNA is the sole type 1 gene, uniquely requiring TFIIIA. Type 1 and type 2 genes both require TFIIIC, a basal factor and targeting complex that recognizes gene-internal A-box and B-box elements at type 2 genes but not type 1 genes. The TFIIIB complex includes the TATA-binding protein, needed for promoter recognition and Pol III initiation. Type 2 and type 3 genes use alternative assemblies of TFIIIB:BRF1 for type 2 and BRF2 for type 3 genes. Type 3 genes lack an internal A or B box and lack reliance on TFIIIC, relying instead on upstream proximal and distal sequence elements (PSEs and DSEs) and specific factors (OCT1, SNAP and others) for targeting. Notably, type 3 Pol III promoters resemble Pol II genes in their architecture, which have upstream regulatory elements rather than gene-internal elements.

Here we have applied genomics approaches toward the following goals: (i) to define human Pol III transcriptomes by occupancy of the Pol III machinery, (ii) to discover new or alternative Pol III loci, (iii) to classify all Pol III genes by the specialized Pol III machinery present and (iv) to provide new insights regarding the placement and regulation of Pol III genes in chromosomes and chromatin.

RESULTS

Localization of Pol III in HeLa reveals gene classes

To define Pol III transcriptomes, we applied chromatin immunoprecipitation (ChIP) of Pol III machinery to determine occupied loci,

[1]Department of Oncological Sciences, Huntsman Cancer Institute, University of Utah School of Medicine, Salt Lake City, Utah, USA. [2]Howard Hughes Medical Institute, University of Utah School of Medicine, Salt Lake City, Utah, USA. [3]Agilent Technologies, Life Science Solutions Unit, Santa Clara, California, USA. [4]Department of Medicine and Experimental Pathology, University of Utah School of Medicine, Salt Lake City, Utah, USA. Correspondence should be addressed to B.R.C. (brad.cairns@hci.utah.edu).

Received 4 December 2009; accepted 10 March 2010; published online 25 April 2010; doi:10.1038/nsmb.1801

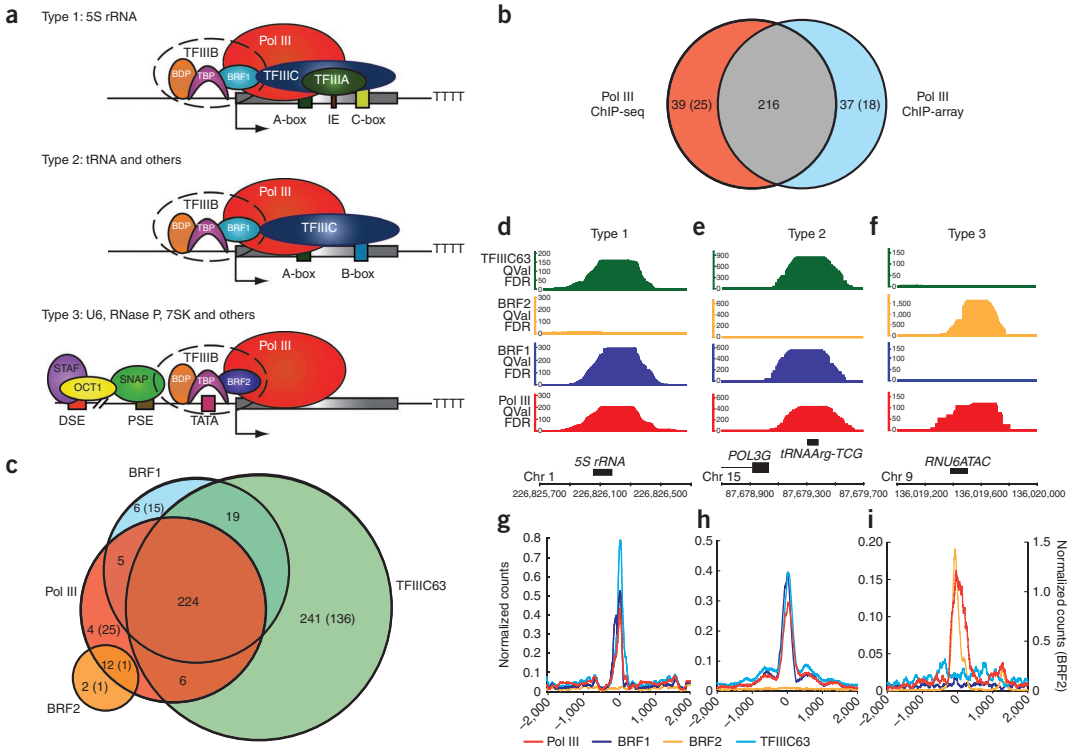

Figure 1 Occupancy analysis of Pol III and associated machinery in HeLa cells. (**a**) Pol III–transcribed genes are classified into three types on the basis of sequence elements and transcription factors. IE, intermediate element. See Introduction for details. (**b**) Comparison of Pol III–enriched regions obtained by ChIP-array (threshold 8.5-fold over background) and ChIP-seq (FDR < 1%). Most sites appearing unique in the ChIP-array can be explained by data thresholding; they are scored as occupied when we lowered the threshold for Pol III in the ChIP-seq format, and they met the high threshold (FDR < 1%) in ChIP-seq experiments with other Pol III factors (TFIIIB or TFIIIC). (**c**) Intersections of Pol III–enriched regions (FDR < 1%) with regions enriched by the basal transcription machinery (BRF1, BRF2 and TFIIIC; FDR < 1%). In the Venn diagram, the numbers outside parentheses denote known annotated Pol III genes, whereas the numbers within parentheses denote previously uncharacterized Pol III targets. (**d**–**f**) Genomic visualization of one random example of each of the three types of Pol III genes. The *y* axis depicts *q* value FDR (QValFDR) significance values, which correspond to *P* values (50 corresponds to $P = 10^{-5}$; 100 corresponds to $P = 10^{-10}$). Values are depicted for Pol III (red), BRF1 (blue), BRF2 (yellow) and TFIIIC63 (green). The physical map (hg18) is plotted on the *x* axis. (**g**–**i**) Class-average maps of Pol III (red), BRF1 (blue), BRF2 (yellow) and TFIIIC63 (turquoise) at type 1 (**g**), type 2 (**h**) and type 3 genes (**i**). The number of read counts at each nucleotide, normalized to the number of genes in the class, is plotted on the *y* axis. The distance from the TSS of the Pol III gene is plotted on the *x* axis. Chr, chromosome.

as RNA sequencing cannot determine all active tDNA loci owing to the small fraction (21%) of uniquely mappable tDNAs (see Online Methods). Thus, Pol III occupancy of the unique flanking region (determined by ChIP coupled with massively parallel sequencing (ChIP-seq) or ChIP followed by complementary DNA microarray hybridization (ChIP-array)) was a proxy measurement of gene activity. We chose HeLa cells for our initial Pol III transcriptome, and we localized RNA Pol III itself (RPC32 subunit) by standard ChIP-array approaches, probing the unique portion of the human genome at ~150–base pair (bp) resolution (Agilent Technologies). A threshold of 8.5-fold enrichment yielded 271 sites bound by Pol III and included the vast majority of formerly verified unique Pol III genes, a few candidate unique loci and approximately half of the predicted tDNAs (**Supplementary Data 1**). With a false discovery rate (FDR) cutoff of 1%, ChIP-seq revealed 257 loci bound by Pol III in HeLa cells, which overlap 255 annotated Pol III genes and 25 unannotated loci (**Table 1**; full data sets in **Supplementary Data 1**). Bound loci occasionally encompass closely linked tDNAs (within 600 bp); for Pol III, 20 bound loci each contain two to four tDNAs. Loci occupied in the ChIP-array experiment largely overlapped with those identified by ChIP-seq ($P < 10^{-7}$; **Fig. 1b**). A small number of Pol III genes reside in nonunique regions (5S, small NF90-associated RNA (snaR) genes and certain tDNAs; **Supplementary Data 1**) but are not included in the analyses below. In summary, the two genomics formats yielded similar Pol III–occupied loci in HeLa cells.

To classify Pol III genes (**Fig. 1a**), we localized BRF1 (types 1 and 2), BRF2 (type 3) and TFIIIC (TFIIIC63 subunit, types 1 and 2, but not type 3) by ChIP-seq in HeLa cells. With an FDR cutoff of 1%, we obtained 242, 16 and 549 occupied loci for BRF1, BRF2 and TFIIIC, respectively. Venn diagrams (**Fig. 1c**), examples (**Fig. 1d**–**f**) and class-average maps (**Fig. 1g**–**i**) reveal two important features. First, BRF1 and BRF2 are mutually exclusive, supporting earlier work on individual genes; here

Table 1 Pol III genes and Pol III–related repeats in the human genome and enrichment with Pol III initiation machinery in HeLa ChIP-seq

Pol III promoter type	Class of RNA	Subclass[a]	Number in human hg18 reference genome[b]	Number and percentage with attribute[c]		Number and percentage occupied with Pol III, BRF1 or BRF2 (FDR < 1%) in HeLa	
Type 1	5S	Consensus	17	17[d]	100.0%	17[e]	100.0%
		5S-related	1,260	175[d]	13.9%	0[e]	0%
Type 2	tRNA	Consensus	513	490[f]	95.5%	242	47.1%
		tRNA pseudogene[g]	172	120[f]	69.8%	2	1.2%
		tRNA-related[g]	1,224	227[f]	18.5%	0	0%
	Alu	Dimer[h]	1,099,242	638,006[f]	58.0%	13	0.001%
		Monomer[h]	90,882	30,301[f]	33.3%	2	0.002%
	MIR	MIR	587,443	65,530[f]	11.5%	1	0.0002%
	snaR	Consensus	21	21[f]	100.0%	21[e]	100.0%
		snaR-related	7	5[f]	71.4%	2[e]	28.5%
	HVG or Vault	Consensus	3	3[f]	100.0%	3	100.0%
		HVG-related	1	1[f]	100.0%	0	0%
	7SL or SRP	Consensus	2	0[f]	0%	1	50%
		7SL-related	954	128[f]	13.4%	0	0%
	BC200	Consensus	1	1[f]	100.0%	1[i]	100.0%
		BC200-related	253	141[f]	55.9%	0	0%
Type 3	Y	Consensus	4	4[j]	100.0%	4	100.0%
		Y-related	1,123	0[j]	0%	0	0%
	U6	Consensus	9	5[j]	55.5%	5	55.5%
		U6-related	1,670	0[j]	0%	0	0%
	7SK	Consensus	1	1[j]	100.0%	1	100.0%
		7SK-related	713	1[j]	0.1%	0	0%
	RNase P	Consensus	1	1[j]	100.0%	1	100.0%
		RNase P–related	1	0[j]	0%	0	0%
	RNase MRP	Consensus	1	1[j]	100.0%	1	100.0%
		RNase MRP–related	6	0[j]	0%	0	0%
	U6atac	Consensus	1	1[j]	100.0%	1	100.0%
		U6atac-related	39	0[j]	0%	0	0%
	$tRNA^{SeC}$	Consensus	3[k]	1[f,j]	33.3%	1[k]	33.3%

[a]'Consensus' subclass is based on high sequence identity (using BLAT, http://genome.ucsc.edu) to the validated RNA, except tRNAs, which are compared to the Genomic tRNA Database (http://gtrnadb.ucsc.edu) and snaRs, which are compared to other studies[31]. [b]Based on UCSC Genome Browser (http://genome.ucsc.edu); tracks 'RNA genes' and RepeatMasker. (http://www.repeatmasker.org) (except for tRNAs and snaRs, see footnote a). [c]Attributes determined with Consensus and Patser programs (http://rsat.ulb.ac.be/rsat; see Online Methods). See **Supplementary Data 1** for consensus matrices. [d]Contains an internal C-box. [e]Mapped allowing multiple alignments with Bowtie (http://bowtie-bio.sourceforge.net; see Online Methods and **Supplementary Data 1**). [f]Contains an internal B-box. [g]'tRNA pseudogene' from the Genomic tRNA Database; 'RNA genes' track; 'tRNA-related' subclass consists of all tRNAs in RepeatMasker track (http://genome.ucsc.edu), not contained in 'Consensus' or 'tRNA pseudogene' subclasses. [h]'Monomer' refers to free left or right element (FLAM or FRAM); 'Dimer' means the Alu has a FLAM and a FRAM. [i]Enriched in Pol III ChIP-array but not ChIP-seq. [j]Contains a TATA (within 50 bp upstream) and PSE (between 100 bp and 25 bp upstream). [k]These are a subset of the tRNAs in the type 2 promoter section.

we show this exclusion genome-wide and reveal all separate type 2 and type 3 genes in HeLa cells. Second, the majority of TFIIIC-bound loci lack Pol III (**Fig. 1c**), an observation that may be noteworthy given the known roles of TFIIIC-only sites in genome organization in lower eukaryotes[8–11], addressed further below. A compilation of gene types and occupancy, including repetitive elements, is provided in **Table 1** and **Supplementary Data 1**. Notably, we verified the single occupied selenocysteine tDNA as the only type 3 tRNA gene in the genome, with clear BRF2 occupancy (**Supplementary Data 1**).

Cell-type variation in Pol III loci

To explore the dynamic and cell type–specific Pol III transcriptome, we next performed ChIP-seq of Pol III in three other cell types: human embryonic kidney HEK 293T cells (bearing adenovirus and T antigen), human foreskin fibroblasts (HFF; immortalized with human telomerase reverse transcriptase (*TERT*) but untransformed) and Jurkat T cells. For comparison, we intersected the top 400 enriched loci from each cell type (**Fig. 2a**), which overlapped 336, 266, 200 or 168 predicted Pol III genes in HEK 293T, HeLa, Jurkat and HFF cells, respectively. Notably, 120 genes are clearly occupied in all four cell types. In addition, HEK 293T cells have a large number (75; see **Fig. 2a**) of unique loci (primarily tDNAs). Region p22.1 of chromosome 6, which harbors the majority of genomic tDNAs, exemplifies cell-type variation (**Fig. 2b**,**c**). Of 24 genes showing variance, nine HEK 293T genes and one HeLa gene (**Supplementary Data 1**) met a stringent threshold for differential occupancy (>38-fold enriched over background in HEK 293T or >14-fold in HeLa; enrichment was <3-fold in other cell types) in a quantitative PCR (qPCR) format. Thus, although the Pol III transcriptomes from these cell types show considerable overlap, cell type–specific Pol III–bound loci do exist. In addition, we observed that three transformed cell lines share a set of 51 genes not occupied in HFF (**Fig. 2a**).

Occupied tDNAs often reside in Pol II promoters

A particularly noteworthy observation was that only a portion of the *in silico*–predicted tDNAs (ranging from ~30% to ~60%) were occupied by Pol III in the different cell lines (52% in HeLa, **Fig. 3a**). This observation does not derive from data thresholding; rather, percentile rank analysis suggests two types of tDNAs, occupied or unoccupied, with variation in the occupied class (HeLa, **Fig. 3b**). This differential occupancy is not a mapping artifact, as most tDNAs lacking Pol III enrichment can be mapped at >85% efficiency (**Supplementary Fig. 1**). These occupancy differences (occupied compared with unoccupied) are also not explained by predicted TFIIIC affinity, as

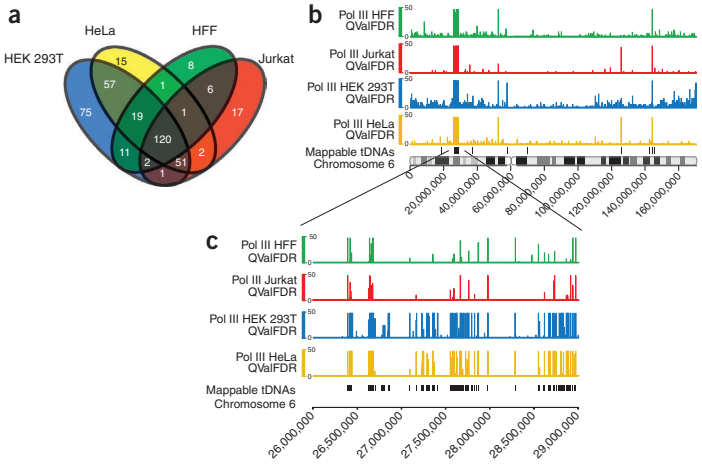

Figure 2 Differential Pol III occupancy in various cell types. (**a**) Intersection analysis of the known Pol III–occupied genes between the four cell types. Pol III–bound regions (top 400 enriched loci) were filtered for unannotated regions, and only known genes were used for the analysis. Total numbers of genes for HEK 293T, HeLa, Jurkat and HFF were 336, 266, 200 and 168, respectively. (**b**) A depiction of chromosome 6 showing Pol III occupancy in HeLa (yellow), HEK 293T (blue), Jurkat (red) and HFF (green). Bottom, mappable tDNAs. (**c**) Detail of a tDNA cluster in 6p22.1 showing Pol III occupancy in the four cell types. Note that many tDNAs are differentially enriched with Pol III in different cell types.

MEME[12] analysis revealed nearly identical A- and B-box elements at occupied and unoccupied tDNAs in HeLa cells (**Fig. 3c**).

Notably, in HeLa cells, 53 occupied Pol III genes (19%) reside just upstream (within 2 kilobases (kb)) of an annotated Pol II gene, a significant enrichment in location ($P < 10^{-7}$). In contrast, only three predicted tDNAs within 2 kb of a Pol II gene were unoccupied by Pol III, and two of those three tDNAs flank Pol II genes that are inactive in HeLa cells. Moreover, histogram plots of all occupied tDNAs residing near Pol II genes reveal a pair of peaks at −300 and −900 (**Fig. 3d**), reflecting the relatively common presence of two tandem tDNAs (~600 bp apart) just upstream of a Pol II gene. In contrast, tDNAs lacking Pol III do not cluster near Pol II genes (**Fig. 3d**). Finally, adjacent Pol II and Pol III genes are often (71%) divergent (see Discussion).

Occupied tDNAs coincide with regions of active chromatin

Intersection analyses revealed Pol III coincident with Pol II protein, monomethylated and trimethylated histone H3 Lys4 (H3K4me1 and H3K4me3), H2A.Z, CTCF and H3.3, at levels that were significant ($P < 10^{-3}$) and that exceeded our enrichment cutoff of ten-fold above random (**Supplementary Data 2** and ChIP-seq data sets from other studies[13–16]). Notably, the extent of Pol III occupancy scaled with the levels of regional Pol II and active chromatin (**Fig. 4a–h**). To reveal this, we separated Pol III–occupied loci into four classes: the top 50, middle 50 and bottom 50 occupied loci (remaining above the FDR cutoff of 1%), and Pol III–unoccupied tDNAs. We compared occupancy of these four classes of loci to levels of Pol II, chromatin modifications and chromatin factors (class-average map, centered on the Pol III gene transcription start site (TSS)). The levels of Pol II, positive histone modifications and H2A.Z all scaled with Pol III occupancy. Also, CCCTC-binding factor (CTCF) was observed at a small subset (10%) of the tDNAs with the highest Pol III occupancy. In contrast, repressive H3K27me3 was more prevalent at predicted tDNAs lacking occupancy (below our cutoff) and was not correlated with Pol III (**Fig. 4f**).

The correlations described above would be expected if all tDNAs simply resided within active annotated Pol II promoters. However,

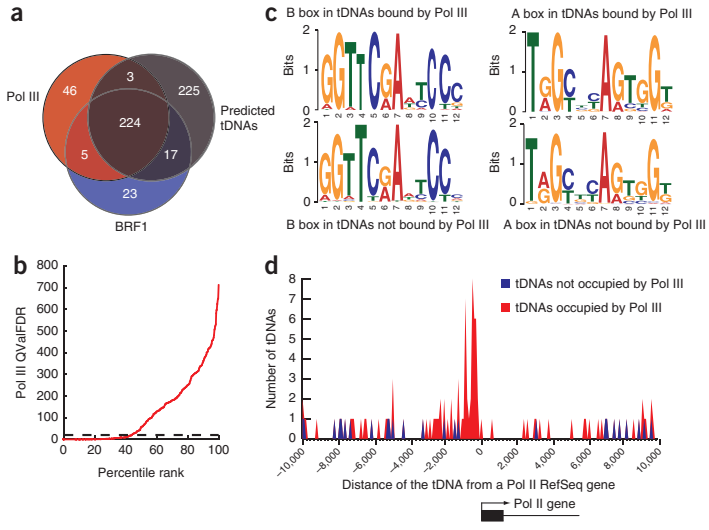

Figure 3 Genomic features of Pol III–occupied and unoccupied tDNAs in HeLa cells. (**a**) Venn diagram illustrating that predicted tDNAs are bound by Pol III or initiation factors (BRF1). These 469 tDNAs represent 467 mappable, predicted tDNAs plus two Pol III–enriched tRNA pseudogenes. (**b**) All predicted mappable tDNAs were ranked by their Pol III occupancy (*x* axis) and plotted against Pol III QValFDR (*y* axis) to show that ~50% of tDNAs are unoccupied by Pol III. The dotted line represents the FDR cutoff of 1% (QValFDR = 20). (**c**) Sequence discovery (MEME)[12] analysis of the regulatory sequence elements (A-box and B-box) of tDNAs bound or not bound by Pol III. Note that the sequences are nearly identical between the two classes of tDNAs. (**d**) Pol III–bound (red) or unbound tDNAs (blue) were clustered on the basis of their distance from the nearest Pol II gene TSS in 100-bp bins. Note that Pol III–bound tDNAs cluster within 1 kb of the Pol II gene TSS ($P < 10^{-7}$), whereas the unbound tDNAs show no such clustering. A tDNA was classified as Pol III bound if it was occupied by RPC32, BRF1 or both. A promoter was defined as being ±2 kb from a Pol II gene TSS.

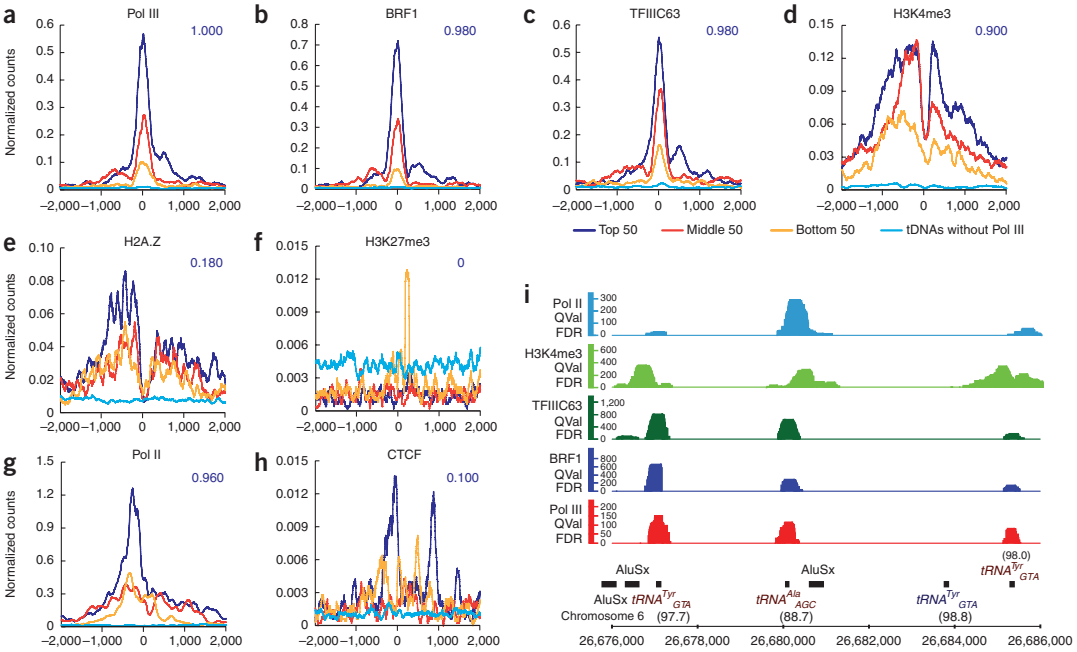

Figure 4 Chromatin features at Pol III–bound tDNAs in HeLa cells. (**a**–**h**) We binned Pol III–bound genes into three categories—top 50 (blue), middle 50 (red) and bottom 50 (yellow)—on the basis of their Pol III levels, and plotted class-average maps for various factors and chromatin marks[13–16]. Class-average plots of factors at tDNAs without Pol III (turquoise) serve as negative controls. The distance from the Pol III TSS is plotted on the *x* axis, and the number of read counts at each nucleotide, normalized to the number of regions in the class, is plotted on the *y* axis. The fraction of each of these factor-bound regions intersecting with the top-50 class is indicated in blue at top right corner of each graph. (**i**) Example of a genomic locus showing a tDNA cluster with differential occupancy of Pol III, BRF1, TFIIIC63, H3K4me3 and Pol II. Note that the $tRNA^{Tyr}$ gene lacking Pol III machinery also lacks Pol II and H3K4me3. The percent mapping efficiency of each of the tRNA genes is indicated in parentheses (see Online Methods).

most tDNAs occupied by Pol III actually reside outside annotated Pol II gene promoters (201, or 82%, in HeLa cells). Therefore, we separated occupied Pol III genes into two classes—those within annotated Pol II promoters, and those outside—and again examined how Pol III occupancy scaled with Pol II and chromatin attributes. Notably, active tDNAs outside annotated Pol II promoters still strongly correlated with adjacent Pol II and chromatin modifications typical of a Pol II promoter or enhancer (including H3K4me1; **Supplementary Fig. 2** and **Supplementary Data 2**). In contrast, unoccupied tDNAs lack adjacent Pol II or active chromatin (**Fig. 4d–h**), and instead bear higher levels of H3K27me3 (**Fig. 4f**). An example of this partitioning is shown in **Figure 4i**, where the two Pol III–occupied genes encoding $tRNA^{Tyr}_{GTA}$ genes also bear Pol II and active chromatin, whereas the single Pol III–unoccupied gene encoding $tRNA^{Tyr}_{GTA}$ lacks these factors or attributes. Thus, active tDNAs outside of annotated Pol II promoters are found in a chromatin region that resembles an active Pol II gene promoter or enhancer. We note that type 3 genes (BRF2-containing) show active chromatin profiles similar to those of type 2 genes.

We found that a considerable fraction (~30%) of Pol III–occupied loci reside within CpG islands—a highly significant overlap ($P < 10^{-6}$)—and that a striking correlation exists between Pol III occupancy and CpG content at Pol II promoters. Others have separated promoters into three types on the basis of their CpG density[17]: high-CpG promoters (HCPs), intermediate-CpG promoters (ICPs) and low-CpG promoters (LCPs). Notably, Pol III–occupied promoters intersect well with HCPs (typically associated with constitutively active genes) and moderately with ICPs, and are anticorrelated with LCPs (**Supplementary Data 2**). Together with the results above, this indicates that Pol III occupancy is enabled by active Pol II promoter–like chromatin.

Jurkat and HeLa cells show similar Pol III chromatin

Genome-wide chromatin maps in HeLa and primary $CD4^+$ T cells are extensive, whereas those in Jurkat, HFF and HEK 293T cells are lacking. Jurkat T cells are similar to $CD4^+$ T cells (Jurkat is also a $CD4^+$ T cell[18]), though proliferative and (in our hands) technically more amenable to Pol III occupancy analysis. ChIP-seq of Pol III in Jurkat cells yielded 211 occupied loci (FDR < 10%), which overlap 182 annotated genes. This list had high overlap (88%) with the list from HeLa cells and showed similar trends; Pol III–occupied loci were correlated with (and scaled with) Pol II and active Pol II promoter-like chromatin (**Fig. 5a**, **Supplementary Figs. 3** and **4**, and chromatin ChIP-seq data sets from other studies[19–22]), and anticorrelated with additional repressing modifications (for example, H3K36me3; **Supplementary Data 2**). However, with resting $CD4^+$ T cells, the correlations of Pol III with adjacent Pol II were weaker, and correlations of Pol III with adjacent H2A.Z were stronger, possibly reflecting the 'poised' nature of many genes in resting $CD4^+$ cells. Consistent with this notion, Pol II levels rise and H2A.Z levels fall

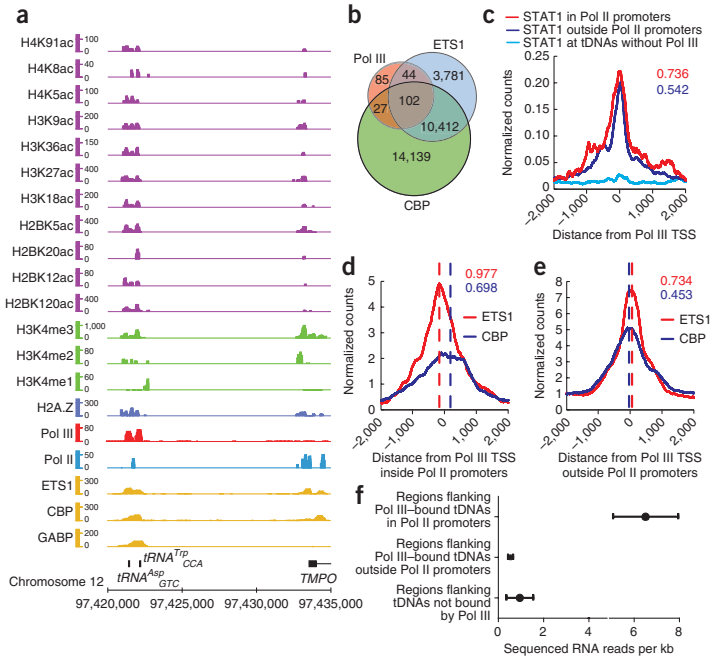

Figure 5 Chromatin marks and factors associated with Pol III–bound regions in Jurkat cells. (**a**) Example of a genomic locus showing a tDNA bound by Pol III (red) in Jurkat cells. Also shown are active acetylation (purple) and methylation (green) marks, H2A.Z (blue), Pol II (turquoise) and transcription factors (yellow). This putative enhancer is ~12 kb upstream of a Pol II gene TSS. Chromatin and factor ChIP-seq are from other studies[19–22]. (**b**) Intersection of Pol III–bound regions (FDR < 10%) with regions bound by ETS1 (FDR < 1%; filtered for regions overlapping DNase I hypersensitivity in CD4$^+$ cells[41]) and CBP (FDR < 1%) in Jurkat cells. (**c**) Pol III–bound genes in HeLa (FDR < 1%) were binned into those inside (red) or outside (blue) annotated Refseq promoters, and a class-average map of STAT1 was plotted; tDNAs without Pol III (turquoise) serve as a negative control. The numbers denote the fraction of total Pol III genes occupied by STAT1 for loci either inside (red) or outside (blue) Refseq promoters. (**d**,**e**) Class-average maps of ETS1 (red) and CBP (blue) at Pol III–bound genes inside (**d**) or outside (**e**) Refseq promoters in Jurkat cells. The red and blue dashed lines indicate approximate peaks of the corresponding factors. The fractions of Pol III regions intersecting with ETS1 (FDR < 1%) and CBP (FDR < 1%) in Jurkat are indicated in red and blue, respectively. (**f**) Average score of HeLa RNA-seq read per kb for each 1-kb region flanking tDNAs. Error bars represent s.e.m. Note that transcripts are seen near tDNAs in Pol II promoters (from neighboring Pol II genes), but not near tDNAs outside Pol II promoters.

adjacent to tDNAs when CD4$^+$ T cells are activated (**Supplementary Data 2**, and Pol II and H2AZ data from other studies[23]).

Occupied Pol III loci correlate with STAT1 and ETS1

Our results prompt two questions regarding the establishment of Pol III–correlated chromatin: (i) whether there are specific DNA binding factors or activators that colocalize with Pol III–occupied regions, and (ii) whether the unannotated loci bearing Pol III and Pol II might represent enhancers or enhancer-like regions. We compared our data sets to the extensive transcription factor binding profiles in T cells (Jurkat and CD4$^+$)—except for STAT1, for which binding profiles[13,24] in HeLa were directly compared. Certain transcription factors have been linked to Pol III regulation (p53, c-MYC and RB)[25,26], but the lack of genome-wide ChIP-seq data sets prevented us from comparing their binding profiles with our data. However, we found a notable overlap between Pol III occupancy and the general transcription factors STAT1 (ref. 13) (in HeLa, FDR < 1%, overlap 161 of 278 loci, $P < 10^{-5}$) and ETS1 (ref. 22) (in Jurkat, overlap 144 of 182 loci, $P < 10^{-5}$; **Fig. 5b**). Moreover, using the list of STAT1-occupied sites generated in ref. 24 (FDR < 0.1%), we derived an overlap of 254 of 278 loci. Notably, STAT1 binding sites reside very near the Pol III gene TSS, for Pol III genes both within and outside of annotated Pol II gene promoters (**Fig. 5c** and **Supplementary Fig. 4f**). ETS1 has different properties at promoters compared with enhancers[22]. For example, sites within Pol II promoters are typically consensus sites, and a feature of promoter-localized ETS1 is that it lacks precise co-alignment with CREB-binding protein (CBP) occupancy. In contrast, ETS1 sites at enhancers show considerable variation from consensus, and they often physically partner with other transcription factors (for example, RUNX1). Also, ETS1 at enhancers is aligned more precisely with CBP occupancy[22]. In keeping with these different properties at promoters and enhancers, we found that Pol III–occupied annotated promoters bearing ETS1 are typically consensus sites (data not shown) and lack precise alignment with CBP (**Fig. 5d**). In contrast, the tDNAs not adjacent to annotated Pol II genes coincide with enhancer-like ETS1 sites (data not shown) that are well aligned with CBP (**Fig. 5e**). This raises the possibility that particular enhancer-binding proteins such as STAT1 and ETS1 help nucleate open chromatin at promoters or enhancers, which then promotes Pol III occupancy (see Discussion). We also saw marked overlap with the transcription factor SRF (FDR < 1%, 52 of 182 loci) and moderate overlap with GABP (FDR < 1%, 29 of 182 loci). However, we observed little overlap with NRSF (FDR < 1%, 10 of 182 loci) in Jurkat cells (**Supplementary Fig. 4g–i** and data from other studies[21]).

Enhancers strongly correlate with three chromatin attributes[27]—H3K4me1, acetylation of H3K27 (H3K27ac) and DNase I hypersensitivity—for which maps are available in CD4$^+$ T cells or HeLa cells. We saw highly significant overlap between Pol III occupancy at unannotated regions and the presence of H3K4me1 ($P < 10^{-5}$) and H3K27ac ($P < 10^{-5}$) (**Supplementary Data 2** and **Supplementary Fig. 3b**,**i**,**r**). Furthermore, of the 150 occupied tDNAs in Jurkat cells, 145 overlap DNase I–hypersensitive sites ($P < 10^{-5}$), whereas only 96 of the 321 unoccupied tDNAs do. Notably, 59 of those hypersensitive sites become enriched with Pol III in HeLa cells.

Occupied tDNAs correlate with enhancer-like chromatin, which typically does not produce RNA. However, the presence of Pol II at these loci prompted us to address whether transcription by Pol II occurs from these enhancer-like loci. We performed RNA sequencing

(RNA-seq) of total RNA in HeLa and quantified reads in the region flanking the tDNAs. This region contains the peak of Pol II (**Supplementary Fig. 2d**) but not the tDNA itself (or Pol III), so that reads from only Pol II were compiled. At these tDNAs in enhancer-like chromatin, we did not generally observe RNA transcripts in the aforementioned region (**Fig. 5f**). This suggests that 'active' chromatin modifications, including those involved in Pol II initiation (for example, H3K4me3), but not Pol II transcripts *per se*, best correlate with Pol III occupancy.

Previously uncharacterized Pol III genes and miRNAs

ChIP-seq data yielded 42 candidates for previously uncharacterized Pol III loci in HeLa cells. From these, we tested 13 by qPCR; ten were enriched at least 3.5-fold above background for Pol III occupancy. One noteworthy unannotated locus is about 2 kb upstream of the *SLC7A2* TSS, which shows nearby STAT1, H3K4me3, Pol II and a transcript by RNA-seq (**Supplementary Fig. 5a–c**). Another candidate locus resides on chromosome 5 among multiple repeats. Here, BRF2 and Pol III colocalized over an L1M5 long interspersed nuclear element (LINE), with STAT1, Pol II and H3K4me3 nearby (**Supplementary Fig. 5d–f**). This could represent a previously uncharacterized type 3 gene; there are only 14 type 3 genes currently known. We also identified one MIR highly enriched with Pol III, BRF1 and TFIIIC in the first intron of *POLR3E* (**Supplementary Fig. 5g**,**h**). These positives, in addition, include other loci in promoters of Pol II–transcribed genes, such as *ADARB1*, *FZR1* and the U1 small nuclear RNA gene, or near other retroviral elements (for example, MER41C LTR) (**Supplementary Fig. 6a**,**b**). Furthermore, we found six annotated tRNA pseudogenes enriched at high levels in various cell types, and we verified two by qPCR (**Supplementary Fig. 6c** and **Supplementary Data 1**). Finally, we also found 17 Pol III genes within Pol II transcriptional units (mostly in introns; data not shown).

For repetitive regions, we applied mapping algorithms that allow multiple alignments (Bowtie; http://bowtie-bio.sourceforge.net), which revealed Pol III enrichment (and often enrichment of other Pol III factors; see **Supplementary Data 1**) at snaR-class genes, at all of the consensus 5S rDNA genes on chromosome 1 (but no other 5S-related genes), at multiple Alu elements and at 35 tDNAs that map inefficiently. However, the human papillomavirus 18 and 45S rDNA loci were not occupied.

Pol III has been reported to transcribe multiple miRNAs on the chromosome 19 miRNA cluster (C19MC)[28], driven by Alu promoters in HEK 293T cells, which would represent the first example, to our knowledge, of Pol III–driven miRNAs. However, after remapping our reads for HeLa, HEK 293T and HFF, allowing multiple alignments, we saw no enrichment of Pol III at any region (or miRNA) in this highly repetitive cluster (data not shown), a negative result supported by recent evidence showing transcription of C19MC by Pol II instead[29]. Another study[30] supports two additional Pol III–transcribed loci, *SNAR-A* (ref. 31; also known as *CBL-1*) and *MIR886* (ref. 32; also known as *CBL-3*), but the authors did not test for occupancy by Pol III. Here we show clear occupancy of both loci (**Supplementary Fig. 7**); we also observed transcripts lacking a 5′ cap derived from the *MIR886* locus by RNA-seq (see Online Methods and **Supplementary Fig. 7d**). To our knowledge, this is the first direct evidence for occupancy and transcription by the Pol III machinery of a miRNA in mammals.

TFIIIC-only and TFIIIB-TFIIIC sites

Given the role in yeast chromatin organization of loci bound by TFIIIC but not Pol III, BRF1 or BRF2 (refs. 8–11), we identified 307 such loci in HeLa cells. TFIIIC-only sites partition into two classes: loci adjacent to Alu or MIR repeats, or both (181), and those that lack repeats (126). Certain loci were adjacent to both an MIR and an Alu element, which accounts for the higher number of total TFIIIC-only loci (377) depicted in **Figure 1c**. Notably, 101 TFIIIC-only loci reside within 2 kb of the TSS of an annotated Pol II gene, 60% of which have HCP Pol II promoters, a highly significant enrichment ($P < 10^{-5}$), whereas 206 reside in unannotated regions (**Supplementary Fig. 8a**). Those within annotated Pol II genes show correlations with active promoter chromatin (**Supplementary Fig. 8b–i** and **Supplementary Data 2**). Those in unannotated regions also show strong correlations with active chromatin, though weaker than with annotated Pol II genes (**Supplementary Data 2**). Notably, TFIIIC-only sites near Alu and MIR elements typically have a B-box (164 of 181) and bear high levels of H3K4me1, H3K4me3 and Pol II, whereas those distal from repeats are generally void of positive marks and typically lack a consensus B-box element (27 of 126 have a B-box) (**Supplementary Fig. 8b–i**), raising the possibility that TFIIIC cooperates with other factors for binding at these loci. MEME[12] and TOMTOM[33] analysis revealed the consistent presence of a G/A-rich site with significant ($P = 0.00028$) similarity to the binding site of Kruppel-like factor 4 (KLF4; **Supplementary Fig. 8j**). Nineteen sites in our HeLa data sets contain both TFIIIB (BRF1) and TFIIIC, but lack Pol III enrichment (at our threshold of FDR < 1%). However, the majority (14 of 19) of these sites become enriched with Pol III in HEK 293T cells, or in HeLa cells if compared with a lower threshold (FDR < 5%, Pol III ChIP-seq) or our Pol III ChIP-array data set (data not shown). At present, it is not clear whether these sites are truly different in their mode of Pol III recruitment or they simply represent sites near our occupancy cutoff thresholds.

DISCUSSION

Our data sets and analyses address the scope and regulation of human RNA Pol III transcriptomes, providing multiple insights (**Fig. 6**). First, we observed the close proximity of Pol III genes to Pol II genes genome-wide. This result is in keeping with previous work at the Pol III–transcribed U6 small nuclear RNA gene (a type 3 gene), which has a proximal Pol II that assists in Pol III expression[34]. Second, we show genome-wide a marked overlap of Pol III with active chromatin. Previous work at U6 supports the notion that nearby chromatin remodeling promotes U6 expression[35], and our work extends this concept genome-wide to all type 2 and type 3 genes, and also to many active histone modifications and compositions. Notably, ~81% of occupied Pol III genes reside at regions outside of annotated Pol II genes, yet those regions bear high levels of H3K4me3 and Pol II protein, properties typical of promoters. Notably, these unannotated regions also have properties of enhancers[27], as they contain H3K4me1 and H3K27ac, and overlap with enhancer-binding proteins and DNase I–hypersensitive sites. In addition, we found few, if any, transcripts adjacent to most of these unannotated Pol II peaks, and those we found generally lack a long downstream open reading frame. Thus, it is not entirely clear whether one should consider these regions new unannotated promoters or instead a subclass of enhancers that contain Pol II and H3K4me3, resembling Pol II 'poised' promoters. We speculate that the promoter-like chromatin formed near either 'poised' or active Pol II might be sufficient for enabling Pol III occupancy. In addition, it will be of interest to determine whether these unannotated promoters or enhancers produce a functional transcript in particular cell types, or whether they are typical enhancers, activating another Pol II gene in the larger region. Regardless, the overlap of Pol III–occupied tDNAs with active chromatin is striking. Notably, Pol III occupancy scaled with active chromatin marks and proximal Pol II, but not with RNA transcript levels for the Pol II gene, emphasizing the

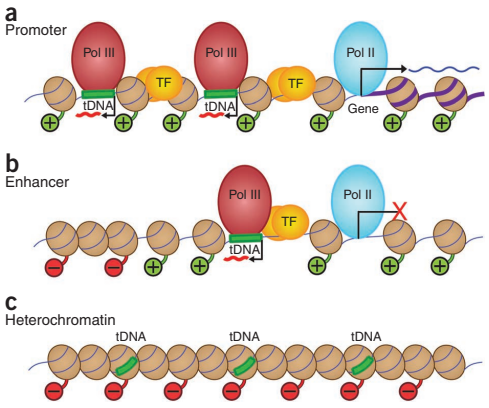

Figure 6 Model depicting how chromatin features affect Pol III recruitment at three different regions: promoters, enhancer-like promoters and heterochromatin. (**a**) Chromatin features at an annotated Pol II gene promoter, where ~20% of active tDNAs with Pol III (red spheroid) reside, typically in a divergent orientation and about 300–400 bp from the peak of Pol II. This region contains transcription factors (TF; yellow spheres, transcription factors and enhancer-binding proteins) and a large region of active chromatin, where nucleosomes (brown spheroids) have histone tails with positive or active modifications (green histone tails with '+' balls). Active tDNAs are frequently found in pairs (shown) or clusters. At promoters, Pol II produces an RNA transcript from the annotated gene (purple thick DNA). (**b**) About 80% of active tDNAs are located distal to annotated Pol II promoters, and these regions have features of both Pol II promoters and enhancers. They contain active local chromatin, have Pol II nearby and have TFs close to the Pol III gene. Although Pol II is present and there is evidence of Pol II initiation (H3K4me3), stable transcripts by Pol II are not detected (although it cannot be ruled out that unstable transcripts are produced). Outside of the local active region, we saw facultative heterochromatin, represented by red histone tails with '–' balls. (**c**) Inactive tDNAs lack active chromatin marks, TFs and Pol II, and instead are associated with repressive chromatin marks (red histone tails with '–' balls), suggesting a more tightly packed chromatin environment that is inaccessible to Pol III machinery.

connection of Pol III occupancy with active chromatin. Finally, DNA hypomethylation may also contribute to the active chromatin state, as occupied Pol III genes correlated with regions having high CpG content (which are typically unmethylated) and as STAT1 consensus sites are strongly correlated with DNA hypomethylation[36].

Occupied Pol III genes often reside 300–900 bp upstream of the Pol II TSS—close enough to overlap with promoter-proximal chromatin, but generally not within the promoter-proximal region where the Pol II basal machinery assembles. Furthermore, tDNAs residing in Pol II promoters are typically transcribed away from the Pol II gene (divergent orientation), with a significant bias ($P = 0.006$). We suggest that these properties allow the Pol III gene to benefit from promoter chromatin dynamics while avoiding interference with the transcription of the Pol II gene itself. Previous Pol III transcriptomes in *Saccharomyces cerevisiae*[10,37,38] have shown that virtually all predicted Pol III genes (including tDNAs) are occupied by Pol III, providing evidence against appreciable Pol III regulation by chromatin or position relative to Pol II genes. Moreover, *S. cerevisiae* lacks key modifications of vertebrate heterochromatin (H3K9me3, H3K27me3 and DNA methylation), suggesting that Pol III in human cells may encounter chromatin obstacles not present in lower yeasts.

Our work also reveals moderate variation in Pol III occupancy among cell types, and cell type–'specific' occupancy of a small number of loci. Here specificity is defined using a stringent criterion, but very low occupancy of these 'specific' loci may exist in other cell types. A key issue is the basis for cell-type variation and specificity. One possibility is that as each cell type varies its repertoire of Pol II gene transcription and active enhancers, the Pol III genes that overlap the permissive chromatin gain access to the Pol III machinery. According to this model, Pol III relies on both general Pol II transcription factors and cell type–specific factors to create open or active chromatin. Although active chromatin may gate Pol III access, it does not constitute all of Pol III regulation: the activity of occupied Pol III genes is probably still regulated by other factors such as the general Pol III repressor MAF1 (ref. 39). Furthermore, we emphasize that although these models are based on extensive sets of strong correlations, genetic experiments are required to determine their dependency relationships.

Notably, tDNAs are thought to have expanded in the genome via retrotransposition[40], and retrotransposons often insert in regions of open chromatin. One interpretation of our data is that the juxtaposition of active Pol III genes (~300) with active Pol II chromatin is largely a consequence of this initial accessibility during transposition, which would imply that these regions were accessible in the germline at some point during evolution. However, there are an additional ~1,396 tRNA-derived elements in the genome, and these are generally not occupied by Pol III machinery (~0.1% occupied). Furthermore, as a class these elements are not coincident with active chromatin (data not shown), raising the possibility that transposition may have occurred in the germline and placed these elementsinto inactive chromatin, with inactive chromatin preventing their subsequent expression and contribution to fitness, allowing sequence drift. Alternatively, it may be that the transposition placed them into active chromatin, but these regions were later converted into heterochromatin, with similar consequences. Regardless, we observed active chromatin coincident with active Pol III genes and not with tRNA-derived elements.

In addition, our work reveals many new Pol III–occupied loci in multiple cell types, and these loci also require functional work *in vivo*. For the three new loci clearly enriched with Pol III machinery (**Supplementary Fig. 5**), we propose names that include a 'P3' (Pol III) designation: for the MIR in the *POLR3E* intron, *MIRP3*; for the chromosome 8 locus conserved in primates, *CPP3*; for the LINE L1M5 locus, *L1M5P3*. Furthermore, we reveal the transcription of a miRNA, clarifying and extending earlier work[30,32]. It will be of interest to identify the Pol III transcriptomes of pluripotent cell lines or early embryos to determine whether additional noncoding RNAs are produced by Pol III.

METHODS

Methods and any associated references are available in the online version of the paper at http://www.nature.com/nsmb/.

Accession codes. Gene Expression Omnibus: GSE20309 (all ChIP-seq data) and GSE20609 (Pol III ChIP-array data).

Note: Supplementary information is available on the Nature Structural & Molecular Biology website.

ACKNOWLEDGMENTS

We thank D. Ayer and S. Lessnick at the Huntsman Cancer Institute for cells, B. Dalley for his expertise in Illumina sequencing, D. Nix for suggestions for ChIP-seq analysis and R. Roeder (Rockefeller University) for the gift of anti-RPB90 antibody. Financial support was from the Howard Hughes Medical Institute (HHMI; supplies and genomics resources), the US National Institutes of Health (grants GM38663 to B.J.G., CA42014 to the Huntsman Cancer Institute for

support of core facilities and CA63640 to C.H.H.), the Huntsman Cancer Institute and Huntsman Cancer Foundation and the Agilent Technologies Foundation (supplies). B.R.C. is an investigator with the HHMI.

AUTHOR CONTRIBUTIONS

B.R.C. and A.J.O., overall scope and design; A.J.O., overall experimental execution; D.N.R. and A.W., ChIP-array experiments; C.A.N. and C.H.H., cap-purified RNA; P.A.C., qPCR; P.C.H., K.J.C. and B.J.G., ETS1 and CBP data sets and analysis; A.J.O., R.K.A. and B.R.C., data analysis and interpretation; A.J.O. and R.K.A., figures, tables and data organization. B.R.C. and A.J.O. wrote the manuscript, with comments from all authors.

COMPETING FINANCIAL INTERESTS

The authors declare no competing financial interests.

Published online at http://www.nature.com/nsmb/.
Reprints and permissions information is available online at http://npg.nature.com/reprintsandpermissions/.

1. White, R.J. *RNA Polymerase III Transcription* (Springer-Verlag, New York, 1998).
2. Dieci, G., Fiorino, G., Castelnuovo, M., Teichmann, M. & Pagano, A. The expanding RNA polymerase III transcriptome. *Trends Genet.* **23**, 614–622 (2007).
3. White, R.J. RNA polymerases I and III, non-coding RNAs and cancer. *Trends Genet.* **24**, 622–629 (2008).
4. Marshall, L. & White, R.J. Non-coding RNA production by RNA polymerase III is implicated in cancer. *Nat. Rev. Cancer* **8**, 911–914 (2008).
5. Willis, I.M. RNA polymerase III. Genes, factors and transcriptional specificity. *Eur. J. Biochem.* **212**, 1–11 (1993).
6. Geiduschek, E.P. & Kassavetis, G.A. The RNA polymerase III transcription apparatus. *J. Mol. Biol.* **310**, 1–26 (2001).
7. Schramm, L. & Hernandez, N. Recruitment of RNA polymerase III to its target promoters. *Genes Dev.* **16**, 2593–2620 (2002).
8. Noma, K., Cam, H.P., Maraia, R.J. & Grewal, S.I. A role for TFIIIC transcription factor complex in genome organization. *Cell* **125**, 859–872 (2006).
9. Simms, T.A. *et al.* TFIIIC binding sites function as both heterochromatin barriers and chromatin insulators in *Saccharomyces cerevisiae*. *Eukaryot. Cell* **7**, 2078–2086 (2008).
10. Moqtaderi, Z. & Struhl, K. Genome-wide occupancy profile of the RNA polymerase III machinery in *Saccharomyces cerevisiae* reveals loci with incomplete transcription complexes. *Mol. Cell. Biol.* **24**, 4118–4127 (2004).
11. Valenzuela, L., Dhillon, N. & Kamakaka, R.T. Transcription independent insulation at TFIIIC-dependent insulators. *Genetics* **183**, 131–148 (2009).
12. Bailey, T.L. & Elkan, C. Fitting a mixture model by expectation maximization to discover motifs in biopolymers. *Proc. Int. Conf. Intell. Syst. Mol. Biol.* **2**, 28–36 (1994).
13. Rozowsky, J. *et al.* PeakSeq enables systematic scoring of ChIP-seq experiments relative to controls. *Nat. Biotechnol.* **27**, 66–75 (2009).
14. Robertson, A.G. *et al.* Genome-wide relationship between histone H3 lysine 4 mono- and tri-methylation and transcription factor binding. *Genome Res.* **18**, 1906–1917 (2008).
15. Jin, C. *et al.* H3.3/H2A.Z double variant-containing nucleosomes mark 'nucleosome-free regions' of active promoters and other regulatory regions. *Nat. Genet.* **41**, 941–945 (2009).
16. Cuddapah, S. *et al.* Global analysis of the insulator binding protein CTCF in chromatin barrier regions reveals demarcation of active and repressive domains. *Genome Res.* **19**, 24–32 (2009).
17. Weber, M. *et al.* Distribution, silencing potential and evolutionary impact of promoter DNA methylation in the human genome. *Nat. Genet.* **39**, 457–466 (2007).
18. Koka, P. *et al.* Increased expression of CD4 molecules on Jurkat cells mediated by human immunodeficiency virus tat protein. *J. Virol.* **62**, 4353–4357 (1988).
19. Barski, A. *et al.* High-resolution profiling of histone methylations in the human genome. *Cell* **129**, 823–837 (2007).
20. Wang, Z. *et al.* Combinatorial patterns of histone acetylations and methylations in the human genome. *Nat. Genet.* **40**, 897–903 (2008).
21. Valouev, A. *et al.* Genome-wide analysis of transcription factor binding sites based on ChIP-Seq data. *Nat. Methods* **5**, 829–834 (2008).
22. Hollenhorst, P.C. *et al.* DNA specificity determinants associate with distinct transcription factor functions. *PLoS Genet.* **5**, e1000778 (2009).
23. Barski, A. *et al.* Chromatin poises miRNA- and protein-coding genes for expression. *Genome Res.* **19**, 1742–1751 (2009).
24. Robertson, G. *et al.* Genome-wide profiles of STAT1 DNA association using chromatin immunoprecipitation and massively parallel sequencing. *Nat. Methods* **4**, 651–657 (2007).
25. Felton-Edkins, Z.A. *et al.* Direct regulation of RNA polymerase III transcription by RB, p53 and c-Myc. *Cell Cycle* **2**, 181–184 (2003).
26. Gomez-Roman, N., Grandori, C., Eisenman, R.N. & White, R.J. Direct activation of RNA polymerase III transcription by c-Myc. *Nature* **421**, 290–294 (2003).
27. Heintzman, N.D. *et al.* Histone modifications at human enhancers reflect global cell-type-specific gene expression. *Nature* **459**, 108–112 (2009).
28. Borchert, G.M., Lanier, W. & Davidson, B.L. RNA polymerase III transcribes human microRNAs. *Nat. Struct. Mol. Biol.* **13**, 1097–1101 (2006).
29. Bortolin-Cavaille, M.L., Dance, M., Weber, M. & Cavaille, J. C19MC microRNAs are processed from introns of large Pol-II, non-protein-coding transcripts. *Nucleic Acids Res.* **37**, 3464–3473 (2009).
30. Mrazek, J., Kreutmayer, S.B., Grasser, F.A., Polacek, N. & Huttenhofer, A. Subtractive hybridization identifies novel differentially expressed ncRNA species in EBV-infected human B cells. *Nucleic Acids Res.* **35**, e73 (2007).
31. Parrott, A.M. & Mathews, M.B. Novel rapidly evolving hominid RNAs bind nuclear factor 90 and display tissue-restricted distribution. *Nucleic Acids Res.* **35**, 6249–6258 (2007).
32. Landgraf, P. *et al.* A mammalian microRNA expression atlas based on small RNA library sequencing. *Cell* **129**, 1401–1414 (2007).
33. Gupta, S., Stamatoyannopoulos, J.A., Bailey, T.L. & Noble, W.S. Quantifying similarity between motifs. *Genome Biol.* **8**, R24 (2007).
34. Listerman, I., Bledau, A.S., Grishina, I. & Neugebauer, K.M. Extragenic accumulation of RNA polymerase II enhances transcription by RNA polymerase III. *PLoS Genet.* **3**, e212 (2007).
35. Yuan, C.C. *et al.* CHD8 associates with human Staf and contributes to efficient U6 RNA polymerase III transcription. *Mol. Cell. Biol.* **27**, 8729–8738 (2007).
36. Straussman, R. *et al.* Developmental programming of CpG island methylation profiles in the human genome. *Nat. Struct. Mol. Biol.* **16**, 564–571 (2009).
37. Roberts, D.N., Stewart, A.J., Huff, J.T. & Cairns, B.R. The RNA polymerase III transcriptome revealed by genome-wide localization and activity-occupancy relationships. *Proc. Natl. Acad. Sci. USA* **100**, 14695–14700 (2003).
38. Harismendy, O. *et al.* Genome-wide location of yeast RNA polymerase III transcription machinery. *EMBO J.* **22**, 4738–4747 (2003).
39. Willis, I.M. & Moir, R.D. Integration of nutritional and stress signaling pathways by Maf1. *Trends Biochem. Sci.* **32**, 51–53 (2007).
40. Weiner, A.M., Deininger, P.L. & Efstratiadis, A. Nonviral retroposons: genes, pseudogenes, and transposable elements generated by the reverse flow of genetic information. *Annu. Rev. Biochem.* **55**, 631–661 (1986).
41. Boyle, A.P. *et al.* High-resolution mapping and characterization of open chromatin across the genome. *Cell* **132**, 311–322 (2008).

ONLINE METHODS

Cell culture and cross-linking. We used cross-linked HeLa S3 cells (Biovest International) for ChIP-array and most HeLa ChIP-seq. For a second replicate of RPC32 ChIP, we obtained HeLa cells from ATCC (Cat. CCL-2.2) and cultured them in DMEM, 10% (v/v) FBS and 10 mM glutamine. We harvested cells at ~80% confluence and cross-linked them in 1% (v/v) formaldehyde for 30 min. We cultured and cross-linked Jurkat, HEK 293T and HFF (with *TERT*) cells as for HeLa (except we grew Jurkat cells in RPMI). We obtained Jurkat E6-1 cells from ATCC (Cat. TIB-152).

Chromatin immunoprecipitation. We used Standard Agilent Technologies Mammalian ChIP-on-chip protocol version 10.0 (http://www.agilent.com) for ChIP-array. For ChIP-seq, we made the following modifications. We lysed nuclei in 50 mM Tris-HCl, pH 8, 100 mM NaCl, 10 mM EDTA and 1% (w/v) SDS. We sheared chromatin by sonicating (Misonix) 10–20 times on setting 4–5 to an average shear length of 200–400 bp. For each immunoprecipitation, we bound 100 µl Dynabeads (Invitrogen) to 5–10 µg antibody in dilution buffer (15 mM Tris, pH 8.0, 150 mM NaCl, 2 mM EDTA, 1% (w/v) Triton X-100, 2 mg ml^{-1} BSA) for 5 h to overnight (16 h). We precleared chromatin sonicate from 20–40 × 10^6 cells in 1.4 ml dilution buffer with 50 µl Dynabeads for 1 h and transferred it to bead–antibody complexes for overnight immunoprecipitation. We washed and eluted the immunoprecipitate and reversed cross-links in 200 mM NaCl as described[42]. We purified DNA from eluate with phenol-chloroform-isoamyl (25:24:1, pH 8; Invitrogen) and Qiagen PCR Purification. We used these antibodies for immunoprecipitation: anti-RPC32 (Santa Cruz Biotechnologies, sc-21754), anti-RPB90 (that is, anti-BRF1), anti-BRF2 (abcam, ab17011) and anti-TFIIIC63 (Bethyl Laboratories, A301-242A).

ChIP-array. We designed ten ~1-million-feature custom microarrays tiling the nonrepetitive human genome (average resolution of 150 bp) from the Agilent ChIP database. We carried out RPC32 ChIP eluate amplification, labeling, array hybridization and wash according to Agilent Mammalian ChIP-on-chip protocol version 10.0. We scanned arrays with Agilent Technologies' Scanner C (cat. G2505C) and performed feature extraction with Agilent Technologies FE version 10.1.1.22 using default ChIP settings. We analyzed arrays using DNA Analytics' ChIP-chip analysis module (Agilent) and determined bound regions using default settings.

RNA-seq. We seeded 10^7 HeLa S3 cells per plate on two 15-cm dishes overnight. We washed cells with warm PBS, added 5 ml Trizol (Invitrogen) per plate and purified total RNA. We subjected RNA to RiboMinus (Invitrogen) or double 7-methylguanosine cap purification[43] plus RiboMinus before preparing RNA-seq libraries.

Sequencing. We used the Illumina GA2 with standard protocols for preparing and sequencing libraries. Read numbers are unique satellite-filtered reads (26–36 bp): input HeLa, 20,691,965; RPC32 HeLa, 13,082,194; BRF1 HeLa, 10,986,064; BRF2 HeLa, 11,053,174; TFIIIC HeLa, 16,076,219; RPC32 Jurkat, 18,173,688; RPC32 HFF, 8,917,992; RPC32 HEK 293T, 7,762,672; total RNA HeLa, 4,392,375; capped RNA HeLa, 5,934,673. When multiple alignments were desired, we remapped reads with Bowtie (http://bowtie-bio.sourceforge.net), retaining either the top 5 or the top 15 alignments.

Analysis of ChIP-seq data. We analyzed ChIP-seq data with the USeq package (http://useq.sourceforge.net). We used Jurkat input reads[21,22] to analyze RPC32 ChIP data from Jurkat, HFF and HEK 293T, as well as ChIP-seq tags for $CD4^+$ and Jurkat from other studies[19–23,44], unless provided. We used HeLa input reads from this study to analyze all HeLa data sets produced in this study, as well as HeLa ChIP-seq tags from other studies[13–16], unless provided. We created the 'random regions' file for IntersectRegions by pooling data from this study and others[13,14,19,20,22] and merging all 110-bp windows with at least one read; this is an estimate of the uniquely mappable genome. We removed duplicate alignments of RPC32 HeLa replicate 2, HEK 293T and HFF data sets. We performed Venn intersections using a Perl script (available upon request). We determined mapping efficiency of a tDNA by tiling every possible 36-bp sequence within the tDNA (plus 100 bp upstream and downstream sequence for ChIP-seq). The expected number of mappable reads for 100% efficiency is the number of tiles. We aligned the tiles uniquely with Bowtie (http://bowtie-bio.sourceforge.net) and calculated percent of observed mapped tiles over expected. We used only tDNAs overlapping the 'random regions' file for analysis. See **Supplementary Data 1** for lists and further descriptions. We used the Integrated Genome Browser (IGB, http://igb.bioviz.org/) for screen shots.

Consensus binding sites. We used Consensus and Patser (http://rsat.ulb.ac.be/rsat) to determine position-weight matrices for consensuses in **Table 1** from Pol III–enriched genes, and to search for the consensus in repeats. We downloaded sequences for repeats in **Table 1** from UCSC (http://genome.ucsc.edu) tracks RepeatMasker (http://www.repeatmasker.org) and 'RNA genes', except that tDNAs were from the Genomic tRNA Database (http://gtrnadb.ucsc.edu). We analyzed A- and B-boxes of tDNAs as well as TFIIIC-only and KLF4 consensuses with MEME and TOMTOM (http://meme.sdsc.edu).

Real-time PCR. For qPCR reactions, we used 1:50 to 1:100 of ChIP eluate, 500 nM primer, and iQ SYBR Green Supermix (Bio-Rad) in a total volume of 20 µl. We serially diluted ChIP input DNA for a standard curve. We designed primers of annealing temperature 62–65 °C with a single melt curve peak (**Supplementary Table 1**). We analyzed PCR results with iCycler (Bio-Rad).

Statistical analysis. Others have detailed a full description of statistical methods used in USeq programs[45]. To generate *P* values and fold enrichment over random in intersections of data sets, as well as to determine statistical significance of the positions of Pol III genes with respect to Pol II Refseq TSS, we used IntersectRegions (USeq package), which uses multiple permutation tests of random regions, as described[46]. We generated the *P* value for the divergent orientation of Pol II and nearest Pol III gene with the binomial *P* value function in R (http://www.r-project.org).

Data availability. The processed data is available for programmatic access using the GenoPub DAS/2 data distribution server (description, http://bioserver.hci.utah.edu/BioInfo/index.php; software, DAS2, GenoPub web app, http://bioserver.hci.utah.edu:8080/DAS2DB/genopub, and the DAS/2 data access URL, http://bioserver.hci.utah.edu:8080/DAS2DB/genome). One can use DAS/2-compliant genome browsers such as the Integrated Genome Browser (http://igb.bioviz.org/) to view the data sets, found under Homo sapiens→H_sapiens_Mar_2006→Cairns Lab→Oler_2010.

42. Gordon, M. *et al.* Genome-wide dynamics of SAPHIRE, an essential complex for gene activation and chromatin boundaries. *Mol. Cell. Biol.* **27**, 4058–4069 (2007).
43. Choi, Y.H. & Hagedorn, C.H. Purifying mRNAs with a high-affinity eIF4E mutant identifies the short 3′ poly(A) end phenotype. *Proc. Natl. Acad. Sci. USA* **100**, 7033–7038 (2003).
44. Schones, D.E. *et al.* Dynamic regulation of nucleosome positioning in the human genome. *Cell* **132**, 887–898 (2008).
45. Nix, D.A., Courdy, S.J. & Boucher, K.M. Empirical methods for controlling false positives and estimating confidence in ChIP-Seq peaks. *BMC Bioinformatics* **9**, 523 (2008).
46. Hammoud, S.S. *et al.* Distinctive chromatin in human sperm packages genes for embryo development. *Nature* **460**, 473–478 (2009).

Supplementary Figure 1

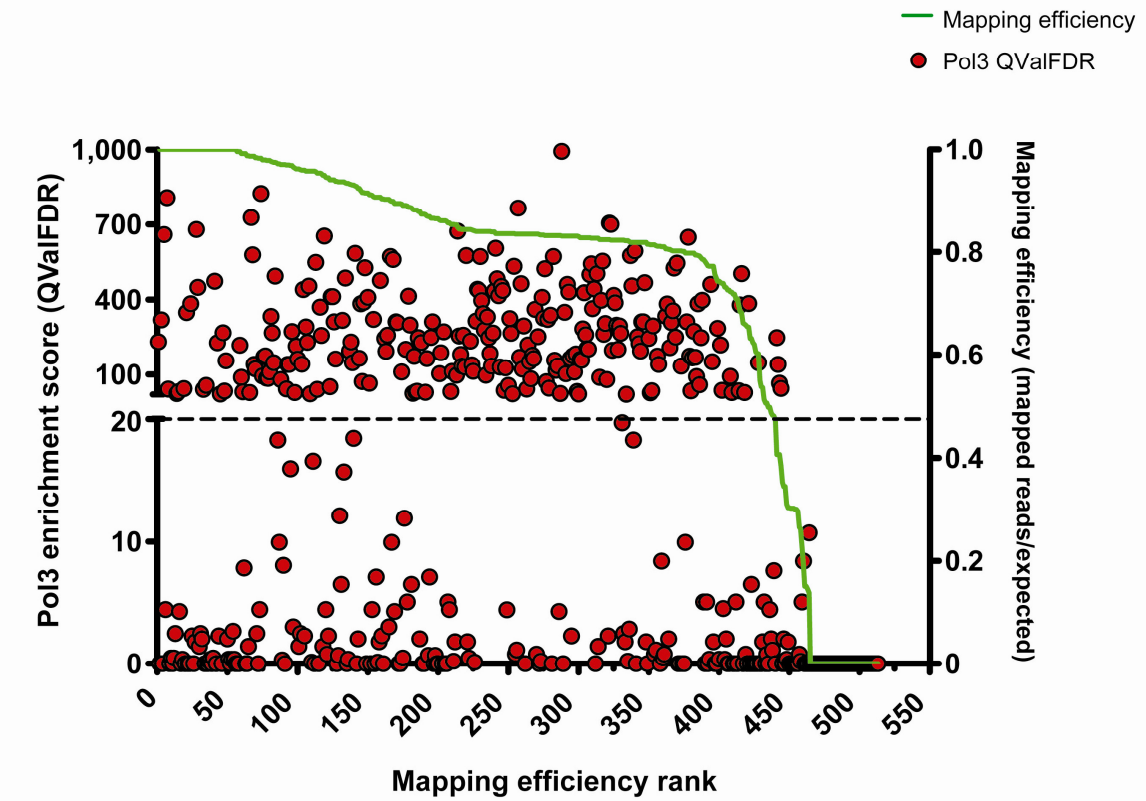

Supplementary Figure 1 Highly mappable tDNAs can be bound or unbound by Pol III. tDNA sequences are non-unique and lack of Pol III occupancy at a certain tDNA could be either because it is not occupied or because it is not uniquely mappable. To distinguish between these possibilities, each of 513 predicted tDNAs is assigned a mapping efficiency rank (*x*-axis) based on how efficiently a tDNA can be mapped (see Methods for a description of determining mapping efficiency). A tDNA with a lower rank number is more uniquely mappable than a tDNA with a higher rank number. The plot shows the QValFDR of Pol III in HeLa (primary *y*-axis) for each of the ranked tDNAs. Highly mappable tDNAs can be bound (QValFDR>20, above dotted line) or unbound (red points with QValFDR between 0–20). Primary *y*-axis is split to enlarge the region from QValFDR 0–20. The secondary *y*-axis shows the mapping efficiency of the tDNA with 100bp flanking sequence (see Methods). Of a total of 513 predicted tDNAs, ~467 are mappable (at rank ~467, the mapping efficiency curve falls steeply from 80% to 0% mapping efficiency).

Supplementary Figure 2

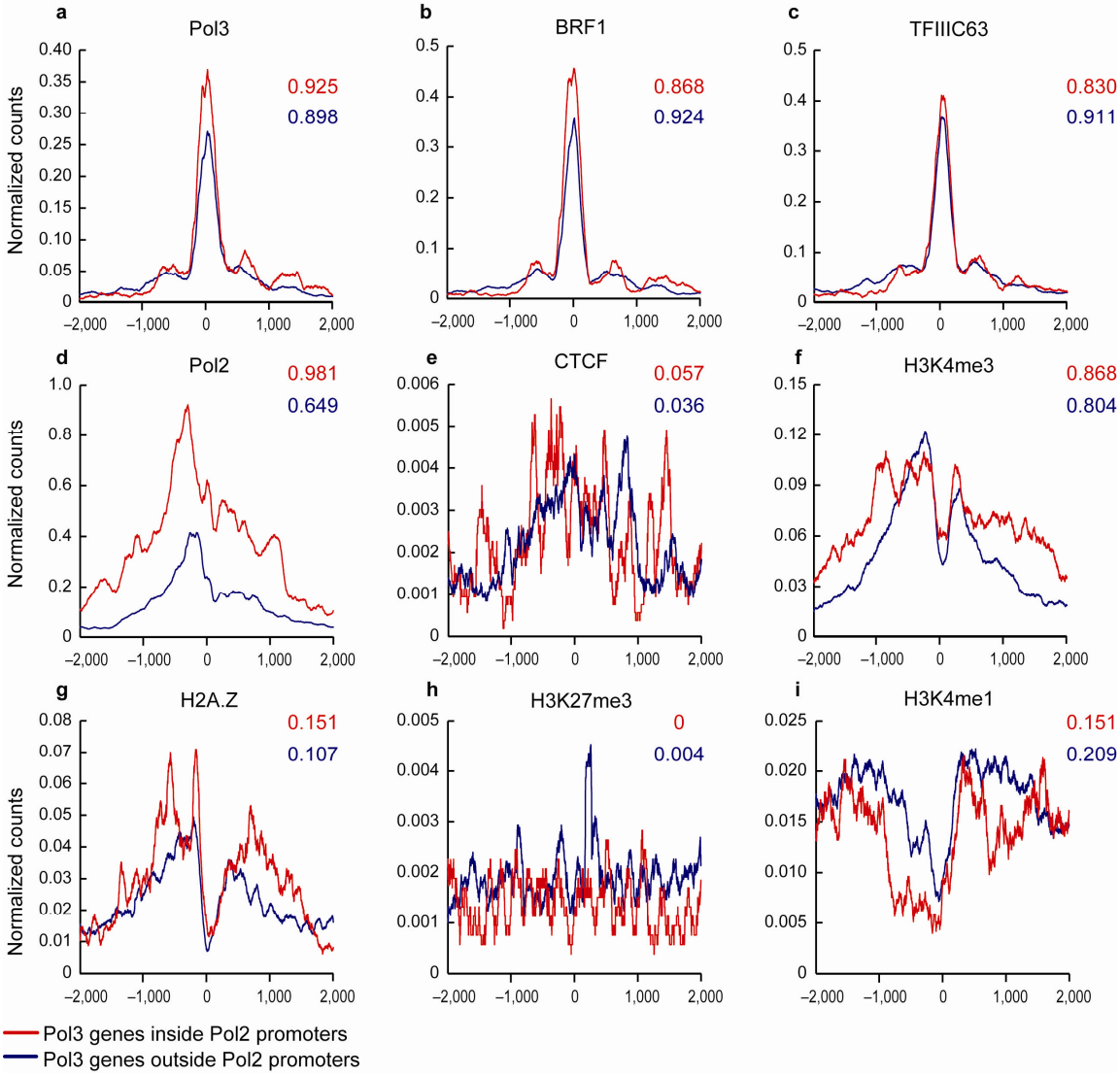

Supplementary Figure 2 HeLa-Pol III bound genes inside and outside Pol II promoters correlate with active chromatin. Pol III bound genes in HeLa (FDR<1%) were binned into those either inside (red) or outside (blue) Refseq promoters, and class average maps of chromatin marks and factors at these two classes of Pol III bound genes were plotted. The *x*-axis is the distance in base pairs from the Pol III transcription start site (TSS). An average Pol III gene is depicted as being transcribed rightward, with zero being the TSS, negative numbers indicating upstream regions and positive numbers indicating downstream regions. The *y*-axis is the number of read counts at each position normalized to the number of genes in the class. The numbers in red and blue indicate the intersection fractions for marks/factor-enriched regions with Pol III bound regions inside and outside Refseq promoters, respectively. Chromatin datasets from others[1–4].

Supplementary Figure 3

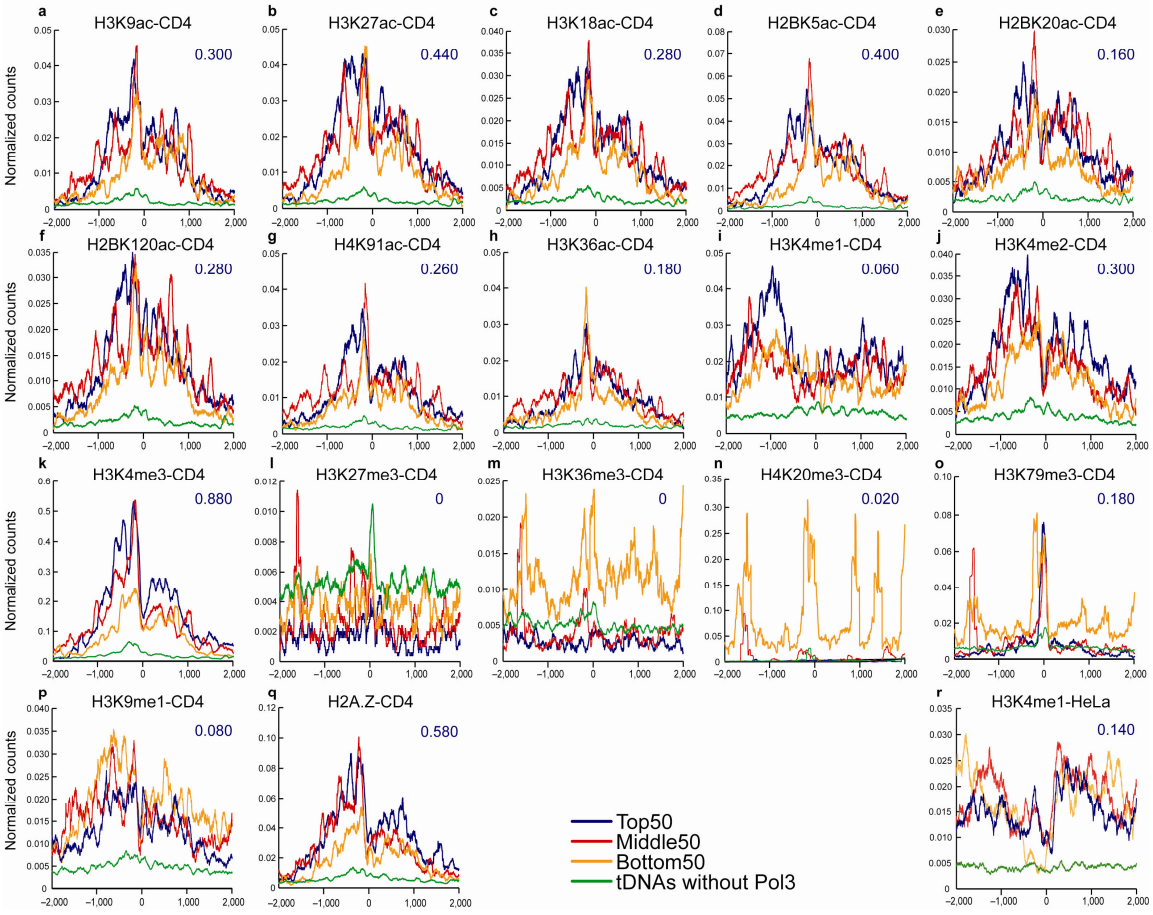

Supplementary Figure 3 Active chromatin marks at Pol III bound genes in Jurkat cells scale with Pol III occupancy. Pol III bound genes in Jurkat cells were binned into Top 50 (blue), Middle 50 (red) and Bottom 50 (yellow) based on their Pol III levels and class average maps were plotted for various marks/factors. Class average plots of marks/factors at tDNAs without Pol III (green) serve as negative controls. The *x*-axis is the distance from the Pol III TSS and the *y*-axis is the number of read counts at each position normalized to the number of regions in the class. The intersection fraction for each of these factor bound regions with the Top 50 class is indicated in blue. Chromatin and factor ChIP-seq from others[2,5–8].

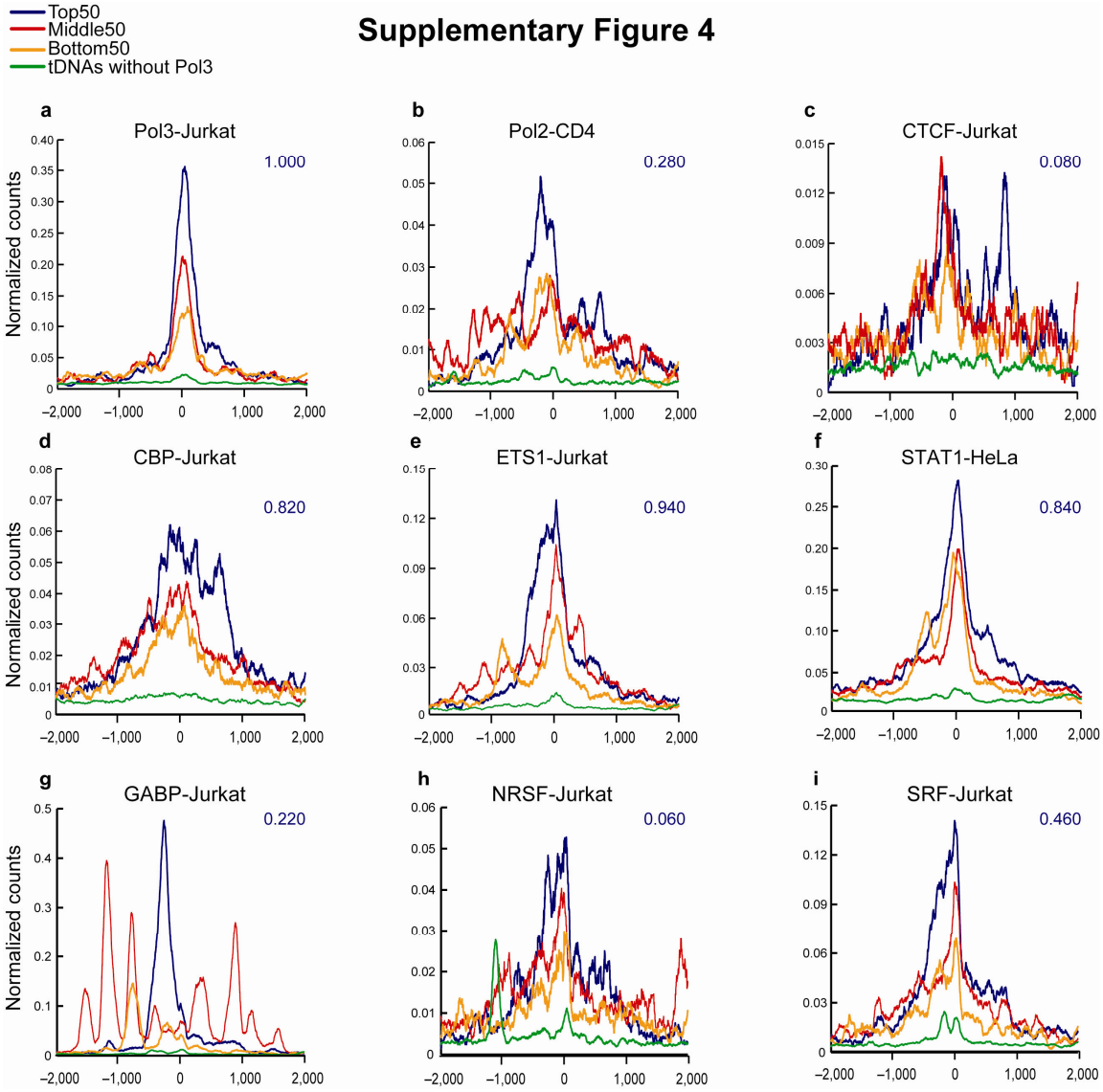

Supplementary Figure 4 Transcription factors at Pol III bound genes in Jurkat cells scale with Pol III occupancy. Pol III bound genes in Jurkat cells were binned into Top 50 (blue), Middle 50 (red) and Bottom 50 (yellow) based on their Pol III levels and class average maps were plotted for various marks/factors. Class average plots of factors at tDNAs without Pol III (green) serve as negative controls. The *x*-axis is the distance from the Pol III TSS and the *y*-axis is the number of read counts at each position normalized to the number of regions in the class. The intersection fraction for each of these factor bound regions with the Top 50 class is indicated in blue. Chromatin and factor ChIP-seq from others[2,5–8].

Supplementary Figure 5

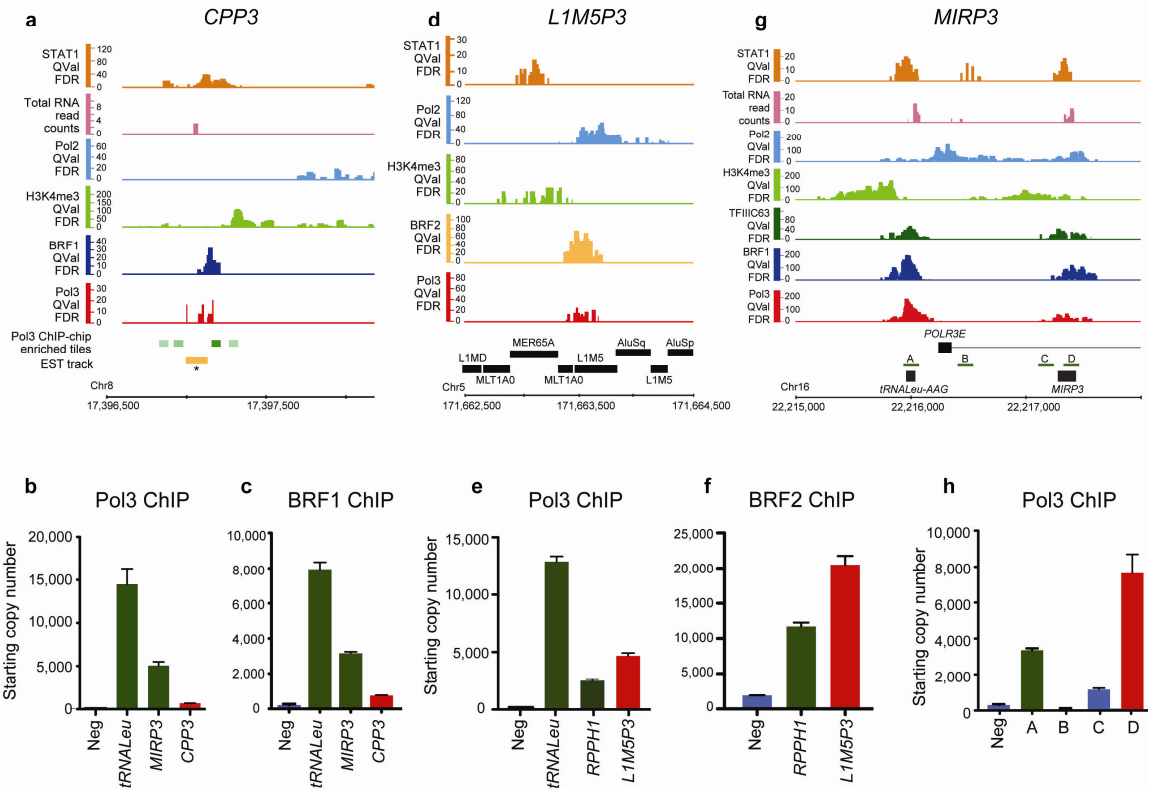

Supplementary Figure 5 Quantitative PCR confirms novel Pol III targets identified by ChIP-seq. (**a,d,g**) Novel Pol III (red), Pol II (turquoise), H3K4me3 (light green), and STAT1 (orange) bound regions. (Pol II, H3K4me3, STAT1 datasets from others[1,2].) (**a**) Novel locus on chromosome 8, *CPP3*, in *SLC7A2* promoter with Pol III (red), BRF1 (blue), STAT1 (orange), and H3K4me3 (light green) nearby. The Pol III ChIP-chip track (dark green) shows the variably enriched (based on color intensity) tiles as assayed by ChIP-array, peaking at 34.8-fold enrichment over background. ESTs (yellow) have been mapped to the reverse strand with the longest EST terminating 128bp downstream of the start at a stretch of five Ts, a typical terminator for Pol III. We also observe a *B-box* (asterix) at +57 from the putative TSS and the putative transcript is predicted to fold into a structure similar to snaR-B RNA (data not shown). Note that the total RNA track (purple) shows a transcript made at this locus in HeLa cells. (**b,c**) Quantitative PCR (qPCR) analysis of (**b**) Pol III or (**c**) BRF1 ChIP eluate in HeLa cells showing occupancy at the novel Pol III bound region as shown by ChIP-seq. Green bars indicate positive controls that are known Pol III targets, blue bars negative controls and red bars novel targets. Error bars represent standard error of the mean (s.e.m.) of three replicates. *y*-axis represents relative starting template copy number based on standard curve of genomic DNA. (**d**) Novel Pol III (red), BRF2 (yellow), Pol II (turquoise) and H3K4me3 (light green) bound region overlapping L1M5 LINE fragment; putative Pol III gene called *L1M5P3*. (**e,f**) qPCR analysis of (**e**) Pol III or (**f**) BRF2 ChIP showing enrichment at *L1M5P3* as seen in ChIP-seq.

qPCR results graphed as in **b,c**. Gene encoding RNase P RNA, *RPPH1*, is a positive control. (**g**) Novel Pol III (red), BRF1 (blue), TFIIIC (dark green), H3K4me3 (light green), Pol2 (turquoise) and STAT1 (orange) bound mammalian-wide interspersed repeat (MIR) in the intron of *POLR3E*; novel Pol III gene called *MIRP3.* This region also shows RNA transcripts (pink). (**h**) Tiling ChIP-qPCR analysis of Pol III genes near TSS of *POLR3E* shows that Pol III is enriched at two separate loci flanking the annotated Pol II TSS: *tRNALeu-AAG* upstream and *MIR* in the first intron. qPCR results graphed as in **b,c**. See **g** for location of amplicons A–D on physical map.

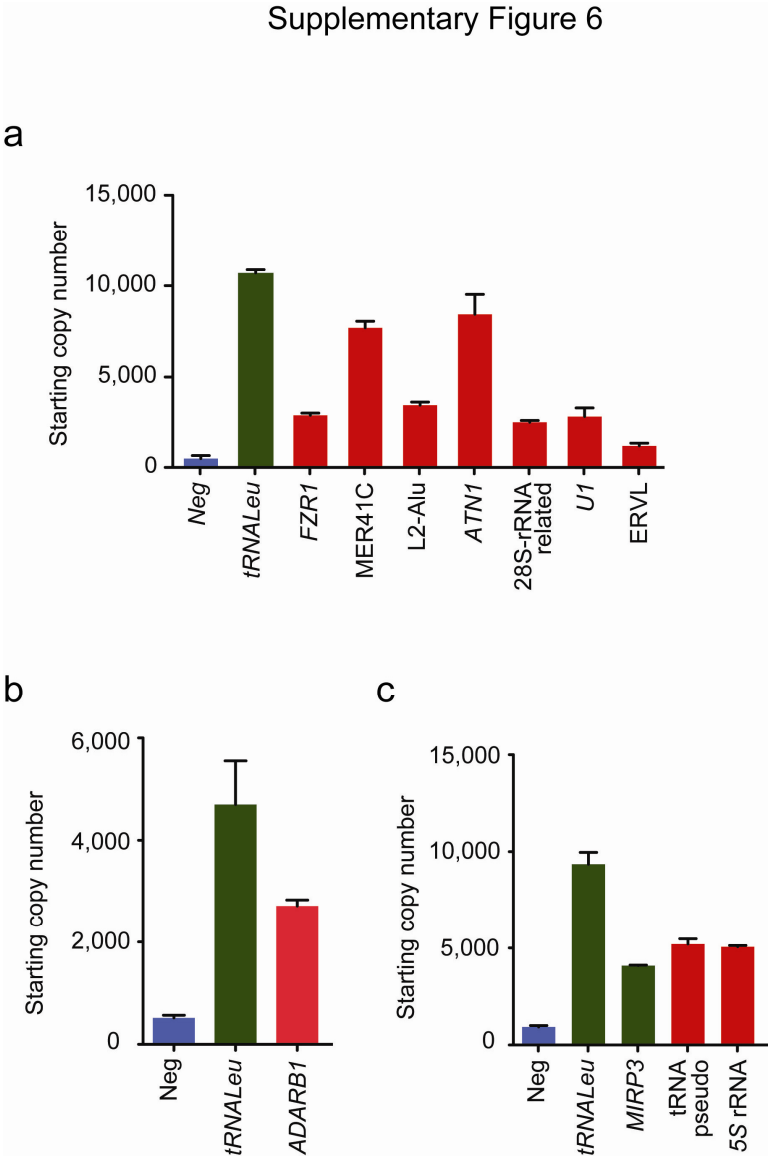

Supplementary Figure 6 Novel unannotated regions bound by Pol III in HeLa cells. (**a–c**) ChIP-qPCR analysis of some novel Pol III-bound sites from ChIP-seq analysis show >3.5-fold enrichment over a negative control locus. Green bars indicate positive controls that are known Pol III targets, blue bars are negative controls, and red bars are novel Pol III bound regions. Error bars represent s.e.m. of three replicates. *y*-axis represents relative starting template copy number based on standard curve of genomic DNA. In **c**, a single *5S* gene bears a point mutation that allows us to query Pol III enrichment at this gene. See Supplementary Table 1 for primer sequences.

Supplementary Figure 7

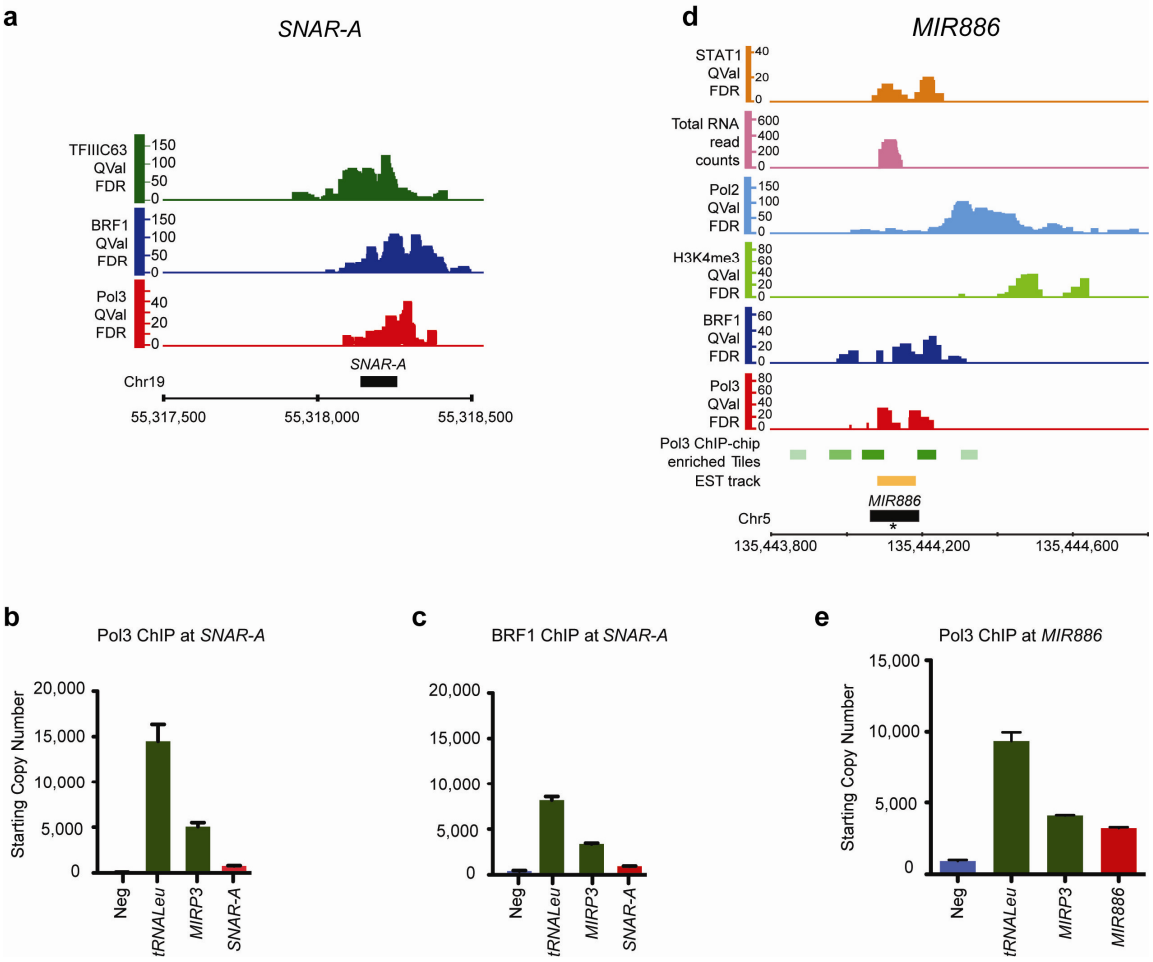

Supplementary Figure 7 Novel demonstration of Pol III machinery binding to *SNAR-A* and *MIR886* in HeLa cells. (**a**) ChIP-seq reads mapped to permit multiple alignments allows us to visualize enrichment of Pol III (red), BRF1 (blue), and TFIIIC (dark green) at *SNAR-A* repetitive locus. Reads mapped with Bowtie to allow up to 15 'best' alignments (bowtie-bio.sourceforge.net). (**b,c**) A single *SNAR-A* gene bears a point mutation, which allows us to query the locus by ChIP-qPCR, showing ~3.5-fold enrichment by (**b**) Pol III and (**c**) BRF1 over a negative control locus. Green bars indicate positive controls that are known Pol III targets, blue bars are negative controls, and red bars are previously annotated genes that are newly shown to be bound by Pol III. Error bars represent s.e.m. of three replicates. *y*-axis represents relative starting template copy number based on standard curve of genomic DNA. (**d**) Novel Pol III (red), Pol II (turquoise), H3K4me3 (light green), and STAT1 (orange) bound regions. (Pol II, H3K4me3, STAT1 datasets from others[1,2].) Novel Pol III (red), BRF1 (blue), Pol II (turquoise), H3K4me3 (light green), and STAT1 (orange) bound regions overlapping the annotated *MIR886* gene. (Pol II, H3K4me3, STAT1 datasets from others[1,2].) Note that the total

RNA track (purple) shows a transcript made at this locus in HeLa cells. No capped transcripts are present for this locus (data not shown). The EST track (yellow) shows putative transcripts. The Pol III ChIP-chip track (dark green) shows the variably enriched (based on color intensity) tiles as assayed by ChIP-array. Consensus *B-box* is indicated (asterisk). (**e**) Quantitative PCR analysis of Pol III ChIP eluate in HeLa cells showing occupancy at *MIR886* as shown by ChIP-array and ChIP-seq. qPCR results graphed as in **b,c**.

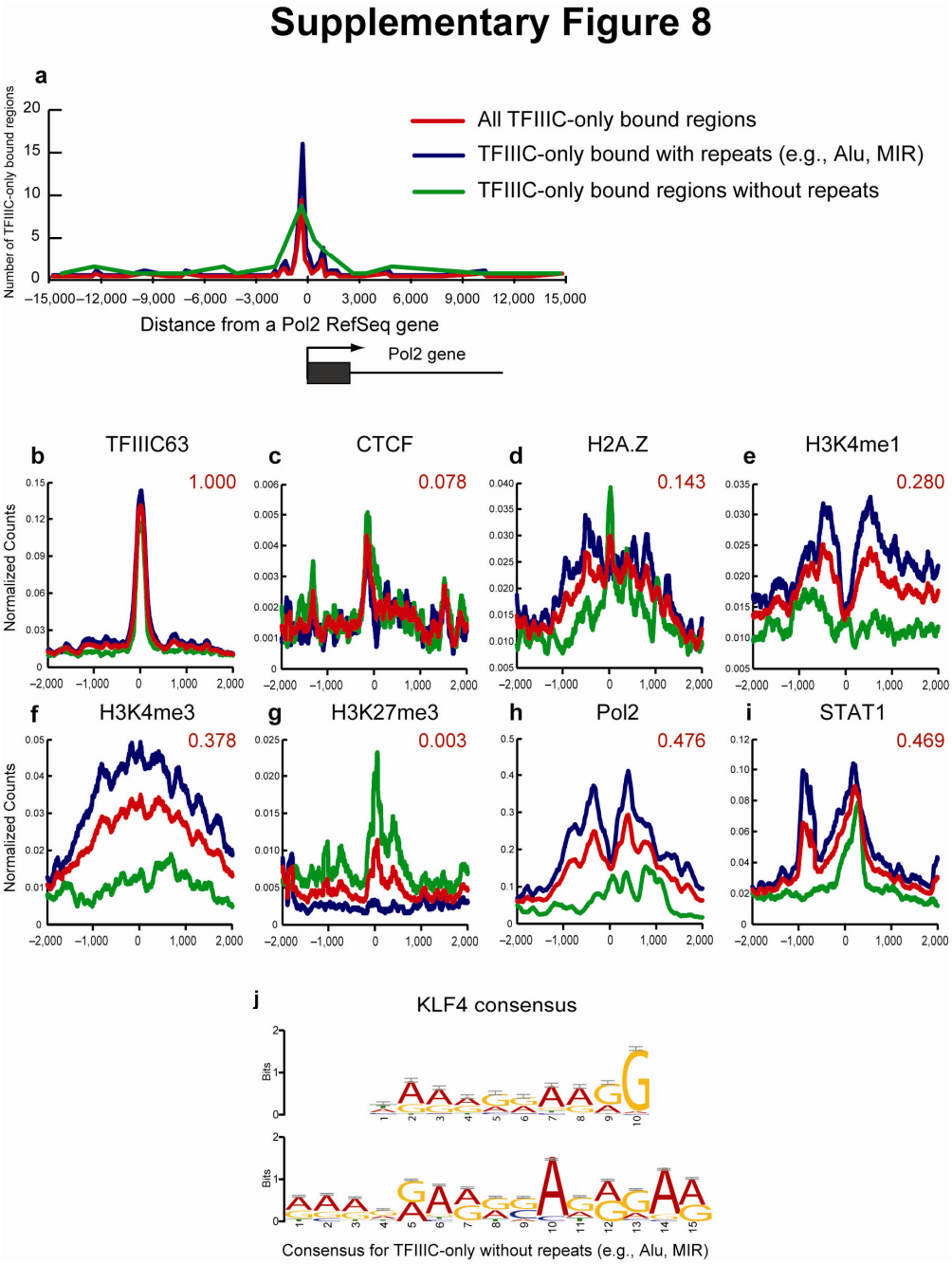

Supplementary Figure 8 TFIIIC bound regions lacking Pol III initiation machinery cluster at Pol 2 promoters and have active chromatin. (**a**) TFIIIC-bound sites lacking Pol III initiation machinery (Pol III, BRF1) show clustering at Pol II promoters, similar to active Pol III genes. (**b–i**) Class average maps for chromatin modifications/factors in HeLa show that TFIIIC-only

sites are associated with active chromatin, including Pol II, STAT1, and H3K4me3. This is more prevalent in TFIIIC-bound sites overlapping repeat elements (e.g., MIR or Alu), although TFIIIC enrichment is similar whether a repeat is nearby or not. The intersection fraction for each of these factor or mark bound regions with all TFIIIC-only sites is indicated in red. (**j**) MEME[9] analysis identifies the G/A-rich sequence for TFIIIC-bound sites outside of predicted repeat elements (e.g., Alu, MIR), which typically lack a consensus *B-box* (bottom panel). Comparison of MEME result with TOMTOM[10] predicts similarity to the KLF4 consensus binding site (top).

Supplementary Table 1. Primer sequences for ChIP-qPCR

Primer Name	Primer ID	Locus Description	Sequence
PGK-F[11]	BC4454	*PGK* promoter	5'-TCGTTGACCGAATCACCGAC-3'
PGK-R[11]	BC4455		5'-AGAGGTTTGCGACAGAGCACAG-3'
GenDes-F[11]	BC4456	Gene Desert chr10	5'-GGCTAATCCTCTATGGGAGTCTGTC-3'
GenDes-R[11]	BC4457		5'-CCAGGTGCTCAAGGTCAACATC-3'
tRNALeu-F[12]	BC4458	tRNALeu Positive control, Pol3 HeLa, HEK293T, Jurkat, HFF	5'-GAGGACAACGGGGACAGTAA-3'
tRNALeu-R[12]	BC4459		5'-TCCACCAGAAAAACTCCAGC-3'
chr8EST-F1.2	BC4934	*CPP3*, novel locus chr8	5'-CGGGTCGGAGTTAGCTCAAGCGGTTACC-3'
chr8EST-R1.2	BC4935		5'-CGTGTAGCCTCGCCTCCTCGAGTG-3'
RNaseP-F1	BC4523	3' end of *RPPH1* gene	5'-GGATGCCTCCTTTGCCGGAGCTTG-3'
RNaseP-R1	BC4524		5'-TGGGCGGAGGAGAGTAGTCTGAATTGG-3'
L1M5-F	BC4936	*L1M5P3*, novel locus enriched with Brf2 and Pol3 in HeLa	5'-TTTTGTATCCTTGACCAAATGAAGGGAAATTTC-3'
L1M5-R	BC4937		5'-GCATGAGCCACTGCACCCAGCCAATATTTAGC-3'
POLR3E-F6	BC4505	tRNALeu in *POLR3E* promoter	5'-CAGCGAAAACGCCTCGCAATGTCCAGATTAAATGC-3'
POLR3E-R6	BC4506		5'-GAGTGTATGCAGCGGGGACAAAAAGACAGCAAC-3'
POLR3E-F5	BC4503	negative control first intron *POLR3E*	5'-GTGGGCCTGGGCTAGATTCCCGAG-3'
POLR3E-R5	BC4504		5'-CCAACTCCCAGGTGTCAGGTCAAGGAAG-3'
POLR3E-F1	BC4497	just downstream of *MIRP3*	5'-ACGGCTCAGTAGAAACCGGGTGACG-3'
POLR3E-R1	BC4498		5'-GGAAGGAGTAAGGACAGGACGCTAATAAACG-3'
POLR3E-F2	BC4499	5' end of *MIRP3*, Pol3 HeLa, HEK293T, Jurkat, HFF	5'-GGGATGAAAATAGGGAGGAATACCAAACCCAG-3'
POLR3E-R2	BC4500		5'-CGGCAGTATGGTTAAGTGGGTAAGAGCTTGG-3'
FZR1prom-F	BC4938	*FZR1* promoter, novel Pol3 HeLa	5'-GCCCTCCATCTACCAGAGCCATTTCTGC-3'
FZR1prom-R	BC4939		5'-GGCATCTCGGGAGGACGTGACGTC-3'
MER41Cchr17-F	BC4940	Near MER41C LTR on chr17, novel Pol3 HeLa	5'-CTGACGGCAGTCAGATTCTGCAGTGAAGTAG-3'
MER41Cchr17-R	BC4941		5'-TCTTTCCATTCAAGTTTACCGCATGTGTTTCACTATCG-3'
L2Aluchr14-F	BC4942	Near L2 repeat and Alu, novel Pol3 HeLa	5'-CACAGTATTAATCTCCCCTGGGCTCAGAGC-3'
L2Aluchr14-R	BC4943		5'-CAGCGATTCTTGCCTATTTTGTTGACTGCTTCC-3'
ATN1-F	BC4944	*ATN1* (aka *C12orf57*) exon, novel Pol3 HeLa	5'-CTCGCGGAGGTGATCCAGGCGTTC-3'
ATN1-R	BC4945		5'-GGCCACGGGCAGCACGAATTGC-3'
28SrRNA-likechr11-F	BC4946	5' end of 28S rRNA-like pseudogene, novel Pol3 HeLa	5'-AAAAGATGCAAATTGGCCCGGGTCTTCC-3'
28SrRNA-likechr11-R	BC4947		5'-CAACTTTCCCTTACGGTACTTGTTGACTATCGGTC-3'
U1chr1-F	BC4948	*U1* snRNA promoter, novel Pol3 HeLa	5'-GGGAGGCGAATTTCAGTCTCTGTTGGTTGGGT-3'
U1chr1-R	BC4949		5'-AAGAGATGTTAGAAGCCCTGGGAGCACTG-3'
ERVLchr1- F	BC4950	Near ERVL1 LTR in *NFIA* promoter, novel Pol3 HeLa	5'-TCGGGAATCAGGAATAAGATTCAATGGGTTTTCCAAC-3'
ERVLchr1- R	BC4951		5'-GTCCCTCCTTGAGTGCCTAGGTTCTGG-3'
ADARB1-F1.3	BC4537	*ADARB1* promoter, novel Pol3 HeLa	5'-GCC CAG CCG CGG TCT CTC AGC TC-3'
ADARB1-R1.2	BC4538		5'-TGC GGC GGA CGG GCG CGG GGC CGT TG-3'
tRNApseudoHLHKchr1-F	BC4952	tRNA-pseudo-Gly, Pol3 HeLa, HEK293T, HFF	5'-TTGATAATTCTCCCAGGGTTGCTAGAGAGAGGC-3'
tRNApseudoHLHKchr1-R	BC4953		5'-GGCAGAAGGGTAAAGAGCCATAGTGAAGAGC-3'
5SrRNAunique-F	BC4954	*5S* rRNA chr1:~226830595	5'-GGCAGCCAGGCGCCTCCTTC-3'
5SrRNAunique-R	BC4955		5'-GTATTCCCAGGCGGTCTCCCG-3'
snaRA-F	BC4956	*SNAR-A* with unique sequence	5'-GGGTTCCAGGGCACGAGTTCG-3'
snaRA-R	BC4957		5'-ATTTCTTCCTATCAAGGCGTCCTCCCTTTAC-3'
hsa-mir-886-F1.2	BC4958	*MIR886* miRNA gene, aka CBL-3	5'-CGGGTCGGAGTTAGCTCAAGCGGTTACC-3'
hsa-mir-886-R1.2	BC4959		5'-CGTGTAGCCTCGCCTCCTCGAGTG-3'
HK1GlnF	BC4960	tRNAGln, Pol3 HEK293T	5'-AGGTTCCACCGAGACTCGAACTCGG-3'
HK1GlnR	BC4961		5'-GGGTGGGAACTAATTCAGACACCTTTAACAAC-3'
HK5ProF	BC4962	tRNAPro, Pol3 HEK293T	5'-GCTCGTTGGTCTAGGGGTATGATTCTCGC-3'
HK5ProR	BC4963		5'-AGGCTCGGTCCCCGATTTTCTAGCTC-3'
HK6LysF	BC4964	tRNALys, Pol3 HEK293T	5'-CCCGGCTAGCTCAGTCGGTAGAGC-3'
HK6LysR	BC4965		5'-TGACCCAGTTGGAACAGAAACTCACAATGC-3'
HK7LysF	BC4966	tRNALys, Pol3 HEK293T	5'-GCCACCCCGCCAATTACTAGACATAAAACG-3'
HK7LysR	BC4967		5'-AGCAAGGAAGAAAACAAGTCGCCCAACG-3'
HK9MetF	BC4968	tRNAMet, Pol3 HEK293T	5'-GCAAGCTTGTCTAAGCAGAGGCCCTC-3'
HK9MetR	BC4969		5'-TCCGAACATTTGCTGCATTCGTAGCACAAC-3'
HK10ValF	BC4970	tRNAVal, Pol3 HEK293T	5'-CTCCCTTAACGAAGGAAGCCAACGCAGC-3'
HK10ValR	BC4971		5'-CAGAAACACCCCGAAAAATTGCAAGTTGTTTCC-3'
HK11pseudoF	BC4972	tRNA-pseudo, Pol3 HEK293T	5'-CAGATTTGCGGTCGGCCGGTTAGC-3'
HK11pseudoR	BC4973		5'-ACCAAATTTCTCGAGGGGGGAAAAAGCC-3'
HK12SerF	BC4974	tRNASer, Pol3 HEK293T	5'-GAAGGACGAGGTGGCCGAGTGG-3'
HK12SerR	BC4975		5'-GACCTGCGACAAAAACCTGGTTACCCTC-3'
HK13SerF	BC4976	tRNASer, Pol3 HEK293T	5'-AGCCGTCAGCGATGGCGTAGG-3'
HK13SerR	BC4977		5'-CTGCACCTGGTAAAACCGTAGTCGGC-3'

Primer Name	Primer ID	Locus Description	Sequence
HL1AluJbF	BC4978	AluJb, Pol3 HeLa	5'-CCTCAGTCTCCCGAGTAGCTAGCACAGG-3'
HL1AluJbR	BC4979		5'-CTTAGGTTACGGTCTGTTTTAATTAGATGCTCGC-3'
HL2TrpF	BC4980	tRNATrp, Pol3 HeLa, HEK293T	5'-GAACACGCAACCTTCTGATCTGGAGTCAG-3'
HL2TrpR	BC4981		5'-GCTGCCTGGTCTTCACCAGTACCG-3'
HL3AspF	BC4982	tRNAAsp, Pol3 HeLa, HEK293T, Jurkat	5'-AGAGGTAGTCAAAACTCGCTGACGCAGAG-3'
HL3AspR	BC4983		5'-GCAACTTTTCTCCCCGTCGGGG-3'
HL5LysF	BC4984	tRNALys, Pol3 HeLa, HEK293T	5'-GAAGTAAAACTTCTGAAGTTCGCCTGAACAGGG-3'
HL5LysR	BC4985		5'-GAGTTAGAGCCCAGTGTAGAGAGCCTGG-3'
HL6AlaF	BC4986	tRNAAla, Pol3 HeLa, HEK293T	5'-ACAACAAGGGTCTATGTGTGGGGATGTAGC-3'
HL6AlaR	BC4987		5'-CGTACGTTGAACAAGAATCAGCGCTAAAACC-3'
HL7AlaF	BC4988	tRNAAla, Pol3 HeLa, HEK293T	5'-CTCATGCGGTCAGGGGGTGTAGC-3'
HL7AlaR	BC4989		5'-CGCATGCAAAGAACCAGAAAGGAGAATGAAG-3'
HL8LeuF	BC4990	tRNALeu, Pol3 HeLa, HEK293T	5'-AGTCGCCTAGTGTTACCCGAGTTGC-3'
HL8LeuR	BC4991		5'-GGGGTTCGAACCCACGCGGATATG-3'
HL9ThrF	BC4992	tRNAThr, Pol3 HeLa, HEK293T	5'-GCTTGGGAAAAGTATTCCTACAGCCGAGG-3'
HL9ThrR	BC4993		5'-GCTCTCTGTGGCGGCTCCATAGC-3'
J1ProF	BC4994	tRNAPro, Pol3 HeLa, HEK293T, Jurkat	5'-GCAAAAGCCATTTCTAAGTGGCTCGTTGG-3'
J1ProR	BC4995		5'-CCTTATTGGGCGAAAATGAAGTGGGCTCG-3'
HF2GluF	BC4996	tRNAGlu, Pol3 HEK293T, HFF	5'-GTCCAGTCATTCCCACACCGGGAG-3'
HF2GluR	BC4997		5'-AGGGCAGGCGGAAATGATTCAATTGGTTTAG-3'
AllMetchr6F	BC4998	tRNAMet-i, Pol3 HeLa, HEK293T, Jurkat, HFF	5'-CCTCTAACAAGTGCAAGATGCAGTGTTTTGG-3'
AllMetchr6R	BC4999		5'-CACAACAGCTGAAGGGGACAGCAGAG-3'
tRNAValHLHKchr6-F	BC5000	tRNAVal, Pol3 HeLa, HEK293T, Jurkat	5'-TCTACAGCCAAACCTGGATTGTCTCACCC-3'
tRNAValHLHKchr6-R	BC5001		5'-ACCACTTGTTTCCGCCTGGTTTTGATCC-3'
tRNALeuHLHKchr6-F	BC5002	tRNALeu, Pol3 HeLa, HEK293T	5'-GTGGTCTAAGGCGCCAGACTCAAGC-3'
tRNALeuHLHKchr6-R	BC5003		5'-GGCGAAACTTTCGGTACAAATCTGGTAGGG-3'

References

1. Rozowsky, J. et al. PeakSeq enables systematic scoring of ChIP-seq experiments relative to controls. *Nat Biotechnol* 27, 66-75 (2009).
2. Robertson, A.G. et al. Genome-wide relationship between histone H3 lysine 4 mono- and tri-methylation and transcription factor binding. *Genome Res* 18, 1906-17 (2008).
3. Cuddapah, S. et al. Global analysis of the insulator binding protein CTCF in chromatin barrier regions reveals demarcation of active and repressive domains. *Genome Res* 19, 24-32 (2009).
4. Jin, C. et al. H3.3/H2A.Z double variant-containing nucleosomes mark 'nucleosome-free regions' of active promoters and other regulatory regions. *Nat Genet* 41, 941-5 (2009).
5. Barski, A. et al. High-resolution profiling of histone methylations in the human genome. *Cell* 129, 823-37 (2007).
6. Wang, Z. et al. Combinatorial patterns of histone acetylations and methylations in the human genome. *Nat Genet* 40, 897-903 (2008).
7. Valouev, A. et al. Genome-wide analysis of transcription factor binding sites based on ChIP-Seq data. *Nat Methods* 5, 829-34 (2008).
8. Hollenhorst, P.C. et al. DNA specificity determinants associate with distinct transcription factor functions. *PLoS Genet* 5, e1000778 (2009).
9. Bailey, T.L. & Elkan, C. Fitting a mixture model by expectation maximization to discover motifs in biopolymers. *Proc Int Conf Intell Syst Mol Biol* 2, 28-36 (1994).
10. Gupta, S., Stamatoyannopoulos, J.A., Bailey, T.L. & Noble, W.S. Quantifying similarity between motifs. *Genome Biol* 8, R24 (2007).
11. Listerman, I., Bledau, A.S., Grishina, I. & Neugebauer, K.M. Extragenic accumulation of RNA polymerase II enhances transcription by RNA polymerase III. *PLoS Genet* 3, e212 (2007).
12. Gomez-Roman, N., Grandori, C., Eisenman, R.N. & White, R.J. Direct activation of RNA polymerase III transcription by c-Myc. *Nature* 421, 290-4 (2003).

Additional supplementary data can be found:

http://www.nature.com/nsmb/journal/v17/n5/abs/nsmb.1801.html

Supplementary Data 1: Lists of genes and enriched regions.

Supplementary Data 2: Intersection analysis of genes and enriched regions.

CHAPTER 3

PP4 DIRECTLY DEPHOSPHORYLATES MAF1 TO COUPLE MULTIPLE STRESS CONDITIONS TO RNA POLYMERASE III REPRESSION

Abstract

Maf1 is required for general repression of RNA polymerase III (Pol III) transcription in response to diverse stresses, including nutrient deprivation, cell wall stress and DNA damage. Interestingly, Maf1 is a phospho-integrator: it is phosphorylated and cytoplasmic under favorable growth conditions, whereas unfavorable growth conditions lead to dephosphorylation, nuclear accumulation, binding to Pol III at Pol III genes, and transcriptional repression. Here, PP4 complex (bearing catalytic Pph3) is established as the main Maf1 phosphatase for acute Pol III repression. First, PP4 components are shown to have major roles in Maf1 dephosphorylation, nuclear localization, and Pol III repression. Second, PP2A is shown to contain Pph21/22, to lack Pph3, and to lack roles in acute repression or acute Maf1 dephosphorylation. Third, PP4 binds directly to Maf1 in extracts and dephosphorylates Maf1 *in vitro*, with purified components. Finally, Pph3 mediates repression in response to diverse stresses, suggesting Maf1 and PP4 as co-integrators of cell nutrition, stress, and integrity for Pol III regulation.

Introduction

Transcription of the protein synthesis machinery (PSM) by all three RNA polymerases is coordinately responsive to nutrient availability and growth conditions. The RNA polymerases work together to produce the PSM, accounting for ~80% of nuclear transcription in proliferating cells[1]. Transcripts produced by each of these polymerases are required for protein synthesis, including ribosomal RNAs (mostly transcribed by Pol I except for 5S rRNA, which is transcribed by Pol III), ribosomal protein-coding mRNAs (transcribed by Pol II), and tRNAs (transcribed by Pol III). In response to multiple stresses such as nutrient deprivation, repression of all components of the PSM is observed via the TOR pathway and other signaling pathways[2,3]. Likewise, Pol III targets undergo rapid repression in nutrient deprivation and other stress conditions, an attribute important for regulation of growth and proliferation in yeast, as well as higher organisms. In humans, many cancer types overexpress components of the Pol III machinery or its target RNA products, and Pol III targets are regulated by many tumor suppressors/oncogenes, including p53, Rb, and Myc[4,5]. Studies in yeast have elucidated many conserved aspects of the regulation of Pol III. While yeast does not possess homologous counterparts to these human tumor suppressors, they do share a conserved regulator with higher organisms: the protein Maf1[6]. Maf1 is emerging as a central regulator of Pol III transcription and is addressed in detail following a description of the Pol III machinery.

Pol III transcribes short (< 550bp) noncoding RNAs involved in translation (e.g., tRNAs, Scr1), splicing (e.g., U6), and a variety of other functions[7].

Normally, Pol III promoters in yeast reside in the transcribed region of the gene. A typical Pol III promoter consists of A- and B-box DNA consensus elements, as well as a stretch of at least four thymidine residues, which terminates transcription. There are three subcomplexes in the basic Pol III machinery, each performing essential functions. In simplified terms, TFIIIC complex recognizes the A- and B-boxes and recruits TFIIIB complex; TFIIIB contains the initiation protein TBP and together with TFIIIC recruits Pol III; and Pol III produces the RNA[8].

Regulation of Pol II transcription is exceptionally complex, due to the many thousands of targets that must be differentially activated or repressed under any particular condition. In contrast, as the Pol III repertoire is largely (though not solely) dedicated to the PSM, a simpler mode of regulation is observed. Also, in contrast to the Pol II system, Pol III promoters and the basal machinery in yeast have a “default on” state, requiring the master repressor Maf1 to attenuate the Pol III system during unfavorable conditions when the demand for PSM is decreased. Notably, all repression signals for Pol III appear to converge on Maf1, which is required for repression of Pol III in response to nutrient deprivation, DNA damage, oxidative stress, and cell wall stress[9,10]. Also, *maf1* mutant cells produce a higher basal level of tRNAs than WT cells. Maf1 interacts in vivo with several subunits of the Pol III machinery, including Pol III components Rpc160, Rpc34, and Rpc82, as well as TFIIIB component Brf1[6,11,12]. Best characterized is the direct interaction of Maf1 with the N-terminus of Rpc160, shown first *in vitro*[13] and verified by the crystal structure of Maf1 bound to Pol

III[14]. Notably, Maf1 is not required for repression of ribosomal protein genes or Pol I-encoded ribosomal RNAs, suggesting that Maf1 is specifically dedicated to repression of Pol III[9]. In summary, Maf1 functions as a master regulator/integrator that specifically represses Pol III transcription in response to multiple stresses by direct interaction with the Pol III machinery.

Previous work by several labs has revealed important aspects of Pol III regulation by Maf1. First, Maf1 is a phosphoprotein, and is phosphorylated and mostly cytoplasmic in favorable growth conditions[12]. Phosphorylation by Sch9 and PKA, and nuclear export by Msn5 are important for maintaining its cytoplasmic localization[15-17]. Upon stress, Maf1 is dephosphorylated, accumulates in the nucleus, and becomes highly enriched at Pol III target genes, as shown by whole-genome ChIP-on-chip studies[12,13]. Furthermore, *in vitro* systems have demonstrated that Maf1 can block recruitment of TFIIIB to preformed TFIIIC-DNA complexes[11]. However, *in vivo*, Maf1 is also able to repress Pol III at a time when all three subcomplexes remain on DNA (TFIIIB, TFIIIC, and Pol III). The data can be reconciled by postulating two phases of repression: 1) the acute phase (within 30 min of stress/nutrient deprivation), during which Maf1 associates with Pol III on DNA and represses transcription, and 2) the prolonged phase, during which TFIIIB and Pol III are displaced from DNA and recruitment of new active Pol III complexes is inhibited. As Pol III specifically interacts with the hypophosphorylated form of Maf1, it is likely that the major role of Maf1 dephosphorylation is in the acute phase of repression[12].

Since Maf1 dephosphorylation is a common mechanism in all reports of Maf1-dependent repression of Pol III to date, the identity of the phosphatase(s) and how it/they are regulated is a central question. As Pol III repression in diverse unfavorable conditions (representing multiple signaling pathways) each require Maf1, diverse phosphatases from each of these pathways could, in principle, act on Maf1. Alternatively, one phosphatase could account for the majority of Maf1 dephosphorylation in response to all Pol III-repressive stresses. Many phosphatases have been tested for their requirement in dephosphorylation of Maf1, with one report strongly pointing to the PP2A family of serine/threonine phosphatases[13]. These phosphatases are interesting as a group, since they are regulated by Target of rapamycin (TOR), and specific inhibition of TOR nutrient signaling with the macrolide antibiotic rapamycin induces rapid inhibition of Pol III transcription[18]. The regulation of PP2A phosphatases by TOR suggests a possible mechanism of integrating nutrient availability and other stresses to dephosphorylation of Maf1. Regulation of PP2A family phosphatases by TOR occurs via the protein Tap42. Tap42 interacts with the PP2A family catalytic subunits Pph21, Pph22, Pph3, and Sit4[19-21] and this interaction is reinforced by TOR phosphorylation of Tap42[22]. Upon inhibition of TOR by the drug rapamycin or by poor nutrient source, the phosphatases become active, probably by dissociating from Tap42 and associating in their respective holoenzymes[23]. While Sit4 is not involved in Pol III repression[3,12], a potential role for Pph21/22 or Pph3 has been reported[13]. Pph21, Pph22 and Pph3 have frequently been reported as alternative catalytic subunits of the PP2A phosphatase complex.

Notably, PP2A has been described as the Maf1 phosphatase, as the triple catalytic mutant of phosphatases *pph21*Δ, *pph22-ts*, and *pph3*Δ is defective for Maf1 dephosphorylation and Pol III repression. However, in other work, the PP2A scaffold and catalytic mutants *tpd3*Δ and *pph21*Δ*pph22*Δ, respectively, were not defective for Maf1 dephosphorylation, initially raising the possibility that PP2A may not be the Maf1 phosphatase[12]. Furthermore, there is a growing body of evidence supporting Pph3 as part of an evolutionarily conserved phosphatase complex, Protein Phosphatase 4 (PP4). Pph3 homologs have been studied in amoeba, budding yeast, human, worms, and fruit flies and found to have a conserved role in the regulation of the DNA damage response[24-26]. In addition, interaction of Pph3 (or its homologues) with PP4-specific subunits has been shown in humans, *S. cerevisiae*, *D. discoideum,* and *C. elegans*[24-26]. In this study, we demonstrate that Pph3 is the catalytic subunit of PP4 and not PP2A in yeast. We then provide multiple lines of evidence that the PP4 complex (Pph3 and certain other components) is the major and direct phosphatase of Maf1 in response to multiple stress pathways in yeast. Notably, Pph3 is needed for acute repression in response to diverse stresses, suggesting that Maf1 and PP4 are co-integrators of nutrition, stress, and integrity. Finally, we develop and utilize a Maf1-Pol III fusion protein that has proven useful in identifying functional PP4 components, and which may be a valuable tool in uncovering and characterizing other components involved in Pol III repression.

Results

A Maf1-Rpc160 Fusion Recapitulates Maf1-dependent Pol III Transcriptional Repression

Our initial goal was to determine the factors required for Maf1-dependent execution of Pol III transcriptional repression. To begin, we created a genetic tool: a fusion protein involving Maf1 fused to the amino terminus of the large subunit of RNA Pol III (Rpc160), a subunit that directly binds Maf1 during repression[13,27](see Introduction). The expressed Maf1-Rpc60 protein is expected to localize to the nucleus, interact with the Pol III machinery, and attenuate its activity–leading to reduced growth–with the relief of repression as the basis for the screen. Maf1-Rpc160 contains the entire open reading frame (ORF) of *MAF1*, a linker of 10 or 25 (not shown) amino acids (aa), the entire ORF of RPC160, and a 3XHA tag (Fig. 3.1A). The *GAL1* promoter enables galactose-inducible expression of Maf1-Rpc160, and a control construct was also created (lacking Maf1) that expresses only tagged Rpc160.

In galactose-containing medium, the Maf1-Rpc160 fusion and Rpc160 constructs express proteins at the expected molecular weights of ~212kDa and ~167kDa, respectively (data not shown). To determine whether the fusion protein affects Pol III transcription, RNA was isolated from cells grown in glucose or galactose for 4 h. Northern blotting was performed using probes complementary to U4 (control Pol II target) and pre-tRNA^{Leu3} (a Pol III target); pre-tRNAs are examined to distinguish new transcription from highly stable spliced tRNAs. As expected, in conditions where the fusion protein is expressed,

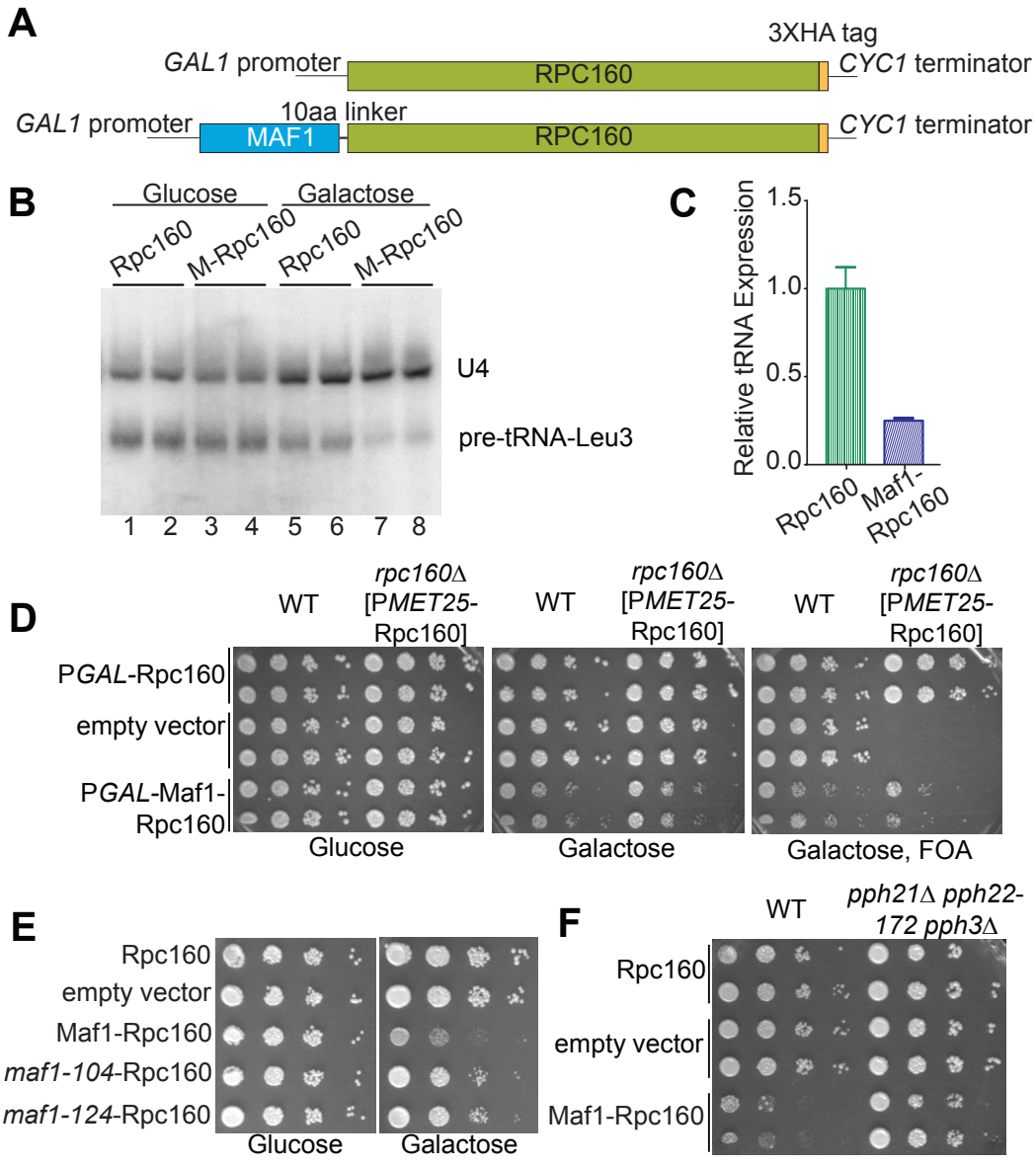

Figure 3.1 A Maf1-Rpc160 fusion functionally represses Pol III transcription and is a screening tool to identify Maf1-dependent repressors of Pol III. (A) Constructs of galactose-inducible Rpc160 or Maf1-Rpc160 fusion. (B) Expression of the Maf1-Rpc160 fusion but not Rpc160 represses pre-*tRNA*^{Leu3} transcription. (C) Quantification of lanes 5-8 of (B) as a ratio of tRNA/U4 band intensity with Rpc160 set to 1. Error bars represent standard deviation. (D) Expression of the Maf1-Rpc160 fusion but not Rpc160 confers a dominant growth defect. (E) The fusion growth defect is dependent on a functional Maf1. Null missense mutations in the Maf1 portion of the fusion partially suppress the fusion growth defect. (F) Partial suppression of the growth defect in triple mutant *pph21Δ pph22-172 pph3Δ* on plates containing galactose validates the Maf1-Rpc160 fusion as a tool for identifying Pol III repression pathway players.

new $tRNA^{Leu3}$ production is reduced to approximately 25% of levels seen in induction of Rpc160 alone (Fig. 3.1B, C), which equates to approximately 10% of normal levels (data not shown). This demonstrates that the fusion protein confers Pol III transcription.

We also tested the fusion for growth inhibition on galactose-containing plates. The reduction in tRNA levels by the fusion protein correlated with a growth defect on galactose-containing plates, as determined by colony size (Fig. 3.1D, left and middle). This is a dominant growth defect as it is seen in WT and *rpc160*Δ [$RPC160^{+}$] cells, both of which also express the WT version of Rpc160 (Fig. 3.1D, middle panel). A similar growth defect was found for the small (10aa) and large (25aa) linker sizes (data not shown), and future experiments were performed with the small linker fusion. The fusion is functional, as it complements *rpc160*Δ when loss of the WT Rpc160 (*URA3*) vector is enforced with FOA (Fig. 3.1D, right). In conclusion, the functional consequence of reduced expression of Pol III targets is a slow-growth phenotype, which we have termed the "fusion growth defect."

Two controls are needed to ensure that the magnitude of the growth defect is meaningful, and not trivial. First, growth inhibition may be solely due to overexpression of Maf1 in the fusion, with no need for the fusion to Rpc160. However, no growth defect was observed on galactose-containing plates, compared to empty vector controls (data not shown). Second, fused Maf1 may simply impair Rpc160 by a nonspecific mechanism. To test this, we created missense mutations in the Maf1 portion of the fusion construct, utilizing mutations

(*maf1-104* and *maf1-124*) that create strong hypomorphic alleles and resist dephosphorylation, based on previous studies[12]. Remarkably, both rescued the fusion growth defect, even while in a fusion context (Fig. 3.1E), suggesting that the fusion growth defect requires a functional Maf1 fused upstream of Rpc160 (and possibly proper phosphorylation dynamics) for full growth repression.

To evaluate the main candidate phosphatases for Maf1-dependent Pol III-repression, we transformed the fusion construct or control plasmids into a triple phosphatase mutant lacking Pph3 and the PP2A catalytic subunit Pph21, and bearing a hypomorph of Pph22. This strain has been shown to be defective for normal Maf1 dephosphorylation and Pol III repression[13]. The fusion growth defect was moderately rescued in this strain (Fig. 3.1F), suggesting that the activity of the fusion protein can be regulated by phosphorylation and that this construct can be used as a tool to look for candidates in the repression pathway.

Pph3 Is Required for Maf1-dependent Acute-phase Repression of Pol III Transcription

We then used the fusion tool to address the important question of the role of Pph3, and whether it resides in PP4 or PP2A (see Introduction). To investigate the role of Pph3 in Maf1-dependent repression of Pol III, we assayed WT and *pph3*Δ null strains by 1) Western blot, 2) Northern blot, 3) our fusion growth assay, and 4) immunofluorescence (IF).

To determine whether Pph3 is required for dephosphorylation of Maf1, HA-tagged Maf1 controlled by its endogenous promoter was transformed into WT or *pph3*Δ strains. Extracts from untreated cells or cells treated with nutrient

deprivation (ND), or rapamycin (125 nM) for 25 min were subjected to Western blot. Cells were pretreated with cycloheximide (CHX) to examine resident, but not newly translated, Maf1. Pph3 is required for dephosphorylation of Maf1 in response to nutrient deprivation and inhibition of TOR, as phosphorylated Maf1 persists following ND or rapamycin treatment (Fig. 3.2A).

When WT cells are treated with rapamycin but not ND, total Maf1 levels decrease (Fig. 3.2A), suggesting there may be two modes of Maf1 regulation by rapamycin: protein stability and dephosphorylation. Importantly, Maf1 degradation in rapamycin treatment also occurs in *pph3*Δ cells (Fig. 3.2A and data not shown), suggesting that Pph3 is required for rapamycin-induced acute dephosphorylation but not degradation of Maf1.

To determine whether inability to dephosphorylate Maf1 in *pph3*Δ cells would confer a Pol III repression defect, we isolated RNA from WT, *pph3*Δ, and complemented *pph3*Δ [PPH3] (*pph3*Δ mutant with WT Pph3 plasmid). As determined by Northern blot, *pph3*Δ is defective for full repression of Pol III transcription in nutrient deprivation (Fig. 3.2B, C). This defect was complemented by a WT cloned version of Pph3 (FLAG-tagged at the N-terminus) (Fig. 3.2B, C). Of note, at longer time-points (e.g., 1 h), repression of Pol III occurs in *pph3*Δ as well as in WT, suggesting that dephosphorylation of Maf1 is important in the acute phase of repression but not prolonged repression (data not shown). Importantly, we see rescue of the fusion growth defect in the *pph3*Δ null (Fig. 3.2D), consistent with an independent role for Pph3 in Maf1-dependent repression of Pol III.

Figure 3.2 Pph3 plays a nonredundant role in global Pol III repression. (A) Nutrient deprivation (ND) and rapamycin treatment (Rap) cause dephosphorylation of Maf1 in WT but not *pph3Δ* mutant strain. (B) Northern blot showing repression of pre-$tRNA^{Leu3}$ transcription in WT strain (top) in response to ND. Repression is absent in *maf1Δ*, attenuated in *pph3Δ* and restored by complementing with Pph3 on a plasmid. (C) Quantification of (B) as a ratio of tRNA/U4 band intensity. Values represent the average of band intensities from two replicate blots. Error bars represent the standard deviation. Significance value calculated as a comparison of WT to mutant strain by Student's t-test. * p-value<0.05 (D) The fusion growth defect is partially suppressed in *pph3Δ* strain. (E, F) Nuclear localization of Maf1-HA in response to nutrient deprivation in (E) WT and (F) *pph3Δ*. Localization of Maf1 to the nucleus is delayed in *pph3Δ* compared to WT. (G) Distribution of Maf1 localization in WT and *pph3Δ* strains at t = 0, 30 min, and 6 h. Significance values calculated as difference between nuclear (N>>C, N>C) and cytoplasmic (C>N, C≈N) Maf1 in WT and *pph3Δ* using Fisher's exact test.

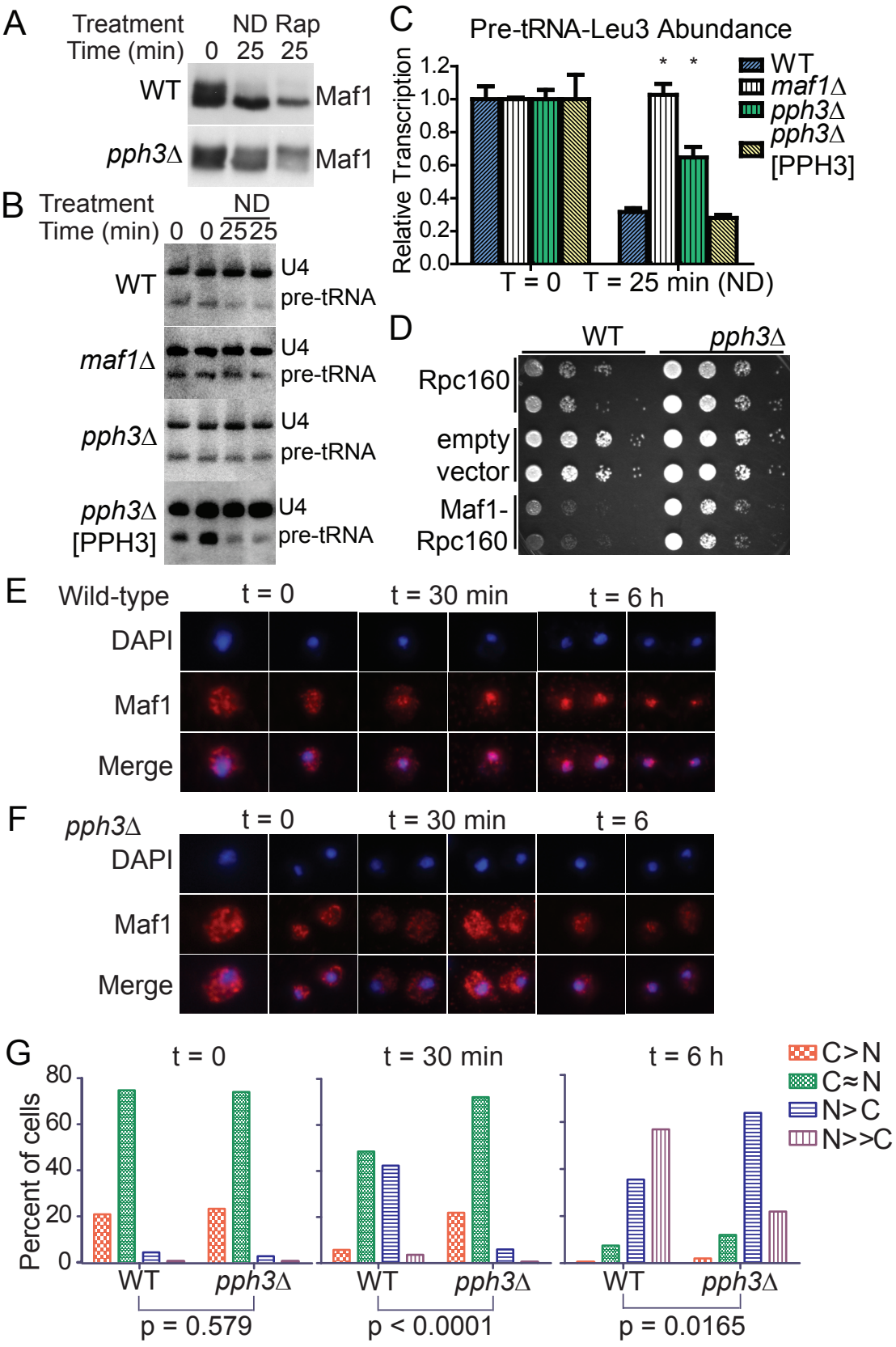
A
Treatment
Time (min)
ND Rap
0 25 25
WT
Maf1
pph3Δ
Maf1
B
Treatment
Time (min)
ND
0 0 25 25
WT
maf1Δ
pph3Δ
pph3Δ [PPH3]
U4 pre-tRNA
C
Pre-tRNA-Leu3 Abundance
Relative Transcription
1.2
1.0
0.8
0.6
0.4
0.2
0.0
* *
T = 0
T = 25 min (ND)
WT
maf1Δ
pph3Δ
pph3Δ [PPH3]
D
WT
pph3Δ
Rpc160
empty vector
Maf1-Rpc160
E
Wild-type
t = 0
t = 30 min
t = 6 h
DAPI
Maf1
Merge
F
pph3Δ
t = 0
t = 30 min
t = 6
DAPI
Maf1
Merge
G
t = 0
t = 30 min
t = 6 h
Percent of cells
80
60
40
20
0
WT
pph3Δ
p = 0.579
p < 0.0001
p = 0.0165
C>N
C≈N
N>C
N>>C

To determine whether nuclear translocation of Maf1 is affected in *pph3*Δ mutants, WT and *pph3*Δ cells were treated with ND and examined after 30 min and 6 h. By IF, *pph3*Δ shows a defect/delay in the translocation of Maf1 to the nucleus compared to WT (Fig. 3.2E-G). In untreated cells, the distribution of Maf1 is similar in WT compared to *pph3*Δ cells. After 30 min treatment, Maf1 localization becomes more nuclear in the WT strain, but in the *pph3*Δ strain, Maf1 localization appears unchanged from the untreated state (Fig. 3.2G). After 6 h of treatment, the Maf1 localization profiles appear similar in WT and *pph3*Δ, consistent with a role for Pph3 in acute but not prolonged repression of Pol III transcription.

Pph3 Is in Protein Phosphatase 4 but not

Protein Phosphatase 2A

To understand the regulation of Pph3 in stress-activated repression of Pol III, we determined which phosphatase complex(es) Pph3 resides in—PP4 or PP2A. Pph3 can stably interact with several yeast proteins *in vivo,* including Psy2 and Psy4[24]. The complex of Pph3, Psy2 and Psy4 (or their homologues) is one form of Protein Phosphatase 4 (PP4). Whether yeast Pph3 can bind to the PP2A scaffold has not been tested.

To test whether Pph3 could interact with Tpd3, we transformed strains with Pph3-FLAG and/or Tpd3-myc constructs and prepared extracts. Immunoprecipitation (IP) of Pph3 with FLAG-agarose beads captures approximately 90% of the Pph3 in the extract, yet no Tpd3 is found to be associated (Fig. 3.3A). To ensure that the conditions allow Tpd3-phosphatase

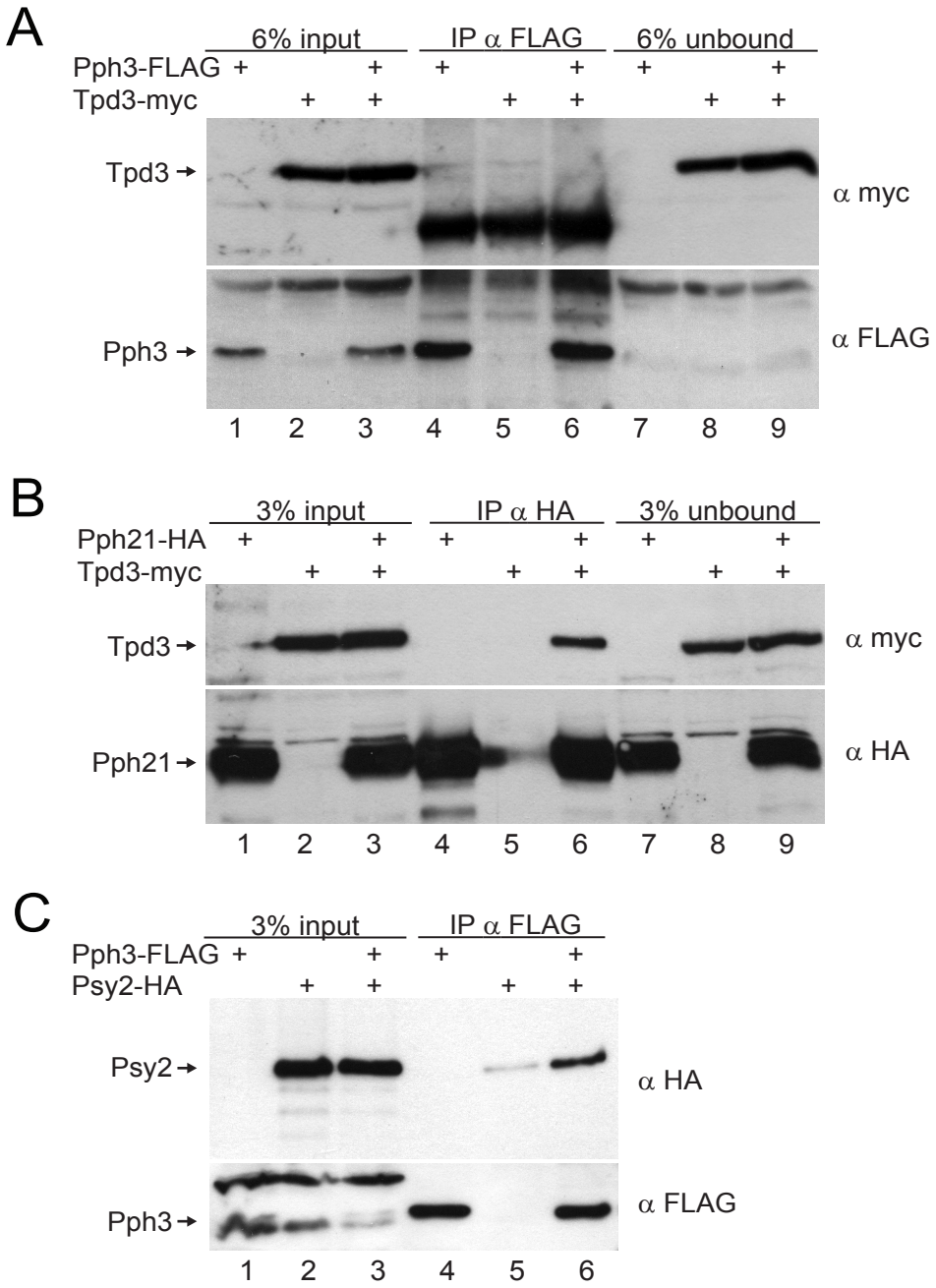

Figure 3.3 Pph3 is part of the Protein Phosphatase 4 complex (PP4) but not PP2A. (B) Pph3 does not interact with Tpd3. (A) Pph21 binds to the PP2A scaffold Tpd3. (C) Pph3 interacts with the PP4-specific subunit Psy2.

association, a control IP was performed between Tpd3 and Pph21 under the same conditions. Strains transformed with the Tpd3-myc construct and Pph21-HA show a specific physical interaction (Fig. 3.3B). Also, as a positive control, we tested whether our Pph3 construct could interact with Psy2, a PP4-specific subunit. Under the same conditions, we found that Pph3 binds to Psy2 (Fig. 3.3C), confirming its presence in the PP4 complex. These results show that yeast Pph3 is present in PP4 but not in PP2A under the conditions tested.

Pol III Repression Requires PP4 Subunit Psy2

but not PP2A Subunits

In order to determine the relative functional roles of PP4 and PP2A regulatory subunits in Maf1-dependent repression of Pol III, we assayed mutants of regulatory subunits for each complex with our fusion growth assay. We also analyzed the ability of these mutants to dephosphorylate Maf1 by Western blot.

Pph3 associates stoichiometrically with Psy2 and Psy4 (ref. 28 and data not shown); therefore, we tested mutants lacking either (or both) of these genes to determine whether either acts with Pph3 in repression of Pol III. In screening these PP4 subunit mutants, we saw that *psy2Δ* mutants rescue the fusion growth defect to the same degree as seen in the *pph3Δ* mutant (Fig. 3.4A, left three panels). In contrast, The *psy4Δ* mutant shows little or no rescue of the fusion growth defect and no additive effect when combined with the *psy2Δ* mutation, illustrating that Psy4 is not required for Pol III repression in this assay (Fig. 3.4A, right three panels). Importantly, Psy2 is required for dephosphorylation of Maf1 as is Pph3 (Fig. 3.4B). By Western blot analysis, we see that Psy4 is not

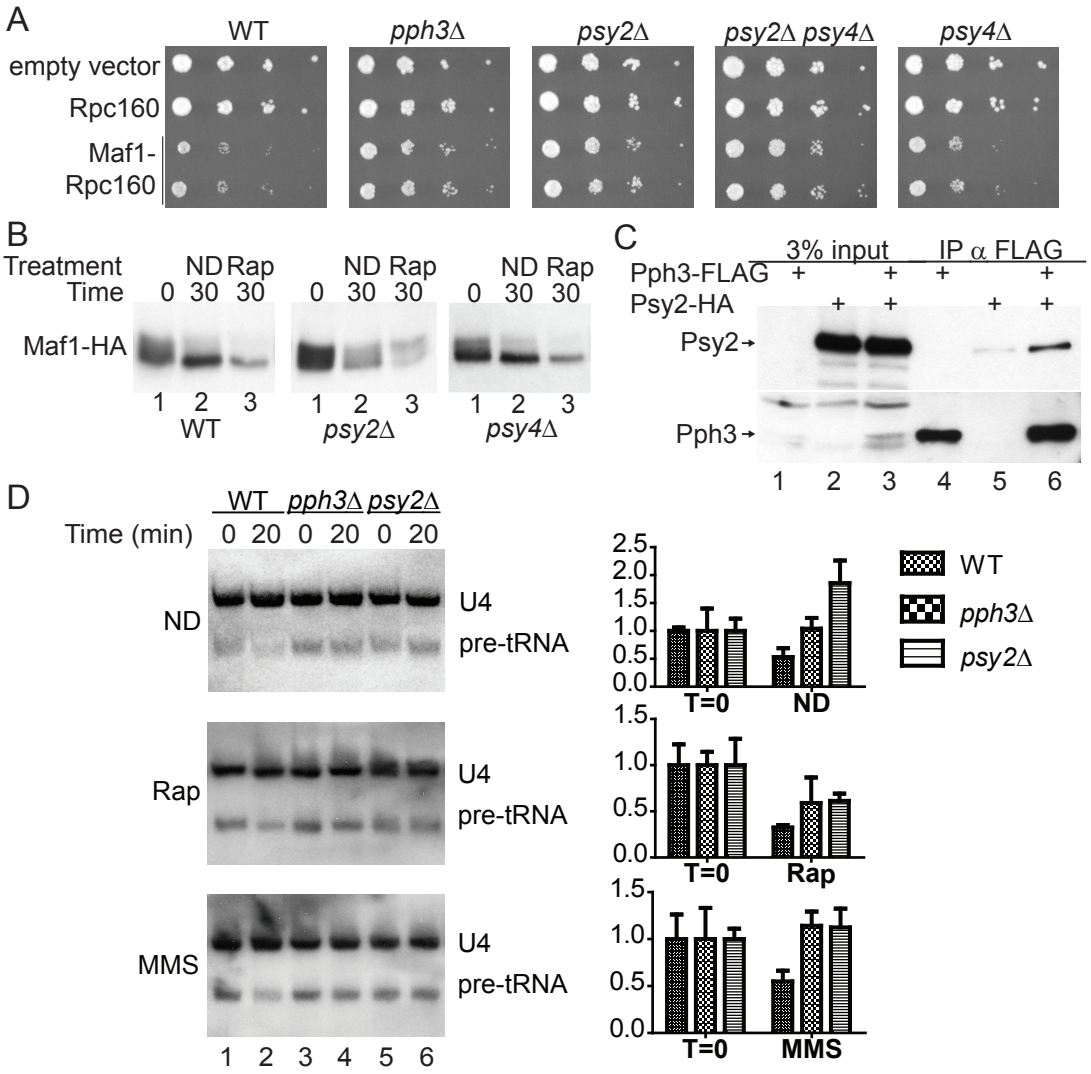

Figure 3.4 PP4 complex members play a role in steps of Pol III repression. (A) The fusion growth defect is partially rescued in some PP4 mutant strains. (B) Maf1 is dephosphorylated in WT but not *psy2Δ* mutant in response to nutrient deprivation (ND) and rapamycin (Rap). Psy4 is not required for dephosphorylation of Maf1. (C) Psy2 and Pph3 can interact in the absence of Psy4. (D) Pph3 and Psy2 are required for reduction of nascent tRNA levels in ND, Rap and MMS treatments. Panels on the right are a quantification of two replicates as a ratio of tRNA/U4 band intensity, with T = 0 set to 1; panels on the left show one representative replicate. Error bars represent standard deviation.

required for dephosphorylation of Maf1 (Fig. 3.4B), consistent with a view that a Pph3-Psy2 complex is acting to direct dephosphorylation of Maf1. This result suggests that Pph3 and Psy2 might interact in the absence of Psy4. Indeed, we performed an IP of Pph3 and Psy2 in the *psy4Δ* strain and found clear interaction (Fig. 3.4C).

To test whether Psy2 is required for repression of Pol III at the transcriptional level, we isolated RNA from WT, *pph3Δ*, and *psy2Δ* strains treated with ND, rapamycin, or MMS, and assayed for new Pol III transcription by Northern blot. We found that *psy2Δ* is defective for Pol III repression in the acute phase in a magnitude similar to *pph3Δ* (Fig. 3.4D).

PP2A is a heterotrimeric complex composed of the scaffold (Tpd3), a catalytic subunit (Pph21 or Pph22) and a regulatory subunit (Cdc55 or Rts1)[29]. Since Pph21 and Pph22 are essentially redundant, we created a double null in the S288C background to test in our assays. Notably, when the double *pph21Δpph22Δ* mutant was tested in the fusion growth assay, it showed no rescue and grew more slowly than the WT strain with the fusion construct (Fig. 3.5A, left two panels). A similar result was obtained with the *tpd3Δ* mutant (Fig. 3.5A, third panel). Furthermore, mutation in either regulatory subunit of PP2A shows no rescue of the fusion growth defect (Fig. 3.5A, right two panels). Previous results showed that W303 background *pph21Δpph22Δ* and *tpd3Δ* mutants[12] are not defective for dephosphorylation of Maf1 in response to nutrient deprivation. Because strain background differences have been reported for different PP2A family phosphatase mutants due to variable *SSD1* alleles[30,31], we

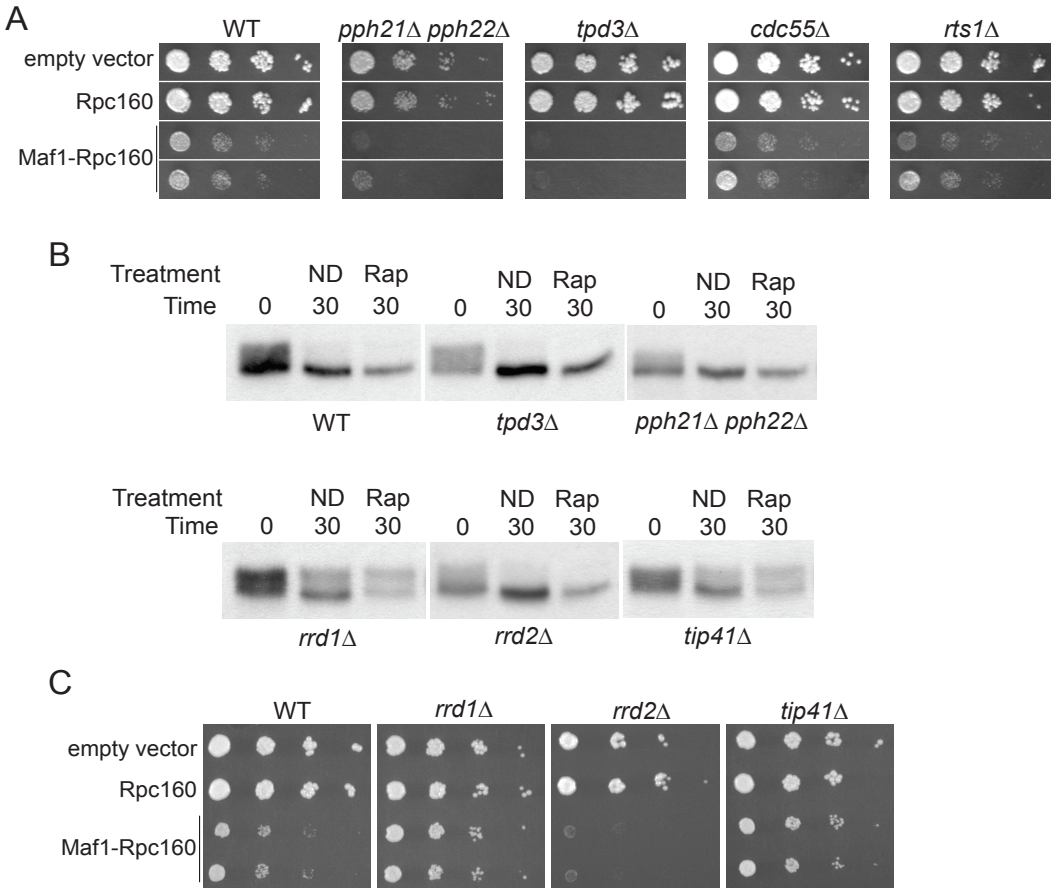

Figure 3.5 Pol III repression requires PP4 accessory factors, but not PP2A subunits. (A) The fusion growth defect remains or is intensified in PP2A mutant strains. (B) Neither Tpd3, Pph21, nor Pph22 are required for dephosphorylation of Maf1 in nutrient deprivation (ND) or rapamycin (Rap) treatment. PP4-associated factors Tip41 and Rrd1 are required for dephosphorylation of Maf1 in ND and Rap, but PP2A-associatd Rrd2 is not required. (C) The fusion growth defect is rescued in *rrd1Δ* and *tip41Δ* mutants, but not *rrd2Δ*, correlating to Western blot data in (B).

tested *pph21Δpph22Δ* and *tpd3Δ* mutants in S288C background and found them to similarly have the ability to dephosphorylate Maf1 in response to nutrient deprivation (ND) or rapamycin treatment (Fig. 3.5B). The lack of rescue of PP2A mutants in the fusion growth assay and the ability of PP2A mutants to dephosphorylate Maf1 strongly suggest that PP2A is not the major phosphatase involved in Maf1-dependent repression of Pol III.

The results above show a high correlation between mutants that rescue the fusion growth defect and those defective in the dephosphorylation of Maf1 (Fig. 3.4B). In order to further investigate the different roles of PP4 and PP2A, we used the fusion construct to screen other genes whose protein products have been shown to be in complex with catalytic subunits of these complexes at substoichiometric levels. The yeast protein tyrosyl phosphatase activators Rrd1 and Rrd2 are conserved proteins involved in activating the PP2A-like family of phosphatases[32]. Rrd1 shows a preference for interacting with PP2A-like phosphatases Pph3, Sit4 and Ppg1, while Rrd2 only interacts with Pph21 and Pph22[32]. Consistent with a role for Rrd1 in activating PP4, *rrd1Δ* mutants show rescue of the fusion growth defect (Fig. 3.5C) and are defective for Maf1 dephosphorylation in ND and rapamycin treatment (Fig. 3.5B). In contrast, *rrd2Δ* mutants show an enhanced fusion growth phenotype similar to *pph21Δpph22Δ* or *tpd3Δ* mutants and are not defective for Maf1 dephosphorylation by Western blot in ND or rapamycin (Fig. 3.5B,C). Again, this is consistent with PP4 as the major phosphatase involved in Pol III repression.

Tip41 is a member of the TOR signaling pathway that physically interacts with PP2A family phosphatases, including Pph3, Pph21/22, and Sit4[20,24,33]. Upon inhibition of TOR, Tip41 binds to the phosphatases and activates them[20,24]. Tip41 interacts with PP4 at substoichiometric levels and a role for Tip41 in Pph3 regulation has been implicated in the DNA damage response[24]. When the fusion construct is transformed into *tip41Δ* mutants, we see rescue of the growth defect, suggesting that Tip41 plays a role in activation of Maf1, likely in concert with Pph3 (Fig. 3.5C). *tip41Δ* mutants were also defective in dephosphorylation of Maf1, consistent with the results of the fusion growth assay (Fig. 3.5B).

Maf1 Interacts Directly with Pph3

Since Maf1 remains phosphorylated in *pph3Δ* and *psy2Δ* strains, it seemed likely that PP4 could dephosphorylate Maf1 directly, although there was a possibility that PP4 could regulate Maf1 indirectly, via a different phosphatase. To distinguish between these two models, we determined whether Maf1 could interact physically with Pph3. Because interactions between an enzyme and its substrate are often transient and difficult to detect, we attempted to maximize the chance of detecting an interaction by cross-linking the cells with 1% formaldehyde. We cloned Pph3 under the control of the *MET25* promoter in order to overexpress the protein in medium lacking methionine. Here, HA-tagged Maf1 was co-expressed with FLAG-tagged Pph3. We looked for an interaction by co-IP in unstressed cells as well as cells stressed with MMS for 30 min to activate the phosphatase. In both stressed and unstressed cells, we detect specific interaction of Pph3, enriched 3-4-fold above background (Fig. 3.6A,B).

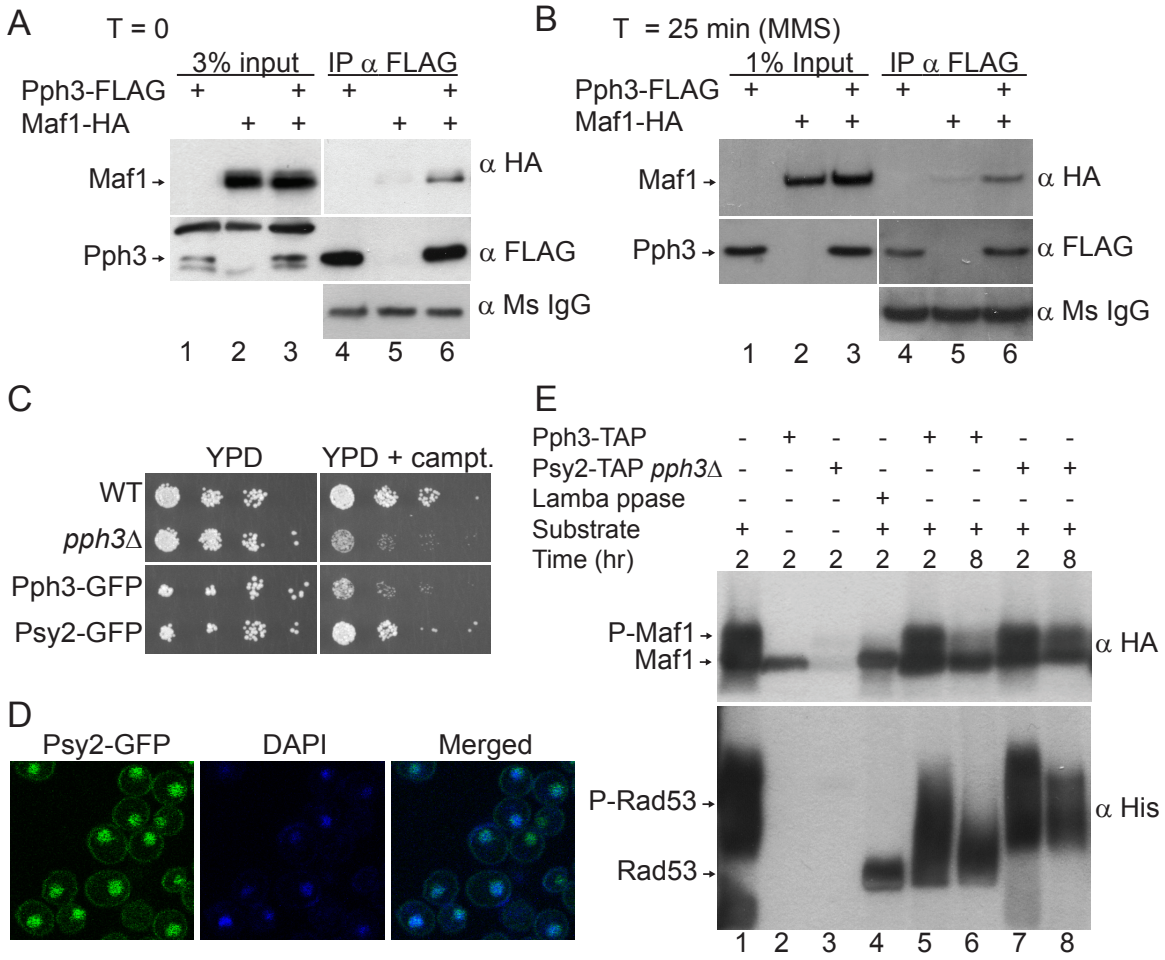

Figure 3.6 Pph3 dephosphorylates Maf1 directly. (A, B) Maf1 interacts with Pph3 in (A) unstressed cells and (B) MMS-treated cells. (C) Psy2-GFP strain grows well on plates with camptothecin, thus the PP4 complex is functional. Pph3-GFP fusion renders PP4 nonfunctional, as indicated by growth on camptothecin similar to *pph3Δ*. (D) Psy2-GFP localizes to the nucleus and cell membrane in unstressed cells. (E) Pph3-TAP complexes (but not Psy2-TAP complexes from *pph3Δ* background) are active on purified phosphorylated Maf1 (top panel) and Rad53 (bottom panel).

We detect only a small fraction of total Maf1 associated with Pph3 (<5%), which may be due to the difficulty of capturing enzyme-substrate interactions by IP. The level of association is similar in uncrosslinked extracts (data not shown), suggesting that the interaction is not an artifact of crosslinking nonspecific proteins.

PP4 Subunit Psy2 Is Localized in the Nucleus

As already mentioned, PP4 plays a role in DNA damage, which is one cellular perturbation that causes Pol III repression. PP4 dephosphorylates Rad53 and γH2AX in order to recover from the intra-S cell cycle checkpoint induced by DNA damage[28,34]. Recent data show that in the nuclear exportin *msn5Δ* mutant strain, Maf1 is constitutively localized in the nucleus but still requires dephosphorylation to repress Pol III[16]. This suggests that the phosphatase of Maf1 must be capable of localizing to the nucleus. All of the known substrates of yeast PP4 are nuclear proteins[34,35] (e.g., Rad53, γH2AX), and PP4 is activated towards these substrates in DNA-damaging conditions, putting PP4 in the proper time and place for filling the role of a Maf1 phosphatase.

In order to determine where Pph3 acts for its cellular function, we created nuclear and cytoplasmic versions of Pph3 (with either a nuclear localization sequence or nuclear export sequence encoded in the protein) and transformed them into *pph3Δ* cells. Both versions complement the null phenotype as well as WT Pph3 by growth on camptothecin plates and by pre-tRNA repression Northern blots (data not shown). This suggests that the action of the enzyme for

its DNA damage function, as well as its Maf1 dephosphorylation function can be in the nucleus or the cytoplasm. Alternatively, Pph3 activity could be required in a particular compartment, but there could be leaky mislocalization of the Pph3 proteins that is sufficient for complementing activity.

We also attempted to enhance the fusion growth defect by overexpression of WT Pph3 by growth of strains with Pph3 under control of Met15 promoter on plates lacking methionine, to no effect. Interestingly, overexpression of cytoplasmic Pph3 caused *suppression* of the fusion growth defect (data not shown). As this phenocopies the growth ability of a *pph3Δ* strain with the fusion, it could be that overexpression of Pph3 in the cytoplasm titrates limiting enzyme complex members (e.g., Psy2) into the cytoplasm, causing nuclear PP4 function to be abrogated. This could suggest that Pph3 enzyme activity causing the fusion growth defect is required in the nucleus. This may reflect the natural localization requirement for enzyme activity, or it could reflect the requirement of enzymatic activity in our fusion assay only, as the fusion likely localizes in the nucleus (as evidenced by its complementation of *rpc160*Δ null lethality [Fig. 3.1D, third panel], which suggests it can incorporate into Pol III complexes and provide activity).

To determine the localization of PP4, we obtained strains with GFP-tagged Pph3 or Psy2. To test whether the GFP fusion proteins allow a functional phosphatase, the growth ability for the strains was assayed on plates containing camptothecin. Psy2-GFP strains show growth similar to WT, although Pph3-GFP strains show growth similar to *pph3Δ* (Fig. 3.6C), suggesting that GFP

fused to Psy2 but not Pph3 permits a functional complex with proper localization. By fluorescent microscopy, we see that Psy2-GFP shows strong nuclear localization, consistent with the predicted location of the Maf1 phosphatase (Fig. 3.6D). This suggests that Maf1 dephosphorylation most likely occurs in the nucleus, and the accumulation of Maf1 in the nucleus during stress is due to the inability to shuttle dephosphorylated Maf1 out of the nucleus[16].

PP4 Dephosphorylates Maf1 *In Vitro*

In addition to the genetic and molecular data shown above, we attempted to reconstitute the dephosphorylation of Maf1 by PP4 *in vitro*. To do this, we incubated IgG-bound complexes from a Pph3-TAP strain, or a Psy2-TAP strain with *pph3Δ* null as a negative control. Both Pph3-TAP and Psy2-TAP have been shown previously to bind stably to the other main components of PP4 (e.g., Pph3, Psy2, and Psy4) and their purified complexes have phosphatase activity, unless *PPH3* is deleted[28]. To verify activity of the enzyme complex, we used phosphorylated Rad53, which was shown previously to be a native substrate[28]. As seen in Figure 3.6E (bottom panel), Pph3-TAP is active at 2 and 8 h against Rad53 and Psy2-TAP *pph3Δ* complexes are not. By quantifying the change in Rad53 mobility, at 2 h, Pph3-TAP has 22.2% (±0.7) of the activity seen by lambda phosphatase and 34.8% (±3.1) of the lambda activity at 8 h (when comparing the change in the bottom band as a percentage of total Rad53 signal per lane; see Methods). Likewise, Pph3-TAP complexes are active at 8 h against phosphorylated Maf1 (Fig. 3.6E, top panel). Because of the poor separation of the phosphorylated species of Maf1 compared to Rad53, it is

difficult to see much difference in phosphorylation at 2 h. The quantified change in Maf1 mobility shows that at 2 h, the Pph3-TAP complex has 5.3% (±3.7) of the activity of lambda phosphatase and 43.0% (±4.1) activity at 8 h. The Psy2-TAP *pph3Δ* complexes show <4% of the activity of lambda phosphatase on both Rad53 and Maf1 at 2 h and 8 h. Taken together, these data show that a PP4 complex containing Pph3 can dephosphorylate Maf1.

Pph3 Is an Integrator of Multiple Signals for Maf1 Dephosphorylation

The simplest explanation for regulation of Maf1 dephosphorylation during acute repression consists of a single phosphatase complex acting in response to all stresses, but there could potentially be multiple phosphatases regulating Maf1 in response to different stresses. To address this, we sought to test for the requirement of Pph3 for dephosphorylation of Maf1 in other, some of which have been reported to repress Pol III. Extracts were prepared from WT and *pph3Δ* cells stressed with the DNA-damaging agent methyl methanesulfonate (MMS), cycloheximide (CHX), chlorpromazine (CPZ), dithiothreitol (DTT), glycerol, glucose deprivation, nitrogen deprivation (ND), amino acid deprivation, or phosphate deprivation, all of which are associated with Pol III repression (except phosphorus deprivation)[3]. Phosphorus deprivation was included as a stress since it causes nuclear accumulation of tRNAs, similar to DNA damage and amino acid deprivation[36-38], although whether it causes Pol III transcription arrest has not been tested. Glucose deprivation is similar to ND treatment (i.e., both lack glucose) and produces similar results, in that Pph3 is required for

dephosphorylation of Maf1 (Fig. 3.7A). Maf1 dephosphorylation in cells with glycerol as the main carbon source is also Pph3-dependent (Fig. 3.7A). Endoplasmic reticulum stress with DTT and cell wall stress with CPZ are also Pph3-dependent stresses (Fig. 3.7B). The remaining stresses tested have been reported to repress Pol III (except phosphorus limitation), but whether they are accompanied by dephosphorylation of Maf1 has not been reported. As seen in CHX treatment, dephosphorylation of Maf1 begins between 30 and 60 min, therefore in treatments longer than 30 min, CHX is not included, in order to ensure the dephosphorylation we see is due to the stress and not the supplemental CHX. Notably, this dephosphorylation seen in CHX is Pph3-dependent (Fig. 3.7C). Pph3 is also required for full dephosphorylation of Maf1 in nitrogen, amino acid, and phosphorus deprivation treatments (Fig. 3.7D–E). These findings demonstrate that the Pph3 phosphatase complex PP4 is able to integrate multiple nutrient and stress signals to effect bulk dephosphorylation of Maf1.

Discussion

PP4 as an Integrator of Multiple Stress Conditions For Dephosphorylation of Maf1

As Maf1 is a conserved, central regulator of Pol III and its phosphorylation status is correlated with activity of Pol III in response to all known Pol III-repressive stresses tested thus far, it is important to understand how phosphorylation of Maf1 is regulated.

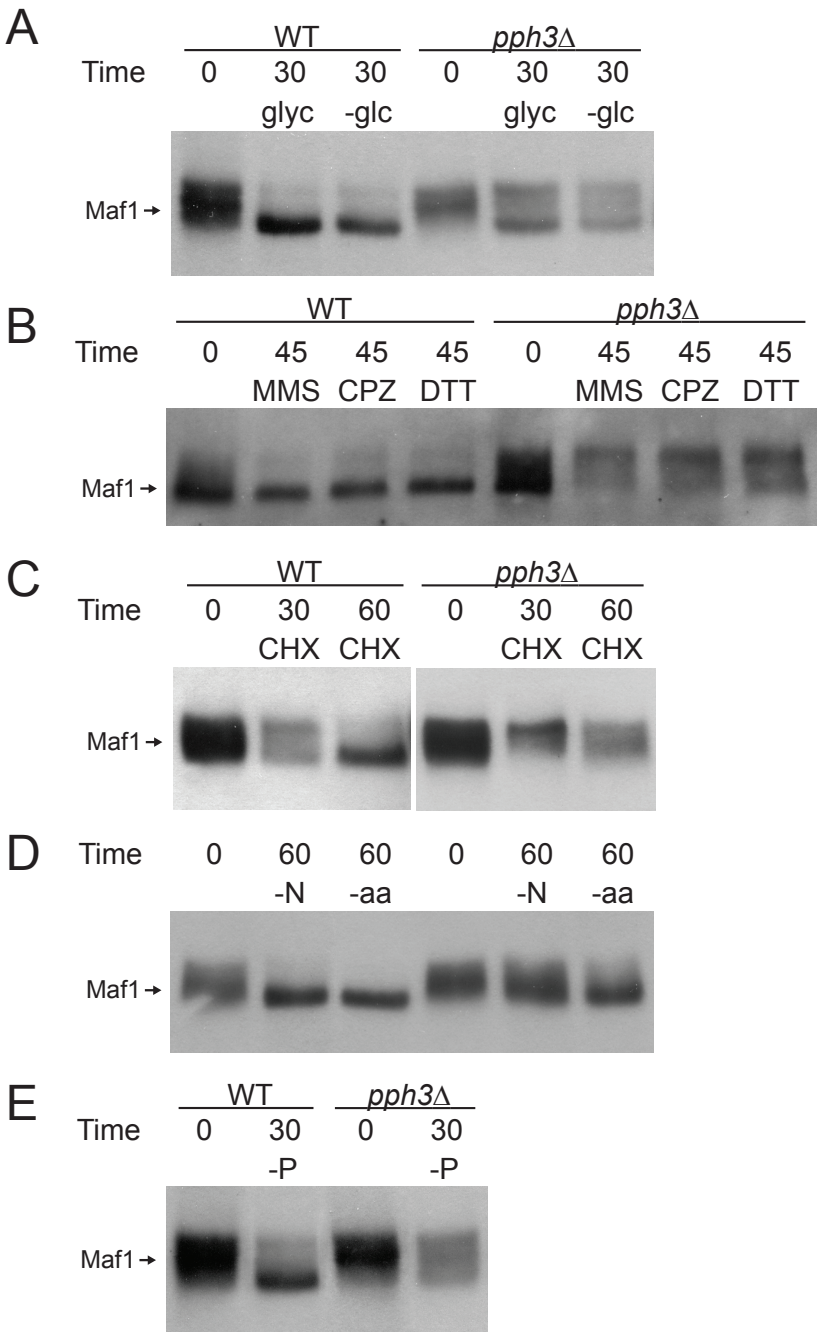

Figure 3.7 Pph3 is required for dephosphorylation of Maf1 in multiple stress conditions. (A-E) Maf1 dephosphorylation requires Pph3 in (A) glycerol as carbon source, no carbon source, (B) extended cycloheximide (CHX), (C) methyl methanesulfonate (MMS), chlorpromazine (CPZ), dithiothreitol (DTT), (D) nitrogen deprivation (-N), amino acid deprivation (-aa), and (E) phosphorus deprivation (-P).

Here, we show that Pph3 is required for full repression of Pol III transcription in response to multiple stresses. Pph3 has previously been identified as a potentially important phosphatase subunit involved in regulation of Maf1[13], but whether it could function independently of PP2A catalytic subunits, as well as the identity of the complex of which it was a member in this process had not been previously determined. Here, we provide evidence that Maf1 is dephosphorylated by Protein Phosphatase 4, composed of Pph3 and Psy2 (plus potential accessory factors Rrd1 and/or Tip41), in response to multiple stresses that lead to Pol III repression. This is further evidenced by the direct interaction of Pph3 and Maf1 herein detected by immunoprecipitation. Previous work investigating the role of Pkc1 in repression of Pol III showed that Pkc1 was required in nutrient deprivation but not rapamycin treatment[12], suggesting that these treatments converge on Maf1 via different pathways. This result, as well as the fact that there is a multitude of different stresses that can cause Pol III repression, argues that there could be multiple phosphatases regulating Maf1. We show here instead that a single phosphatase, PP4, is able to regulate phosphorylation of Maf1 in response to rapamycin, DNA damage, chlorpromazine, cycloheximide, and multiple types of nutrient deprivation.

Conserved Role for PP4 in the Stress Response

PP4 plays a role in the environmental stress response in many other species. PP4 has been shown to play a role in the DNA damage response in multiple species, including yeast, human, *C. elegans*, and *Drosophila*[24,25]. This has been shown to be in part via interaction with and dephosphorylation of

Rad53, which allows the cell to overcome G2/M arrest[28]. The human form of Pph3—PP4C—interacts with the human form of Tap42—IGBP1—suggesting that the involvement of human PP4 in mTOR and nutrient signaling might be conserved in humans[39]. Human PP4 was found to play a role in the inflammatory response via activation of nuclear factor-κB (NF-κB) p65 and c-Jun N-terminal kinase (JNK) in tumor necrosis factor (TNF-α) signaling[40,41]. In *Dictyostelium discoideum*, the PP4 complex is activated in response to starvation conditions in order for the cells to differentiate into fruiting bodies[26,42]. In addition to its role in the DNA damage response, *C. elegans smk-1* (homologue of Psy2) is required for the response to oxidative and innate immune stress required for long-lived worms[43]. Given the role for PP4 in the environmental stress response of higher organisms, it will be interesting to see if PP4 also plays a conserved role in dephosphorylation of Maf1.

PP4 Versus PP2A in Pol III Regulation

Initially, PP2A appeared to be a good candidate for regulation of Pol III. It was shown that in *tpd3Δ* cells, Pol III transcription was inhibited[44,45]. *In vitro* studies have shown that compared to free PP2A phosphatase subunits, the scaffold-catalytic dimer has less activity towards nonphysiological substrates[46], leading to the conclusion that Tpd3 is an inhibitor of PP2A and that *tpd3Δ* cells have overactive PP2A. However, genetic data suggest that Tpd3 is rather *required* for proper activity of PP2A, as *tpd3Δ* cells have similar phenotypes to *pph21Δpph22Δ* cells[47]. Instead of being required for repression of Pol III, the reduction in Pol III transcription seen in *tpd3Δ* cells suggests that PP2A is

required for proper Pol III transcription[3]. This idea can be explained with the following: since *tpd3Δ* cells have a slow growth phenotype and are lacking appropriate PP2A activity, it is likely that certain stress pathways are activated, which could activate PP4 and lead to repression of Pol III. Furthermore, it has been suggested by some that Pph3 is an alternative catalytic subunit of PP2A, although much evidence suggests that this is not the case. For example, initial reports showed that the rabbit homolog of Pph3, PPX, cannot bind to the homolog of the PP2A scaffold, $PP2A_A$, *in vitro*[48]. In contrast, recent studies in human cells using quantitative mass spectrometry report that there is a detectable amount of PP4C in complex with $PP2A_A$ and a few regulatory subunits of PP2A[49-51]. However, the low ratio of PP2A scaffold/regulatory subunits in complex with PP4C versus canonical PP2A catalytic subunits—approximately 1:60—suggests this type of complex is not abundant[51]. Importantly, there is no evidence suggesting that PP2A catalytic subunits can bind to PP4-specific subunits, such as Psy2. Here, we confirm that Pph3 is not a regular component of yeast PP2A and suggest rather that it is the catalytic subunit of PP4.

Potential Mechanisms for Regulation of PP4

In addition to the core phosphatase of Maf1, we also identify the proteins Tip41 and Rrd1 as potential accessory factors to PP4 in dephosphorylating Maf1. Tip41 was suggested to act in concert with PP4 in DNA damage[24] and has been shown to activate Sit4 and PP2A catalytic subunits towards their substrates Gln3[20] and Msn2[33], respectively. Rrd1 is the yeast homologue of human phosphotyrosyl phosphatase activator (PTPA) and is able to activate PP2A

family phosphatases *in vitro*[32], including Pph3. PTPA has been shown to have prolyl isomerase activity, by which it activates PP2A[52]. PTPA in complex with the catalytic subunit acts as a composite ATPase, required for its ability to activate PP2A[53]. The proline residue in human $PP2A_C$ required for this reactivation is Pro190, which is conserved in all yeast PP2A and PP2A-like phosphatase subunits, suggesting that a similar mechanism of activation could be occurring in yeast. It will be interesting to determine how PP4 is regulated by these or other proteins to dephosphorylate Maf1.

DNA damage often causes replication fork arrest, which appears to be the causative insult leading to repression of Pol III in response to DNA damaging agents[54]. Replication fork arrest-induced repression of Pol III was shown to be Maf1-dependent and to require both Rad53 and its target Dun1[54]. It was suggested that Pph3 could be a target downstream of Dun1. Interestingly, in a recent large-scale proteomics screen to identify targets of DNA damage pathway kinases one member of PP4, Psy4, was identified as a substrate of Mec1 and/or Tel1, however neither Pph3 nor Psy2—the subunits essential to regulation of Maf1—was identified as a substrate of either Mec1, Tel1, Rad53 or Dun1[55]. It is possible that other members PP4 are also targets of one of these kinases, since the screen was not saturating. Or, alternatively, a target of Dun1 could potentially regulate PP4 in response to DNA damaging reagents. In the likely scenario that PP4 is acting downstream of Rad53 in regulating Maf1, there arises the intriguing idea that PP4 could act in a feedback loop where Rad53 activates PP4 for dephosphorylation of Maf1, after which PP4 inactivates Rad53 to exit

from the DNA damage checkpoint[28], thus allowing Rad53 to be active only transiently.

Perspectives on Maf1-Pol III Fusion Action

While this manuscript was in preparation, the co-structure of Maf1 with yeast Pol III was solved[14], which provides interesting insights into the mechanism of action of the Maf1-Rpc160 fusion construct. The co-structure showed that Maf1 indeed binds to the complex in a manner to interact with the clamp domain of Rpc160 (aa 1-245). Therefore, Maf1 fused to the amino-terminus of Rpc160 is an ideal position to poise the complex for repression. In the crystal structure, it was determined that binding of Maf1 to Pol III causes a shift in the position of the C34 subunit within the complex that does not permit Brf1 to bind, effectively inhibiting Pol III from binding to TFIIIB-containing promoters. Other structural studies of Maf1 protein have shown that the phosphorylated form of Maf1 is correlated with absence of interaction between its amino-terminal A domain and its carboxyl-terminal BC domain, while dephosphorylation is correlated with their interaction[56]. This suggests that dephosphorylation helps to create a more compact Maf1 that could bind in the pocket between C34 and C82 in the Pol III complex. These results can help us understand how the fusion growth defect is seen at variable levels. As shown in the results, induction of the fusion protein in WT strain by galactose causes slower growth than normal (Fig. 3.1D). However, if a condition of stress, such as 10 nM rapamycin, is added to galactose plates, this causes the cells to arrest completely (data not shown). Alternatively, the fusion growth defect can be attenuated by deletion of the phosphatase. These

results can be explained by the idea that Maf1 in the fusion context is dephosphorylated and binding more strongly to the complex than usual, inhibiting interaction with TFIIIB, which is required for transcriptional initiation and reinitiation. In the same light, in the phosphatase mutant, Maf1 is not phosphorylated, so the A and BC domains are not interacting, and Maf1 doesn't bind in a way that occludes Brf1 association, leading to normal Pol III activity and growth. Based on this interpretation, the Maf1-Rpc160 fusion provides a strong genetic test for the involvement of a factor in regulation of Maf1 phosphorylation by monitoring the colony size phenotype on galactose-containing plates of mutants harboring the fusion. By this manner, we also determined some of the accessory factors that are most likely acting with PP4 to dephosphorylate Maf1 (e.g., Tip41 and Rrd1). It will be interesting to use this tool to look for other activators and repressors of Maf1 phosphorylation and Pol III activity, or to further investigate the mechanism of repression by Maf1.

Materials and Methods

Growth Conditions

We used standard culture methods. See Table 3.1 for strains used. All strains were S288C background unless indicated. For monitoring phosphorylation status of Maf1, we grew initial cultures to OD600 ~0.5–0.7 (T=0), after which we applied a stress treatment. We added cycloheximide (5 ug ml^{-1}) to cultures 5 min prior to application of stress treatment, unless otherwise indicated. Stress treatments are as follows: rapamycin (125 nM, Sigma); methyl methane-sulfonate (0.13%, Sigma); chlorpromazine (250 uM, Sigma); nutrient

Table 3.1

Strain genotypes

Strain	Genotype	Source
YBC1894	*his3Δ1 leu2Δ0 met15Δ0 ura3Δ0 MATa*	Ref. a
YBC1895	*his3Δ1 leu2Δ0 lys2Δ0 ura3Δ0 MATα*	Ref. a
YBC2026	*his3Δ1 leu2Δ0 lys2Δ0 ura3Δ0 maf1Δ::KanMX MATα*	Ref. a
YBC2077	*ura3-52 trp1Δ63 his3Δ200 leu2::PET56 RPC82-13×Myc MAF1-3×HA::KanMX MATα*	Ref. b
YBC2600	*his3Δ1 leu2Δ0 met15Δ0 ura3Δ0 pph3Δ::KanMX MATa*	Ref. a
YBC2699	*his3Δ1 leu2Δ0 met15Δ0 ura3Δ0 pph21Δ::KanMX MATa*	Ref. a
YBC2784	*ade2-1 his3-11, 15 le2-3, 112 trp1-1 ura3-1 lys2-953 pph22-172::URA3 pph21Δ1::HIS3 pph3Δ1::LYS2 can1-100 ssd1-d2* Gal+ *MATa*	Ref. c
YBC2831	*his3Δ1 leu2Δ0 ura3Δ0 RPC160* Gal+ p2265 *MATa*	This study
YBC2833	*his3Δ1 leu2Δ0 ura3Δ0 rpc160Δ::KanMX* Gal+ p2265 *MATa*	This study
YBC2846	*his3Δ1 leu2Δ0 met15Δ0 ura3Δ0 psy2Δ::KanMX MATa*	Ref. a
YBC2847	*his3Δ1 leu2Δ0 met15Δ0 ura3Δ0 psy4Δ::KanMX MATa*	Ref. a
YBC2920	*his3Δ1 leu2Δ0 met15Δ0 ura3Δ0 rts1Δ::KanMX MATa*	Ref. a
YBC2932	*his3Δ1 leu2Δ0 met15Δ0 ura3Δ0 cdc55Δ::KanMX MATa*	Ref. a
YBC2934	*his3Δ1 leu2Δ0 met15Δ0 ura3Δ0 psy2Δ::KanMX MATα*	This study
YBC2939	*his3Δ1 leu2Δ0 met15Δ0 ura3Δ0 tpd3Δ::KanMX MATa*	Ref. a
YBC2940	*his3Δ1 leu2Δ0 met15Δ0 ura3Δ0 pph21Δ::KanMX pph22Δ::KanMX MATα*	This study
YBC3000	*ura3-52 trp1Δ63 his3Δ200 leu2::PET56 RPC82-13×Myc MAF1-3×HA::NatMX MATα*	This study
YBC3048	*his3Δ200(his3Δ1) ura3-52(ura3Δ0) trp1Δ63(TRP1) leu2::PET56(leu2Δ0) RPC82-13xMyc::TRP1 MAF1-3xHA::NatMX pph3Δ::KanMX MATα*	This study
YBC3083	*his3Δ1 leu2Δ0 met15Δ0 ura3Δ0 ppm1Δ::KanMX MATa*	Ref. a
YBC3086	*hisΔ1 leu2Δ0 met15Δ0 ura3Δ0 psy2Δ::KanMX psy4Δ::KanMX MATα*	This study
YBC3109	*his3Δ1 leu2Δ0 met15Δ0 ura3Δ0 rrd1Δ::KanMX MATa*	Ref. a
YBC3110	*his3Δ1 leu2Δ0 met15Δ0 ura3Δ0 rrd2Δ::KanMX MATa*	Ref. a
YBC3111	*his3Δ1 leu2Δ0 met15Δ0 ura3Δ0 tip41Δ::KanMX MATa*	Ref. a
YBC3429	*his3Δ1 leu2Δ0 met15Δ0 ura3Δ0 PSY2-GFP::His3MX MATa*	Ref. d
YBC3430	*his3Δ1 leu2Δ0 met15Δ0 ura3Δ0 PPH3-GFP::His3MX MATa*	Ref. d
YBC3146	*ade2-1 can1-100 his3-11,15 leu2-3,112 trp1-1 ura3-1 PPH3-TAP::KanMX MATa* (W303)	Ref. e
YBC3147	*ade2-1 can1-100 his3-11,15 leu2-3,112 trp1-1 ura3-1 PSY2-TAP::KanMX pph3Δ::HIS5 MATa* (W303)	Ref. e

a. Research Genetics (Invitrogen).

b. Roberts, D.N., Wilson, B., Huff, J.T., Stewart, A.J. & Cairns, B.R. *Mol Cell* **22**, 633-44 (2006).

c**.** Evans D.R. & Stark M.J. *Genetics* **145**, 227-41 (1997).

d. Invitrogen.

e. O'Neill B.M., et al., *Proc Natl Acad Sci U S A* **104**, 9290-5 (2007).

deprivation (0.15× SC, no glucose); glucose deprivation (1× SC, no glucose); glycerol (1× SC, 2% glycerol); amino acid deprivation (1× synthetic defined medium containing auxotrophic amino acids only); phosphate deprivation (synthetic complete made without nitrogen base mix [Difco], re-adding ammonium sulfate, biotin, calcium pantothenate, inositol, all trace elements, magnesium sulfate, magnesium chloride, sodium chloride, and calcium chloride but not potassium phosphate)[57]; nitrogen limitation (synthetic complete made with sodium sulfate instead of ammonium sulfate); dithiothreitol (5 mM). At harvest, we cross-linked cells for 15-30 min in 1% formaldehyde at room temperature (RT, 23 °C), and washed them three times with cold TBS. For co-immunoprecipitation (co-IP), we grew cultures to OD600 ~1 and did not cross-link them, unless otherwise indicated. For Northern blot, we grew cells to OD600 ~0.5–0.7, then applied treatment. We froze cells in liquid nitrogen, or prepared extracts immediately. For fusion growth assay spot dilutions, we prepared overnight cultures in SC plus glucose and spotted to plates with glucose, galactose, and/or 5-fluoroorotic Acid (FOA). We incubated plates RT 4–6 days, until the size of control colonies (i.e., those containing plasmid p2266 or p518) was equivalent between strains.

Extract Preparation, Co-immunoprecipitation

and Western Blot

For Maf1 phosphorylation Western blot and cross-linked co-IP, we broke cells with 1 mm glass beads in ChIP lysis buffer[12], sonicated six times for 30 s on

highest setting, and clarified by centrifugation. For noncrosslinked co-IP, we prepared extracts in a similar manner, except using lysis buffer (50 mM Tris-HCl pH 7.5, 200 mM NaCl, 0.1% Triton, 1 mM EDTA, 10% glycerol, 0.1 mM DTT and protease inhibitors) and no sonication. We incubated protein concentration with Biorad assay and loaded equal protein amounts (usually 30 ug per lane). For co-IP, we incubated 40 ul Dynabeads (preincubated with BSA plus 2 ug anti-HA [12CA5] antibody) or FLAG-agarose beads (Sigma) with 1 mg of extract for 4–6 h at 4 °C, eluted with 2× sample buffer or FLAG peptide (Sigma), and used half of the eluate for Western blot. For Maf1 phosphorylation Western blot, we used 10% gels with a 1:125 bis-acrylamide ratio. We performed Western blot with anti-HA antibody (12CA5 or Abcam 9110), anti-FLAG (Sigma), or anti-Myc (9E10).

Northern Blot

We isolated RNA and performed Northern blot as described[12], using 20 ug per lane and overnight hybridization with end-labeled probes. Blots were exposed to phosphoimager screen for 24 h, scanned, and the images were quantified using ImageQuant.

Fluorescence Microscopy

We performed immunofluorescence for Maf1 as described[12]. We treated live Psy2-GFP yeast cells with Hoechst to stain nuclei and visualized with confocal microscope.

***In Vitro* Dephosphorylation Assay**

We purified yeast 6xHis-Rad53 from BL21 codon plus electro-competent *E. coli* as described[58]. We pooled Rad53 fractions, diluted in storage buffer (50 mM Tris, pH 7.5, 250 mM NaCl, 30% glycerol), concentrated, and repeated. We stored aliquots at -80 °C. We isolated phosphorylated Maf1 by galactose induction in *pph3Δ* strain containing p2811. We diluted overnight cultures containing 2% raffinose, 0.1% glucose into 4 L of medium with 1.5% raffinose (OD600 ~0.06) and incubated RT for 8 h. We induced cultures with 2% galactose (OD600 ~1.584) for 4 h and YPGal 2% (1:4 ratio) for one additional hour. To induce increased phosphorylation of Maf1, we added glucose to 2% final concentration and incubated for 1 h. We harvested the cells by centrifugation, freezing in liquid nitrogen and breaking by pulverizing in liquid nitrogen bath. Cell powder (~10 g) was lysed in 30 ml lysis buffer (50 mM Tris pH 7.5, 300 mM NaCl, 0.1% NP-40, 10 mM imidazole, 1 mM BME, 5% glycerol and protease inhibitors (PIs)). We centrifuged lysate to clarify and incubated with 200 ul pre-washed Ni^{2+} beads for 3 h, washed twice with nickel wash buffer (20 mM Tris pH 7.5, 250 mM NaCl, 5% glycerol, 20 mM imidazole, 1 mM BME), and eluted with wash buffer containing 300 mM imidazole. We pooled the fractions, diluted them with storage buffer, concentrated, and repeated. We stored aliquots at -80 °C. For Pph3-TAP and Psy2-TAP *pph3Δ* complex preparation, we diluted starter YPD cultures containing 200 ug ml^{-1} G418 into 2L 2× YPD with 4% glucose (OD600 ~0.3), incubated for 9 h (OD600 ~1.3), harvested by centrifugation and frozen in liquid nitrogen. We broke cells (~15 g per strain) by

pulverizing in liquid nitrogen bath and stored powder at -80 °C. For one experiment, we lysed 3 g of cell powder in 25 ml lysis buffer (50 mM Tris pH 7.5, 250 mM NaCl, 5% glycerol, 2 mM EDTA, 1% NP-40, PIs). We centrifuged lysate to clarify, we reduced NaCl to 150 mM, and incubated with 100 ul prewashed IgG bead slurry for 5 h. We washed IgG-bound complexes three times in 50 ml wash buffer (same as lysis, except 150 mM NaCL and no EDTA or PIs), and once with 700 ul reaction buffer (25 mM Tris pH 7.5, 100 mM NaCl, 5 mM $MnCl_2$ 0.5 mM DTT). We mixed reactions with 10 ul of IgG-bound complex (or 2 ul lambda phosphatase) and 5 ul of Rad53 or Maf1 substrate, brought to 50 ul with reaction buffer. We incubated the reactions on rotator at RT for 2 or 8 h, then quenched with 25 ul 4× SDS loading buffer and stored at -20 °C. Half of each reaction was loaded per lane. We made 7.5% (for Rad53) or 10% (for Maf1) gels with 1:125 bis:acrylamide. Western blot image was scanned and analyzed using ImageQuant. The Pph3-TAP and Psy2-TAP preparations contain proteins that cross-react with the anti-HA antibody at the approximate size of dephosphorylated Maf1 when either is alone in a lane (e.g., Fig. 3.6E, lanes 2–3, top panel), but since the total signal from HA antibody is unchanged when combined with either complex (lanes 6, 8), this background signal has a minimal effect on the signal of the combined reactions. We calculated enzyme activity by determining the percent of the bottom band (indicated by lambda phosphatase reaction, Fig. 3.6E, lane 4) as a fraction of the total signal for each lane. We set the difference between the percent for lambda and the percent for phosphorylated Maf1 (Fig. 3.6E, lane 1) to 100% and we adjusted the

bottom/total percentages for each enzyme+substrate reaction accordingly. We expressed the percent of lambda phosphatase activity as the average of two replicates with standard error of the mean as confidence interval.

Plasmid Construction

We amplified the 3xHA tag from p2217 with oligos BC3359 and BC3360 and ligated into p521 XhoI and XmaI sites to create plasmid p2264. Plasmid p2264 contains a polylinker that has sites not found in *MAF1* or *RPC160* (i.e., Met25 promoter, then polylinker—XbaI, SpeI, BamHI, XmaI, SacII, AvrII, SalI, NotI—then 3XHA, XhoI, Cyc1 terminator), derived from BC3359. We amplified the coding region of *RPC160* from genomic DNA with BC3361 and BC3362 and ligated into p2264 SalI and NotI sites to create p2265. We inserted the XmaI-XhoI fragment containing *RPC160-3xHA* into p528 to create p2266 (expression under control of *GAL1* promoter). We amplified *MAF1* from p1863 with oligos BC3363 and BC3364 and inserted into p2266 SacII and AvrII sites to create p2268. We inserted annealed oligos BC3432 and BC3433 at a 1:2 ratio of vector:insert into AvrII and SalI sites of p2268 to create p2320; we used oligos BC2552 and BC3405 to confirm that only one copy was inserted. We amplified the coding region of *PPH3* from genomic DNA with BC3534 and BC3430, BC3531, BC3532, or BC3533 and ligated into p518 BamHI and EcoRI sites to create p2352, p2353, p2354, and p2355, respectively. We inserted the same *PPH3* fragments into p522 BamHI and EcoRI sites to create p2356, p2357, p2358, and p2359, respectively. We created p2424 by site-directed mutagenesis (SDM) with BC2883, BC2884 in p2268, followed by subcloning SacII-AvrII

fragment into p2266. We created p2425 by sequential SDM with BC2549 and BC2552 and then with BC2883 and BC2884, followed by subcloning SacII-AvrII fragment into p2266. We created p2531 by amplifying *PSY2* coding region (plus 750bp upstream) from genomic DNA with BC3848 and BC3849 and ligating into p7 SacII and BamHI sites along with PacI-BglII fragment from p709 (HA tag plus Adh1 terminator). We created p2811 by SDM of p1625 with oligos BC5163 and BC5164 to add 10 histidine residues between Maf1 coding region and the first HA tag. All thermo-cycler-amplified fragments were confirmed after insertion by sequencing. See Table 3.2 for a list of plasmids and Table 3.3 for a list of oligos.

Acknowledgements

We thank David Virshup (Duke-NUS Graduate Medical School Singapore) for PP2A plasmids, and Floyd Romesberg (Scripps Research Institute, La Jolla, CA) for Rad53 clone, and for Pph3-TAP and Psy2-TAP strains.

Table 3.2

Plasmids

Plasmid	Description	Source
p7	pRS315	Ref. a
p8	pRS316	Ref. a
p709	pFA6a:3HA:KanMX6	Ref. b
p521	p416.MET25 (FB1521)	Ref. c
p518	p413.MET25 (FB1518)	Ref. c
p528	p415.GAL1 (FB1528)	Ref. c
p1625	pRS416.GAL1prom.MAF1-4HA	Ref. d
p1841	316.MAF1-4HA.4 or maf1-104	Ref. e
p1863	316.MAF1.4HA	Ref. e
p2217	pMaf1(Δ50-139).3XHA	Ref. f
p2264	521.MET25.3XHA	This study
p2265	521.MET25.RPC160.3XHA	This study
p2266	528.GAL1.RPC160.3XHA	This study
p2268	528.GAL1.MAF1.RPC160.3XHA	This study
p2276	pRS315-PPH21-HA	Ref. g
p2279	pRS316-Myc-TPD3	Ref. g
p2320	528.MAF1.linker.RPC160.3XHA.1	This study
p2352	413.PPH3.Met25.CEN	This study
p2353	413.PPH3.FLAG.Met25.CEN	This study
p2354	413.PPH3.FLAG.NES.Met25.CEN	This study
p2355	413.PPH3.FLAG.NLS.Met25.CEN	This study
p2356	413.PPH3.Met25.2u	This study
p2357	413.PPH3.FLAG.Met25.2u	This study
p2358	413.PPH3.FLAG.NES.Met25.2u	This study
p2359	413.PPH3.FLAG.NLS.Met25.2u	This study
p2424	528.maf1-124.RPC160.3XHA	This study
p2425	528.maf1-104.RPC160.3XHA	This study
p2531	315.PSY2.3HA.CEN	This study
p2645	pET-Rad53	Ref. h
p2811	Gal1-Maf1-10xHis-HA	This study

a. Sikorski R.S. & Heiter P. *Genetics* **122**, 19-27 (1989).
b. Longtine M.S. et al., *Yeast* **14** 953-61 (1998).
c. Mumberg D, Müller R, Funk M. *Nucleic Acids Res* **22**, 5767-8 (1994).
d. Constructed by Jason Huff & Brad Cairns, unpublished.
e. Roberts, D.N., Wilson, B., Huff, J.T., Stewart, A.J. & Cairns, B.R. *Mol Cell* **22**, 633-44 (2006).
f. Constructed by Boris Wilson & Brad Cairns, unpublished.
g. Gift from David Virshup.
h. O'Neill B.M., et al., *Proc Natl Acad Sci U S A* **104**, 9290-5 (2007).

Table 3.3

Oligo sequences for plasmid construction

Oligo	Sequence
BC2549	CGTTGGCTCAACCGATGCAAAATCATGGTCAGGATAAGCAGCGTTGAGGAT
BC2552	TGGTAGACAACCAGAGGAATG
BC2883	GAACCGTCAAGCCACAAAATATTTGCTTATCTGATTGCT
BC2884	AGCAATCAGATAAGCAAATATTTTGTGGCTTGACGGTTC
BC3359	CCCCGCCCCGGGAATAAACCGCGGAAAGAAGCCTAGGAGGGTCGTCGACA ATAAAGCGGCCGCATCTTTTACCCATACGATGTT
BC3360	CCCCCCTCGAGAAACTAGCTCTAGAACTGAGCAGCGTAATCTGG
BC3361	CCCCGCGTCGACGGGCGTAAACATGAAGGAAGTCGTTGTAAGTGAAACCCC
BC3362	CCCGCCCCGCGCGGCCGCTCCCCGCGTTCGCTTTTAAAGCTGCCTCATTTG AGAG
BC3363	CCCCGCCCGCGGTTAAACATGAAAGTATGTTATCACTCTAAAACTGCC
BC3364	CCCCGCCCTAGGCTCTGTAGGGATTCTTCTTGATCTGATTTATC
BC3405	GGTTGAATAGGACCACATCACC
BC3430	CCCCGCGGATCCTAAACATGATGGACTTAGATAAGATTATAGCATC
BC3432	CTAGGAGGGTCGAGTGCTGCCGGAGCGGGTACCGCTGGGGCAAGCGCCG CAGGGTCG
BC3433	TCGACGACCCTGCGGCGCTTGCCCCAGCGGTACCCGCTCCGGCAGCACTC GACCCTC
BC3531	CCCGCCGCGGATCCTAAACATGGACTACAAAGATGACGATGACAAGGGGAT GATGGACTTAGATAAGATTATAGCATC
BC3532	CCCGCCGCGGATCCTAAACATGAACGAACTTGCGCTTAAGCTGGCGGGCCT GGACATAAACAAGACAGGGGACTACAAAGATGACGATGACAAGGGGATGAT GGACTTAGATAAGATTATAGCATC
BC3533	CCCGCCGCGGATCCTAAACATGCCCAAGAAAAAGAGGAAGGTGGGGGACT ACAAAGATGACGATGACAAGGGGATGATGGACTTAGATAAGATTATAGCATC
BC3534	CCCCGCGAATTCTTATTATAAGAAATAGTCCATTTGAGATTTTTTGG
BC3848	CCCGCCCGCGGTCCCGATTGTTTCGGTGGACG
BC3849	CCCGCTTAATTAAAGTACTTGCATTCATTTGGTCAACG
BC5163	GATCAAGAAGAATCGATGGCCCGCGGGCATCATCACCATCACCACCACCAT CACCATGGCCGCATCTTTTACCC
BC5164	GGGTAAAAGATGCGGCCATGGTGATGGTGGTGGTGATGGTGATGATGCCCG CGGGCCATCGATTCTTCTTGATC

References

1. Moss, T. & Stefanovsky, V.Y. At the center of eukaryotic life. *Cell* **109**, 545-8 (2002).

2. Wullschleger, S., Loewith, R. & Hall, M.N. TOR signaling in growth and metabolism. *Cell* **124**, 471-84 (2006).

3. Willis, I.M., Desai, N. & Upadhya, R. Signaling repression of transcription by RNA polymerase III in yeast. *Prog Nucleic Acid Res Mol Biol* **77**, 323-53 (2004).

4. Felton-Edkins, Z.A. et al. Direct regulation of RNA polymerase III transcription by RB, p53 and c-Myc. *Cell Cycle* **2**, 181-4 (2003).

5. Gomez-Roman, N., Grandori, C., Eisenman, R.N. & White, R.J. Direct activation of RNA polymerase III transcription by c-Myc. *Nature* **421**, 290-4 (2003).

6. Pluta, K. et al. Maf1p, a negative effector of RNA polymerase III in Saccharomyces cerevisiae. *Mol Cell Biol* **21**, 5031-40 (2001).

7. Dieci, G., Fiorino, G., Castelnuovo, M., Teichmann, M. & Pagano, A. The expanding RNA polymerase III transcriptome. *Trends Genet* **23**, 614-22 (2007).

8. Schramm, L. & Hernandez, N. Recruitment of RNA polymerase III to its target promoters. *Genes Dev* **16**, 2593-620 (2002).

9. Upadhya, R., Lee, J. & Willis, I.M. Maf1 is an essential mediator of diverse signals that repress RNA polymerase III transcription. *Mol Cell* **10**, 1489-94 (2002).

10. Boisnard, S. et al. H2O2 activates the nuclear localization of Msn2 and Maf1 through thioredoxins in Saccharomyces cerevisiae. *Eukaryot Cell* **8**, 1429-38 (2009).

11. Desai, N. et al. Two steps in Maf1-dependent repression of transcription by RNA polymerase III. *J Biol Chem* **280**, 6455-6462 (2005).

12. Roberts, D.N., Wilson, B., Huff, J.T., Stewart, A.J. & Cairns, B.R. Dephosphorylation and genome-wide association of Maf1 with Pol III-transcribed genes during repression. *Mol Cell* **22**, 633-44 (2006).

13. Oficjalska-Pham, D. et al. General repression of RNA polymerase III transcription is triggered by protein phosphatase type 2A-mediated dephosphorylation of Maf1. *Mol Cell* **22**, 623-32 (2006).

14. Vannini, A. et al. Molecular basis of RNA polymerase III transcription repression by Maf1. *Cell* **143**, 59-70.

15. Moir, R.D. et al. Protein kinase A regulates RNA polymerase III transcription through the nuclear localization of Maf1. *Proc Natl Acad Sci U S A* **103**, 15044-9 (2006).

16. Towpik, J., Graczyk, D., Gajda, A., Lefebvre, O. & Boguta, M. Derepression of RNA polymerase III transcription by phosphorylation and nuclear export of its negative regulator, Maf1. *J Biol Chem* **283**, 17168-74 (2008).

17. Lee, J., Moir, R.D. & Willis, I.M. Regulation of RNA polymerase III transcription involves SCH9-dependent and SCH9-independent branches of the target of rapamycin (TOR) pathway. *J Biol Chem* **284**, 12604-8 (2009).

18. Zaragoza, D., Ghavidel, A., Heitman, J. & Schultz, M.C. Rapamycin induces the G0 program of transcriptional repression in yeast by interfering with the TOR signaling pathway. *Mol Cell Biol* **18**, 4463-70 (1998).

19. Di Como, C.J. & Arndt, K.T. Nutrients, via the Tor proteins, stimulate the association of Tap42 with type 2A phosphatases. *Genes Dev* **10**, 1904-16 (1996).

20. Jacinto, E., Guo, B., Arndt, K.T., Schmelzle, T. & Hall, M.N. TIP41 interacts with TAP42 and negatively regulates the TOR signaling pathway. *Mol Cell* **8**, 1017-26 (2001).

21. Wang, H., Wang, X. & Jiang, Y. Interaction with Tap42 is required for the essential function of Sit4 and type 2A phosphatases. *Mol Biol Cell* **14**, 4342-51 (2003).

22. Jiang, Y. & Broach, J.R. Tor proteins and protein phosphatase 2A reciprocally regulate Tap42 in controlling cell growth in yeast. *EMBO J* **18**, 2782-92 (1999).

23. Inoki, K., Ouyang, H., Li, Y. & Guan, K.L. Signaling by target of rapamycin proteins in cell growth control. *Microbiol Mol Biol Rev* **69**, 79-100 (2005).

24. Gingras, A.C. et al. A novel, evolutionarily conserved protein phosphatase complex involved in cisplatin sensitivity. *Mol Cell Proteomics* **4**, 1725-40 (2005).

25. Kim, S.H., Holway, A.H., Wolff, S., Dillin, A. & Michael, W.M. SMK-1/PPH-4.1-mediated silencing of the CHK-1 response to DNA damage in early C. elegans embryos. *J Cell Biol* **179**, 41-52 (2007).

26. Mendoza, M.C., Booth, E.O., Shaulsky, G. & Firtel, R.A. MEK1 and protein phosphatase 4 coordinate Dictyostelium development and chemotaxis. *Mol Cell Biol* **27**, 3817-27 (2007).

27. Boguta, M., Czerska, K. & Zoladek, T. Mutation in a new gene MAF1 affects tRNA suppressor efficiency in Saccharomyces cerevisiae. *Gene* **185**, 291-6 (1997).

28. O'Neill, B.M. et al. Pph3-Psy2 is a phosphatase complex required for Rad53 dephosphorylation and replication fork restart during recovery from DNA damage. *Proc Natl Acad Sci U S A* **104**, 9290-5 (2007).

29. Jiang, Y. Regulation of the cell cycle by protein phosphatase 2A in Saccharomyces cerevisiae. *Microbiol Mol Biol Rev* **70**, 440-9 (2006).

30. Sutton, A., Immanuel, D. & Arndt, K.T. The SIT4 protein phosphatase functions in late G1 for progression into S phase. *Mol Cell Biol* **11**, 2133-48 (1991).

31. Evans, D.R. & Stark, M.J. Mutations in the Saccharomyces cerevisiae type 2A protein phosphatase catalytic subunit reveal roles in cell wall integrity, actin cytoskeleton organization and mitosis. *Genetics* **145**, 227-41 (1997).

32. Van Hoof, C. et al. Specific interactions of PP2A and PP2A-like phosphatases with the yeast PTPA homologues, Ypa1 and Ypa2. *Biochem J* **386**, 93-102 (2005).

33. Santhanam, A., Hartley, A., Duvel, K., Broach, J.R. & Garrett, S. PP2A phosphatase activity is required for stress and Tor kinase regulation of yeast stress response factor Msn2p. *Eukaryot Cell* **3**, 1261-71 (2004).

34. Keogh, M.C. et al. A phosphatase complex that dephosphorylates gammaH2AX regulates DNA damage checkpoint recovery. *Nature* **439**, 497-501 (2006).

35. Huh, W.K. et al. Global analysis of protein localization in budding yeast. *Nature* **425**, 686-91 (2003).

36. Shaheen, H.H. & Hopper, A.K. Retrograde movement of tRNAs from the cytoplasm to the nucleus in Saccharomyces cerevisiae. *Proc Natl Acad Sci U S A* **102**, 11290-5 (2005).

37. Ghavidel, A. et al. Impaired tRNA nuclear export links DNA damage and cell-cycle checkpoint. *Cell* **131**, 915-26 (2007).

38. Hurto, R.L., Tong, A.H., Boone, C. & Hopper, A.K. Inorganic phosphate deprivation causes tRNA nuclear accumulation via retrograde transport in Saccharomyces cerevisiae. *Genetics* **176**, 841-52 (2007).

39. Chen, J.L. et al. Enhancer action in trans is permitted throughout the Drosophila genome. *Proc Natl Acad Sci U S A* **99**, 3723-8 (2002).

40. Hu, M.C. et al. Protein phosphatase X interacts with c-Rel and stimulates c-Rel/nuclear factor kappaB activity. *J Biol Chem* **273**, 33561-5 (1998).

41. Zhou, G. et al. Protein phosphatase 4 is involved in tumor necrosis factor-alpha-induced activation of c-Jun N-terminal kinase. *J Biol Chem* **277**, 6391-8 (2002).

42. Mendoza, M.C. et al. Loss of SMEK, a novel, conserved protein, suppresses MEK1 null cell polarity, chemotaxis, and gene expression defects. *Mol Cell Biol* **25**, 7839-53 (2005).

43. Wolff, S. et al. SMK-1, an essential regulator of DAF-16-mediated longevity. *Cell* **124**, 1039-53 (2006).

44. van Zyl, W.H., Wills, N. & Broach, J.R. A general screen for mutant of Saccharomyces cerevisiae deficient in tRNA biosynthesis. *Genetics* **123**, 55-68 (1989).

45. van Zyl, W. et al. Inactivation of the protein phosphatase 2A regulatory subunit A results in morphological and transcriptional defects in Saccharomyces cerevisiae. *Mol Cell Biol* **12**, 4946-59 (1992).

46. Turowski, P., Favre, B., Campbell, K.S., Lamb, N.J. & Hemmings, B.A. Modulation of the enzymatic properties of protein phosphatase 2A catalytic subunit by the recombinant 65-kDa regulatory subunit PR65alpha. *Eur J Biochem* **248**, 200-8 (1997).

47. Wang, Y. & Ng, T.Y. Phosphatase 2A negatively regulates mitotic exit in Saccharomyces cerevisiae. *Mol Biol Cell* **17**, 80-9 (2006).

48. Brewis, N.D., Street, A.J., Prescott, A.R. & Cohen, P.T. PPX, a novel protein serine/threonine phosphatase localized to centrosomes. *EMBO J* **12**, 987-96 (1993).

49. Glatter, T., Wepf, A., Aebersold, R. & Gstaiger, M. An integrated workflow for charting the human interaction proteome: insights into the PP2A system. *Mol Syst Biol* **5**, 237 (2009).

50. Chen, G.I. et al. PP4R4/KIAA1622 forms a novel stable cytosolic complex with phosphoprotein phosphatase 4. *J Biol Chem* **283**, 29273-84 (2008).

51. Wepf, A., Glatter, T., Schmidt, A., Aebersold, R. & Gstaiger, M. Quantitative interaction proteomics using mass spectrometry. *Nat Methods* **6**, 203-5 (2009).

52. Jordens, J. et al. The protein phosphatase 2A phosphatase activator is a novel peptidyl-prolyl cis/trans-isomerase. *J Biol Chem* **281**, 6349-57 (2006).

53. Chao, Y. et al. Structure and mechanism of the phosphotyrosyl phosphatase activator. *Mol Cell* **23**, 535-46 (2006).

54. Nguyen, V.C. et al. Replication stress checkpoint signaling controls tRNA gene transcription. *Nat Struct Mol Biol* **17**, 976-81.

55. Chen, S.H., Albuquerque, C.P., Liang, J., Suhandynata, R.T. & Zhou, H. A proteome-wide analysis of kinase-substrate network in the DNA damage response. *J Biol Chem* **285**, 12803-12.

56. Gajda, A. et al. Full repression of RNA polymerase III transcription requires interaction between two domains of its negative regulator Maf1. *J Biol Chem* **285**, 35719-27.

57. Sherman, F. Getting started with yeast. *Methods Enzymol* **350**, 3-41 (2002).

58. Sweeney, F.D. et al. Saccharomyces cerevisiae Rad9 acts as a Mec1 adaptor to allow Rad53 activation. *Curr Biol* **15**, 1364-75 (2005).

CHAPTER 4

SUMMARY AND PERSPECTIVES

Human RNA Polymerase III

Human Pol III Transcriptomes

The studies in this work were motivated by the need for a comprehensive view of the Pol III transcriptome in human cells and the need to understand key mechanistic steps of the regulation of Pol III transcriptional activity. To understand the breadth of Pol III transcription in human cells, we performed ChIP-seq of multiple Pol III factors in multiple cell types. We saw strong evidence for cell-type-specific expression of multiple genes, with normal cells showing fewer active genes (e.g., foreskin fibroblasts, 168 genes) and transformed cells showing more active genes (e.g., HEK293T, 336 genes). To investigate the potential reasons for differences in enrichment of the Pol III machinery, we compared active and inactive genes with chromatin ChIP-seq profiles in two cells types and found that active genes were associated with positive chromatin modifications (e.g., H3K4me3) while inactive genes lacked positive chromatin modifications and had higher levels of repressive modifications (e.g., H3K27me3), suggesting a chromatin regulatory component in Pol III occupancy. We also characterized the interesting association of Pol II at

Pol III genes. Active Pol III genes are frequently found in promoters of Pol II genes (proximal) and outside of annotated Pol II promoters (distal), Pol II enrichment is at similar levels. These distal sites are characterized by active chromatin and enrichment of transcription factors, and may represent a special type of Pol II promoter or enhancer. We also identified several novel Pol III genes based on enrichment of Pol III machinery, chromatin status, RNA-seq expression data and Pol II enrichment. It will be interesting to characterize these novel transcripts further. This would involve identifying whether they are part of ribonucleoprotein complexes, determining whether the expression is restricted to particular tissues, and determining whether these transcripts play a role in cancer progression. Notably absent among our findings of active Pol III genes were the previously reported miRNAs produced from the chromosome 19 miRNA cluster (C19MC)[1].

New Ideas About Pol III and Pol II Regulation

The human Pol III transcriptome study presents new ideas about Pol III regulation in relation to Pol II regulation. We found a statistically high correlation between Pol III occupancy and Pol II occupancy genomewide. In both distal and proximal sites, high levels of positive chromatin indicative of a Pol II promoter were present. The result solicits the question of whether Pol III is responsible for Pol II recruitment or *vice versa.* Pol III could require transcription factors and Pol II activity to open up the chromatin environment by recruiting histone modifiers that place H3K4me3 and other positive chromatin marks, thus permitting Pol III to gain access to these genes. Alternatively, Pol III transcription in this region could

open up the chromatin by its ability to displace nucleosomes over the body of the gene, thereby allowing opportunistic binding of Pol II transcription factors, which then recruit Pol II and its accompanying chromatin modifiers. In the latter model, the reason for choice of active genes in each tissue is unexplained. The question is whether Pol II activity and basal machinery is required for recruitment of Pol III. This will be an important question to address in future studies. Simple inhibition of Pol II is confounding, since disruption of Pol II in the cell can have a major impact on the cellular processes in the cell, which would most likely lead to a stress response that could cause indirect repression of Pol III. In order to address this, it will be important to isolate a Pol II/Pol III distal unit and restrict access by Pol II to this unit alone (and not the rest of the genome), and test for a change in recruitment of Pol III.

Another important aspect of Pol II and Pol III regulation that deserves further study is the influence of active Pol III genes upon nearby Pol II genes. Approximately 20% of active Pol III genes are found in a promoter of an annotated Pol II gene, but whether the activity of one can regulate the activity of the other in these particular examples is not known. To address this, specific repression of a particular Pol II gene, containing a Pol III gene within its promoter, by siRNA could be performed and expression of the Pol III gene could be monitored. Alternatively, global repression of Pol III could be performed with a specific inhibitor (e.g., ML-60218, Calbiochem) and expression of Pol II genes, containing Pol III genes within their promoters, could be monitored. An important characteristic of these promoters that should be considered when studying the

regulation of these shared promoters is the fact that 70% are in a divergent orientation, while 30% are arranged so that the Pol III gene is expressed from the same strand as the Pol II gene. It would be interesting to see whether Pol III expression in one orientation (e.g., same strand) might be repressive for Pol II gene expression, while expression in a separate orientation (e.g., divergent) might be activating or neutral for Pol II gene expression.

Cell Type-specific Pol III Gene Expression

Related to the regulation of Pol II with Pol III is the phenomenon of cell type-specific, or tissue-specific, regulation of Pol III gene expression. Is this a cause of variability in expression of Pol II genes with Pol III genes in their promoters? This would not explain this phenomenon at distal sites that have no Pol II genes in the immediate vicinity, e.g., chr6 tRNA clusters, where we see the highest rate of tissue-specific enrichment of Pol III. Or, it could be that these Pol III-bound genes are in enhancers of distant Pol II genes. If that is the case, it would be interesting to identify any Pol II genes of which the Pol III units could be an enhancer to see if those genes are coordinately regulated with Pol III in the various cell types.

Pol III "Enhancer" Class and DNA Looping

One small but potentially important detail from our study is that Ets1 DNA binding sites found at distal sites were quite divergent from the consensus sequence, or absent. This raises a possibility that the ChIP signal we see could be a shadow of Ets1 bound to DNA that has looped to this "enhancer" site. In this case, the Ets1 DNA consensus site could be in the promoter of any

housekeeping gene, and the Pol III transcription unit, acting as an enhancer, has looped over to this promoter; because the DNA is in proximity to this promoter, it would be crosslinked to Ets1, even if Ets1 is not bound to the DNA of the Pol III transcription unit at all. This would also invoke a shadow of all other elements of the promoter bound by Ets1 as well, including Pol II and positive chromatin modifications. One way to rule out this "shadow" hypothesis would be to identify any transcripts produced at the location where Pol II appears adjacent to the Pol III gene. Interestingly, this hypothesis involving DNA looping is another potential interpretation for the fact that many of the TFIIIC-only sites showed no *A-box* or *B-box* consensus sites[2]. Incorporation of 3C (or Hi-C) technology[3] in analysis of Pol III distal sites could determine whether the DNA at distal Pol III units is in proximity to another annotated Pol II gene.

Phosphorylation of Maf1 in Regulation of Pol III

Evidence for PP4 as the Phosphatase of Maf1

Since Pol III is only repressed by unphosphorylated Maf1, we sought to address the yet open question of the identity of the phosphatase of Maf1. For this, we took a candidate approach and studied protein phosphatase 2A (PP2A) and protein phosphatase 4 (PP4). We showed that yeast genetically disrupted for components of PP4 but not PP2A are defective for dephosphorylation of Maf1, nuclear accumulation of Maf1, and acute phase repression of Pol III. We showed that Maf1 interacts with Pph3 and that PP4 purified from yeast is able to dephosphorylate Maf1 *in vitro,* suggesting the action of PP4 on Maf1 is direct. We also showed that Pph3 (the catalytic subunit of PP4) is required for

dephosphorylation of Maf1 in response to multiple stress conditions, suggesting that PP4 and Maf1 are co-integrators.

Regulation and Activation of PP4 in Repression of Pol III

A central issue for the future will be how PP4 is activated to dephosphorylated Maf1. It will be important to determine whether there is a single key step in activation of PP4 in all stresses, or whether the mechanism of activation of PP4 will vary by the stress condition. Multiple factors that have been shown to interact with PP4, such as Tip41 and Rrd1 were also shown to play a role in dephosphorylation of Maf1. It will be important to define the mechanism of action of these co-factors for PP4 function. PP4 complex could be purified from various mutants, e.g., *rrd1Δ*, to see if and in what manner PP4 is deactivated in *in vitro* dephosphorylation of Maf1 when lacking the component. Rrd1 is a prolyl isomerase that acts on Pro190[4] of human PP2A, which is conserved in yeast Pph3 as Pro184. Rrd1 has been shown to activate all PP2A family phosphatases *in vitro*[5], so it is likely that it could use a similar mechanism to activate Pph3 as is used to activate PP2A. Mutation at this amino acid might provide further information about the mechanism of Rrd1 action.

Another potential mechanism for PP4 activation is phosphorylation. Psy4 was shown to be a target of phosphorylation in the DNA damage pathway[6]. Human PP4C was shown to gain serine and threonine phosphorylation during after JNK activation and concurrent with PP4 activation[7]. It is possible that conserved residues are also functioning in yeast Pph3 to allow for activation.

The physical and genetic interaction of Psy2 and Pph3 with Tip41[8], as well as the requirement of Tip41 in Maf1 dephosphorylation is intriguing as it may shed light on the important issue of how PP4 could be regulated by Target of rapamycin complex 1 (TORC1). It is generally thought that TORC1 regulates the PP2A family of phosphatases, including Pph3, via phosphorylation of Tap42, which affects the interaction of Tap42 with the phosphatase[9]. Tap42 interaction with the phosphatase is thought to inhibit the incorporation of the phosphatases into their respective holoenzymes[10]. Tip41 interacts with Tap42, and it is thought that this interaction breaks the interaction with the phosphatase so that it can again incorporate into the holoenzyme, e.g., PP4. Intriguingly, Tip41 is associated with the PP4 holoenzyme, since Psy2 and Psy4 were found in the complex with it[8]. This is also true of the PP6 (Sit4) holoenzyme, since it was found in complex with Sap4, Sap155, and Sap185, which interact with Sit4 in the PP6 holoenzyme[11,12]. However, Tip41 does not interact with PP2A regulatory subunits (e.g., Tpd3, Rts1, Cdc55), therefore it is not likely incorporating into the holoenzyme of PP2A. Initial studies of Tip41 were performed in relation to Tap42 interaction with yeast PP2A, but given these differing results, it may be that Tip41 (and potentially Tap42 as well) has a different, unknown mode of action on PP4 compared to PP2A. The role of Tap42 in regulation of Maf1 is unclear. *tap42-11* mutant yeast are resistant to rapamycin and they show no defect in dephosphorylation of Maf1 or Pol III repression at the non-permissive temperature[13]. Interestingly, Tap42 also shows interaction with Rrd1 and Rrd2[14]; one potential mechanism by which Tap42 could repress PP2A family

phosphatases is by sequestering their prolyl isomerase activators. If Tap42 were sufficient to keep PP4 in an inactive state, then it would be expected that a mutation in Tap42 would permit PP4 to be constitutively active, thus Maf1 might be dephosphorylated at a greater rate. Since Maf1 is dephosphorylated at the same rate in WT and *tap42-11* cells[13], it is likely that PP4 needs an additional activating signal, provided by environmental stress. Whatever the function of Tap42, the ability of a *tap42-11* mutant to repress Pol III is nevertheless consistent with PP4 being the phosphatase of Maf1.

Maf1-Pol III Fusion as a Screening Tool

In our Maf1 study, we also created a Maf1-Pol III tool that could potentially be used to look for other players in the pathway of repression of Pol III. This might include other co-activators of PP4, or factors involved in PP4-independent mechanisms of Maf1-dependent repression of Pol III. There are several pathways that have not been clearly defined that lead to repression of Pol III, including the pathway to nutrient deprivation stress, which requires PKC[15]. It has also been suggested that there might be other steps involved in execution of repression after Maf1 binds to Pol III, and this fusion tool might be useful in identifying factors responsible for this step. To the end of performing screens with the fusion construct, we integrated the fusion at the Lys2 gene locus and isolated integrants in which the fusion growth defect was still visible on galactose-containing plates (data not shown). Initial work was done to find high copy suppressors of the fusion growth defect combined with rapamycin (to arrest growth); most suppressors were members of the TORC1 signaling pathway,

which lead to rapamycin resistance (data not shown), but a few galactose-specific suppressors were also identified. One such was Rrd1; although not intuitive, it could be that overexpression of Rrd1 could be repressive for PP4 in some way, by titrating essential components, thereby inhibiting Maf1 from being dephosphorylated. The screen was not saturated, and it should be redesigned in order to avoid off-target suppressors, such as the rapamycin suppressors we found. One way to potentially avoid this is to perform the screen with a low concentration of rapamycin and MMS (in galactose-containing plates), as it would be more difficult to find suppressors of both rapamycin *and* MMS, so suppressors would more likely be related to the fusion. We also showed that Maf1 can be mutated in the fusion context to relieve the fusion growth defect, so another type of screen would be to mutate the Maf1 sequence in the fusion context by PCR mutagenesis to identify other key residues in Maf1 function.

PP4 as a Potential Human Maf1 Phosphatase

It is noteworthy that PP4 has many conserved functions including dephosphorylation of γH2AX in the DNA damage response from human to yeast. It would be interesting if PP4 were also important for dephosphorylation of Maf1 in human cells. Future studies in human Pol III regulation will show whether PP4 is the major phosphatase of human Maf1.

References

1. Borchert, G.M., Lanier, W. & Davidson, B.L. RNA polymerase III transcribes human microRNAs. *Nat Struct Mol Biol* **13**, 1097-101 (2006).

2. Oler, A.J. et al. Human RNA polymerase III transcriptomes and relationships to Pol II promoter chromatin and enhancer-binding factors. *Nat Struct Mol Biol* **17**, 620-8 (2010).

3. Lieberman-Aiden, E. et al. Comprehensive mapping of long-range interactions reveals folding principles of the human genome. *Science* **326**, 289-93 (2009).

4. Jordens, J. et al. The protein phosphatase 2A phosphatase activator is a novel peptidyl-prolyl cis/trans-isomerase. *J Biol Chem* **281**, 6349-57 (2006).

5. Van Hoof, C. et al. Specific interactions of PP2A and PP2A-like phosphatases with the yeast PTPA homologues, Ypa1 and Ypa2. *Biochem J* **386**, 93-102 (2005).

6. Chen, S.H., Albuquerque, C.P., Liang, J., Suhandynata, R.T. & Zhou, H. A proteome-wide analysis of kinase-substrate network in the DNA damage response. *J Biol Chem* **285**, 12803-12.

7. Zhou, G. et al. Protein phosphatase 4 is involved in tumor necrosis factor-alpha-induced activation of c-Jun N-terminal kinase. *J Biol Chem* **277**, 6391-8 (2002).

8. Gingras, A.C. et al. A novel, evolutionarily conserved protein phosphatase complex involved in cisplatin sensitivity. *Mol Cell Proteomics* **4**, 1725-40 (2005).

9. Jiang, Y. & Broach, J.R. Tor proteins and protein phosphatase 2A reciprocally regulate Tap42 in controlling cell growth in yeast. *EMBO J* **18**, 2782-92 (1999).

10. Inoki, K., Ouyang, H., Li, Y. & Guan, K.L. Signaling by target of rapamycin proteins in cell growth control. *Microbiol Mol Biol Rev* **69**, 79-100 (2005).

11. Kuepfer, L., Peter, M., Sauer, U. & Stelling, J. Ensemble modeling for analysis of cell signaling dynamics. *Nat Biotechnol* **25**, 1001-6 (2007).

12. Breitkreutz, A. et al. A global protein kinase and phosphatase interaction network in yeast. *Science* **328**, 1043-6.

13. Huber, A. et al. Characterization of the rapamycin-sensitive phosphoproteome reveals that Sch9 is a central coordinator of protein synthesis. *Genes Dev* **23**, 1929-43 (2009).

14. Zheng, Y. & Jiang, Y. The yeast phosphotyrosyl phosphatase activator is part of the Tap42-phosphatase complexes. *Mol Biol Cell* **16**, 2119-27 (2005).

15. Roberts, D.N., Wilson, B., Huff, J.T., Stewart, A.J. & Cairns, B.R. Dephosphorylation and genome-wide association of Maf1 with Pol III-transcribed genes during repression. *Mol Cell* **22**, 633-44 (2006).